Study of the molecular mechanisms involved in the formation of hindbrain boundaries

Simone Calzolari

DOCTORAL THESIS UPF - 2013

THESIS DIRECTOR

Cristina Pujades, PhD

DEPARTAMENT DE CIÈNCIES EXPERIMENTALS I DE LA SALUT

Universitat Pompeu Fabra Barcelona

A colei che mi è sempre accanto

Agraïments

Han pasado 5 años desde que empecé la tesis y ahora estoy aquí, un día antes de ir a la copistería, con pocas horas de sueño y muchas de ordenador, pensando en todas las personas que me habéis ayudado en este largo proceso. Seguro que me olvidaré de alguien.

Primero quiero agradecer a Cristina, per haberme dado esta oportunidad y haberme aguantado durante todo este tiempo. Pero sobretodo te quiero agradecer Cris porque siempre sabes cómo tratarnos a nosotros los estudiantes y porque siempre te pones a nuestro nivel. Hemos tenido algún que otro roce en estos tiempos pero sabes que te respeto muchísimo. Eres una gran jefa Cris.

También quiero dar las gracias a los otros jefes del grupo (aunque somos tres grupos diferentes yo siempre nos veo como un grupo único). A Fernando por su enorme dedicación a la ciencia y a los estudiantes y a Berta por siempre intentar motivarnos. Vuestro esfuerzo es lo bueno de la ciencia.

I want to thank also Nadine to give me the possibility to stay in her lab last year where I learned a lot of things and I knew many people. Thanks.

Gracias Javi, porque gran parte de este proyecto lo hicimos juntos y sin tu aportación no hubiera avanzado tanto.

Grazie Daviduzzo, per essere la rappresentazione della pace e della tranquillità.

Grazie Andrea, perchè senza di te questo labo sarebbe piu monótono.

Gracias Sylvia, por tener tanta energía y fuerza como un volcán.

Gracias Jelena, por alegrarnos las comidas con tus miedos hacia los tiburones.

Gracias Laura, porque siempre transmites alegría y das ánimo.

Gracias Esteban, por ver siempre las cosas bonitas de este trabajo.

Gracias a Miquel y Marta, nuestros grandes técnicos, sin vosotros nuestro trabajo no podría funcionar.

Gracias támbien a los nuevos, Hector, Adriá. Y Gina que es nueva pero también antigua.

Gracias a los anitguos miembros: Eva, Dora, Marija, Joana.

Gracias a Andrés, aunque no hemos coincidido en el lab, luego hemos recuperado.

Gracias Alex, bueno yo creo que el labo es lo de menos. Hemos compartido salidas, pizzas, beer session y alguna excursión cultural.

Y ahora fuera del lab.

Grazie anche a te Davide: laureati insieme, dottorati insieme e adesso la nuova sfida con l'impresa. Grazie per aver condiviso queste cose con me.

Grazie anche a te Valery perchè, a parte l'impresa anche tu ci sei sempre stata.

Gracias al Paquillo, por las muy largas noches de juerga.

Gracias a todo el grupo de PRBB extendido: Egidia, Carluzzo, Maury, Luchiño, Matteo, Serena, Anna, Silvia, Jose y Paula.

A todo el grupo del volley: Diogo, Christos, Mari, Romi, Tobias. Muchas gracias por todas las tardes, por los partidos, las finales y las cervezas.

Gracias a los socios, a dos ya les di las gracias, pero faltaba Ignasi fundamental pieza de friquismo catalán.

Gracias a todo los amigos de "Poble Sec": Natxo, Joana, Mariano, Ali, Romén, María, Braulio, Paz, Lorena y Sam. Algunos ya están lejos otros han vuelto y otros van a volver pronto, pero todos sabemos que Barna es nuestra casa.

Grazie ai regaz di Bologna. Grazie perché quando torno è come se vivessi lì da sempre anch'io, grazie per le zingarate, le uscite e tutto quello che il 2013 ha portato. In primis Teo, Pol compagni di una vita e poi Pino, l'Artista, il Frenky, il Modolo.

Infine lascio per ultimi i miei familiari.

Grazie alla mamma e al babbo per avermi sostenuto in tutti i modi possibili in questo sforzo, grazie perché siete due genitori stupendi e se sono arrivato fin qui è merito vostro. Grazie davvero.

Grazie alle mie due sorelle, perché vi voglio un bene immenso e anche se lontano vi porto sempre con me. Grazie anche alla Patty.

Grazie anche ai miei nonni e alla cara e vecchia zia.

Grazie al mitico e grande Dave, molto piú che un fratello. Grazie per essere la persona piú buona e generosa che io abbia mai conosciuto. Ti voglio bene zio.

Ringrazio la mia nipotina, appena arrivata ed é già la donna piú bella del mondo. Non vedo l'ora di conoscerti. Grazie anche a te Stefy per averla portata al mondo.

Per ultimissima lascio la piú importante, grazie di cuore Giulia. Grazie per la felicitá che mi dai ogni giorno e perché sei davvero una persona meravigliosa. Grazie perchè questa tesi é anche merito tuo.

Merci a tothom.

Septiembre 2013.

Abstract

During development, embryonic tissues are gradually patterned and they eventually are committed to a specific fate. In vertebrates, the entire Central Nervous System (CNS) derives from the neural tube, a transient embryonic structure that is regionalized along the anteroposterior (AP) axis in three different brain vesicles and the spinal cord. The hindbrain, the posterior brain vesicle, is the most evolutionary conserved and it will give rise to important structures such as the cerebellum. The hindbrain itself is transiently patterned along the AP axis in different metameric segments called rhombomeres (r). This organization dictates the temporal and the spatial development of structures that are formed in a repeated pattern, like cranial nerves and reticular neurons. Rhombomeres are cell-lineage compartments, divided by boundaries where cell mixing is restricted. A specific combinatory of gene expression confers molecular identity to each rhombomere. Rhombomeric-restricted genes are progressively refined during development transiting from jagged to sharp limits of expression, therefore establishing molecular boundaries. After that, morphological borders become visible and impede cell intermingling.

Up to date, it was still not clear which are the cellular and molecular mechanisms responsible for boundary refinement and responsible of rhombomeric cell segregation.

In this work we demonstrate that cell sorting is the main mechanism responsible for refinement of molecular boundaries in the hindbrain. For this, we performed *in vivo* cell tracking and fake-cell tracing analysis. We show that once molecular boundaries are refined cell movement is restricted between adjacent rhombomeres due to the formation of an actomyosin cable in the cellular cortex of the cells at the boundary. Finally, we demonstrate that this process is mediated by the Eph/Ephrin signaling pathway.

Resum

Durant el desenvolupament embrionari, els teixits s'especifiquen gradualment fins a que adquireixen un destí final. En els vertebrats el Sistema Nerviós Central (SNC) deriva del tub neural, una estructura embrionària transitòria que està regionalitzada al llarg de l'eix anteroposterior (AP) en tres diferents vesícules cerebrals i en la medul·la espinal. El romboencèfal, la vesícula cerebral posterior, és la més conservada evolutivament i donarà lloc a estructures importants com el cerebel. La part posterior del cervell està segmentada de manera transitòria al llarg de l'eix AP en diferents compartiments anomenats rhombòmeres (r). Aquesta organització segmentada determina el desenvolupament temporal i espacial de les estructures que es formen en un patró repetit, com els nervis cranials i les neurones reticulars. Els rombòmers són compartiments de llinatge cel·lular separats per fronteres, que restringeixen la barreja de cèl·lules dels diferents compartiments. Una combinatòria gènica específica confereix identitat molecular a cada rombòmer. Aquests gens refinen progressivament el seu límit de expressió, establint fronteres moleculars que prefiguren on es formaran les fronteres morfològiques que impediran que les cèl·lules es barregin. Fins avui, encara no està clar quins són els mecanismes cel·lulars i moleculars responsables de refinament de les fronteres i de la segregació cel·lular.

En aquest treball es demostra que el *cell-sorting* és el principal mecanisme responsable del refinament dels límits moleculars en el romboencèfal. Per a això, vam realitzar un seguiment de les cèl·lules *in vivo* i una anàlisi de les seves trajectòries. Es demostra que el moviment cel·lular està restringit entre rombòmeres adjacents un cop els límits moleculars han estat refinats, a causa de la formació d'un cable de actomiosina a la part apical de les cèl·lules de la frontera. Finalment, hem demostrat que aquest procés està mediat per la via de senyalització Eph/Ephrin.

Preface

Identification of the mechanisms involved in patterning is fundamental in developmental biology. We tried to answer to basic and historical questions that are still attractive for their enormous impact. In this context, the development of the Central Nervous System (CNS) is one of the most fascinating field for its extraordinary sophistication that has an implication in the complexity of the adult brain, in which the scientific community has still a lot of work to do in its understanding.

Regionalization of territories is an intelligent way by which the Nature separates cells and control better their behaviour. Earlier in the 70's were published the first evidences in this sense in fly (Garcia-Bellido and Santamaria, 1972) and then it was shown that in different developmental tissues this process occurs. In vertebrates appears immediately clear that it is a fundamental process in correct formation of organs. Like in the hindbrain, in which its particular transient segmentation converts it in a fantastic model to work with.

In this work we decided to elucidate the process of hindbrain patterning using zebrafish, which offers many more advantages compared to the classical animal models and among them the possibility of *in vivo* and genetic studies. We combine classical *in vitro* approaches with the most modern advances in the confocal microscopy that nowadays allow us to observe what happens inside every single cell during time. Only with this possibility we could understand first cellular behaviours and then the molecular mechanisms.

We were able to comprehend how the cells behave to form linear boundaries in hindbrain segments, the mechanism involved in restriction maintenance and finally how a special population is originated in the interface of these segments.

During this work I could make a short stay in the laboratory of Nadine Peyrieras (Gif-sur-Yvette, France) where I had the possibility to acquire a valuable knowledge in 3D+time imaging. I performed several time-lapse videos to visualize the behaviour of specific cell population in the hindbrain and I could also work with specific software dedicated to the acquisition and the treatment of data imaging.

Our results made step forward in the field of basic developmental biology and confirm again that exists a link between gene regulation and the biomechanics in morphogenetic processes and importantly that many more mechanisms than expected are conserved between vertebrates and flies.

Part of this work is now in the process of second revision by an international journal (see annex). At this very same time, we are performing other experiments to be included with the last part of thesis and send it for publication. The work was presented in different national and international meetings: in the European Zebrafish Meeting 2013, in the International Zebrafish development meeting 2012, Barcelona Developmental Biology Joint Retreat 2011, EMBO frontiers in sensory and Development 2011.

INDEX

INTRODUCTION

1. Patterning and regionalization during embryogenesis

1.1 Embryonic development

Embryonic development is the biological event by which a multicellular organism is generated from a fertilized egg. This consists in a complex temporal and spatial coordination of the following cell- and tissue- processes: cell division, c

ell differentiation and growth, patterning, and morphogenesis. Developmental processes are mutually influencing and controlling and finally they generate organized structures, such functional tissues and organs in the adult, from a group of multipotent embryonic cells.

During development, embryonic cells gradually acquire complexity and lose potentiality of differentiation, passing through different states in which eventually they are committed to a specific cellular fate. The genetic program of development is established by a subgroup of genes named *developmental genetic toolkit* (Carroll, 2005) conserved even from very evolutionary distant species. *Toolkit* genes codify for both transcription factors that modulate the expression of other genes, and for members of signaling pathways called morphogenes. Those genes are fundamental for controlling the embryonic patterning that represents the mechanism by which an homogeneous tissue assumes complete multiple forms and functions; in other words, the ability to generate differences in an undifferentiated territory.

The first patterning event is during the gastrulation period when, after several events of morphogenesis and cell-migration in the developing embryo, the body plan is established and the main axes are formed: anteroposterior (AP), dorsoventral (DV), left-right (LR), and in triblastic animals the three germ layers are generated (endoderm, mesoderm and ectoderm). After gastrulation, organogenesis occurs and the definitive adult structures are generated.

1.2. Mechanisms of patterning

Embryonic cells or tissues use different strategies to create patterns that can be classified as i) cell autonomous mechanisms, ii) inductive mechanisms, or iii) morphogenetic mechanisms (Fig.1).

1.2.1 Cell autonomous mechanisms

In different organisms, the egg can contain proteins or mRNAs differentially distributed that can result in an asymmetric heritance of the cells during oogenesis. This strategy is used very often to generate differences among cells in development and the best-studied case is *D. melanogaster* oocyte that is patterned by the gonads that assembly the determinants in specific domains (Langdon and Mullins, 2011).

An analogue case is when, later in development, embryonic cells transform their internal polarity of transcripts or proteins in two daughter cells containing different material. Asymmetric mitosis is found also in *Drosophila* during neuroblast generation (Doe and Bowerman, 2001) and also in other animal groups like nematodes (Bossinger and Cowan, 2012) and many others (Freeman, 1976).

1.2.2 Inductive mechanisms

Cells can communicate to the neighboring tissues by the secretion of diffusible or by membrane-bound molecules. In this mechanism class the tissue.pattern changes as a direct consequence of cell-fate change after the interpretation of the signals received. The territories that are able to instruct the closest tissues -the embryonic organizers- are defined in different organisms at the gastrula stage. In *Xenopu*s for example, the organizer is called the Nieuwkoop center, which sends signals that induce the formation of the mesoendoderm (Joubin and Stern, 2001).

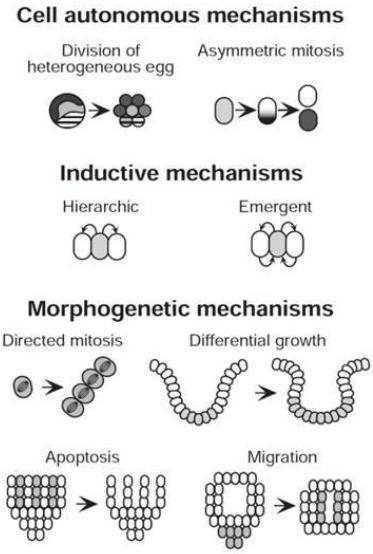

Figure 1. Schematic representation of basic developmental mechanisms. Division of an heterogeneous egg: different shedding of the egg represents distribution of different molecules inherited by different blastomeres. Asymmetric mitosis: determinants differentially localized in the mother cell result in different daughter cells. Hierarchic induction: inducing cells affect neighboring cells. Emergent induction: inducing cells affect neighboring cells, which signal back. Directed mitosis: organization of mitotic spindle orientation affects tissue growth. Differential growth: tissue shape is altered by different rates of cell division. Apoptosis: new patterns are created by apoptosis of specific cells. Migration: cells can migrate to a new position. From Salazar-Ciudad et al., 2003.

a)Hierarchic mechanism

Generally the organizer acts in a **hierarchic** mechanism (Salazar-Ciudad et al., 2000) in which it sends the inductive stimulus and the receiving cells either only receive it or either respond back, but in such a way that the back-signal does not affect the capacity of the first territory to maintain the signal. This is the classical way as the organizer works.

The organizer can establish a morphogen-gradient that can influence the closest tissues respecting the French Flag model (Fig.2a): a scenario in which a gradient of secreted signal causes a concentration-dependent activation of target genes in non-overlapping domains across a field of initially

undifferentiated cells, and this can create different or periodic patterns. In this context the receiving cells interpret positional identity information.

b) Emergent mechanism

Another case is the **emergent genetic** mechanism in which receiving cells or territories the back-signal is itself an inductive stimulus, and affects the first signaling territory in a way that there is a mutual induction upon cell contact (Salazar-Ciudad et al., 2000).

One example is the reaction-diffusion model proposed by Turing in 1952 (Fig.2b), in which dynamic interactions between activator and inhibitor molecules in an initial uniform tissue can result in the generation of periodic patterns. This relevance has been recently demonstrated for the digit patterning in limb development and probably in other systems (Marcon and Sharpe, 2012).

The Notch-Delta system represents the best known example of cell-to-cell reciprocal communication: involved in the so-called processes of lateral inhibition and lateral induction (Artavanis-Tsakonas et al., 1999).

1.2.3 Morphogenetic mechanisms

Different cellular processes can be involved in patterning the tissue rather than in signaling; these mechanisms change the relative arrangement of the cells in the space.

Directed mitosis refers to the capability of modifying and to orientate in the same way the mitotic spindle in order to force cells to position at specific place. This strategy is used during neuroblast generation in the fruitfly (Sousa-Nunes and Somers, 2013) where asymmetric mitosis determine which cell will be a neuroblast but then its position is controlled by this morphogenetic mechanism. The first divisions of *C. elegans* are also governed by this mechanism (Sawa, 2012).

Another strategy is **differential growth,** where cells with different fate divide at different rates, such in the formation of long bones in vertebrates (Sandell and Adler, 1999).

Apoptosis of specific cells in developing tissues after interaction of surrounding cells is responsible of the generation of patterns in different systems: development of neural circuitry (Kuan et al., 2000), generation of the digits in limb development (Chen and Zhao, 1998) or the correct formation of outflow tract and valves of the heart (Poelmann et al., 2000).

Finally cells can change their relative position without changing their fate by **migration**. This can be driven by: chemokinesis, speed random movement, chemotaxis, and directional migration in response to chemical gradients or haptotaxis insoluble substrate gradients. For example, neural crest cells are a migratory population that responds to chemotactic stimuli (Erickson, 1988;Kubota and Ito, 2000).

Collective migration is the more interesting mechanism of this category. This mode differs from single cell migration in that cells remain connected as they move, which results in migrating cohorts and varying degrees of tissue organization. Collective migration of cohesive groups of cells is particularly common during embryogenesis and drives the formation of many complex tissues and organs such as: the migration of the primordium of the lateral line in zebrafish (reviewed in(Lecaudey et al., 2008), during epiboly in zebrafish (Lepage and Bruce, 2010), and for trachea branching in fruitfly (Affolter and Caussinus, 2008).

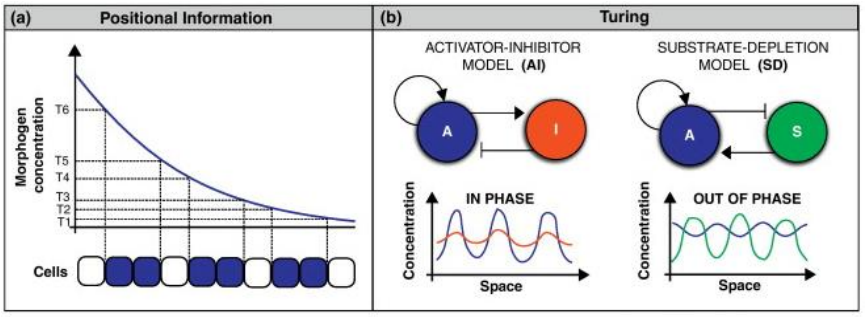

Figure 2. Positional information and Turing model. a) Wolpert French flag model. Six different thresholds of a unique morphogene-concentration gradient settle the boundary of a periodic fate (blue cells). b) Turing pattern generated by the interaction of diffusible molecules. On the left, Activator (A) promotes itself and activates its own inhibitor (I). In the space a periodic pattern is established where A and I are in phase. On the right A auto-activates itself and consumes its own substrate (S) that in turn activates A. In the space a periodic pattern is established where A and I are out of phase. From Marcon and Sharpe, 2012.

1.3 The concept of segmentation

In different embryonic territories a tissue is divided in repeated sequences of the same unit along one body axis; this is a strategy adopted by the organism to create very similar structures but displaying small differences that are reflected in the anatomy of the adult (Fig.3).

Each segment or compartment is morphologically distinguishable, defined by a combinatory of genes that confers an identity to the cells of the same segment, and they are separated by boundaries that prevent cell intermingling. Segmental organization was initially described in the embryonic ectoderm of *Drosophila melanogaster* (Akam, 1987), where the embryo is regionalized along the AP axis in several segments that will generate different structures of the head, thorax and abdomen.

In vertebrates two embryonic territories are segmented: the hindbrain and the somites. It is still controversial if the anterior vesicle of the brain -the forebrain- is segmented during development (Larsen et al., 2001; Puelles and Rubenstein, 2003; Shimamura et al., 1995).

The ability to maintain cells segregated and create borders between them is a key process in development and it has been extensively studied; in particular, the hindbrain represents a perfect vertebrate system for this purpose. In this sense extensive effort has been spent to understand the signaling pathways and transcription factors involved in regional organization of embryonic tissues.

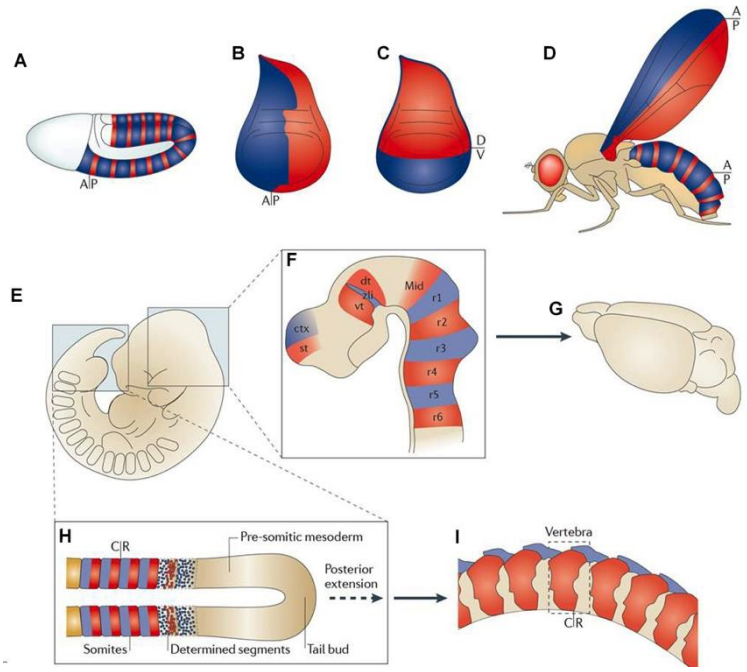

Figure 3. Representation of compartments in developing *D. melanogaster* and in the vertebrate embryo. Red and blue are used to illustrate the compartments. A) Diagram of fruitfly embryo during stages 8-11; B) and C) larval imaginal discs. D) Adult frutifly. E) Mouse embryo at 12.5 days post coitum (dpc) showing developing brain and somites. F) Boundaries of the neural tube: ctx, cortex; dt, dorsal thalamus; mid, midbrain; r1–r6, hindbrain segment rhombomeres 1–6; st, striatum; vt, ventral thalamus; zli, zona limitans intrathalamica. G) Adult mouse brain. The forebrain gives rise to the two anterior lobes and the cortex. Next lobe is the cerebellum. The last structure at the base is the hindbrain, where rhombomeric segmentation is lost in the adulthood. H) Presomitic mesoderm of extending embryo. Solid colors are formed somites, divided by C|R, and the dotted patterns are cells with emerging identities. I) The architecture of the axial skeleton of the mouse. Caudal somite forms ossified bone of the vertebral body and pedicle, rostral somite forms the spinous process. From Dahmann et al., 2011.

1.4 Zebrafish as a model system to study developmental biology

Since 20 years a new animal model is acquiring popularity in the scientific community: the zebrafish (*Danio rerio*). The zebrafish is a small tropical fish that lives in rivers of northern India and Pakistan, Nepal and Bhutan. Its name is given by the characteristic stripes all along the body and the fins. Adult zebrafish measures 4-5 cm in length. Sexual maturity is enriched at 3-4 months and adult pair can generate 200 eggs per week in a single day. Zebrafish embryos are transparent and embryonic development is completely external and rapid: at 24 hours post fertilization (hpf) all the major organs are formed and at 3 days post fertilization (dpf) the fish hatches and it starts to swim.

In the last ten years several transgenic fish lines expressing fluorescent reporter proteins or functional genes have been reported and also a large number of gene-mutants has been isolated and characterized. Zebrafish shares with humans similar physiology, organs and also the 70% of the genome that is completely sequenced. The easy manipulation of the embryos gives the possibility of mRNAs or plasmidic DNAs injections for gain-of-function experiments, or injection of morpholinos for knock-down of target genes.

Finally, zebrafish is becoming famous in drug discovery as pre-clinical model system for High-Content-Screening (HCS) tests. The reduced dimensions of embryos and larvae and its rapid development enables this model to fill the gap between *in vitro* cell culture test, relatively cheap but with limitation in terms of scientific relevance, and *in vivo* studies with murine models, much more effective but very expensive (Parng et al., 2004; Terriente et al., 2012; Terriente and Pujades, 2013).

2. The hindbrain as a model system for studying segmentation

2.1 Neurulation process in teleost is different compared with amniotes

After gastrulation in vertebrates, in the anterior part of the embryo, signals from surrounding tissues induce the ectoderm to thicken and then to form the neural plate, that after folding it will form the neural tube, the primordium of the Central Nervous System (CNS) This process is called "primary neurulation", different, from the "secondary neurulation" in the posterior part where an epithelial tube is formed by mesenchimal cell population that condenses to form a solid rod.

In amniotes the neural plate organizes as a single cell layered epithelium, then two neural folds are formed at the lateral extreme of it, they elevate and converge to the midline and the neural plate invaginates inside. A free space in the center of the forming tube, called neural groove, is generating by the initial elevation of the neural plate (Clarke, 2009; Lowery and Sive, 2004) (Fig.4B).

In teleost this process occurs in a different way, because the epithelialization of the cells occurs during neurulation, such as the neural plate cavitates rather than invaginates and the apical lumen is formed after the complete tube is formed. The neural plate generates a solid neural keel and later neural rod while the cells suffer a global rearrangement and once they are completely epithelialized they create the lumen (Fig.4A).

Neural plate cells converge to the midline where they complete a mediolaterally-oriented cell division, the so-called crossing or C-division. One daughter cell is deposited on the left hand side of the neural keel or rod and the other daughter cell on the right hand side. The daughter cell that stays on its side of origin is always the one closest to its ipsilateral basal surface and the crossing daughter is always the one closest to the midline.

Once C-division is formed the daughter cells progressively separate and form a lumen (Tawk et al., 2007).

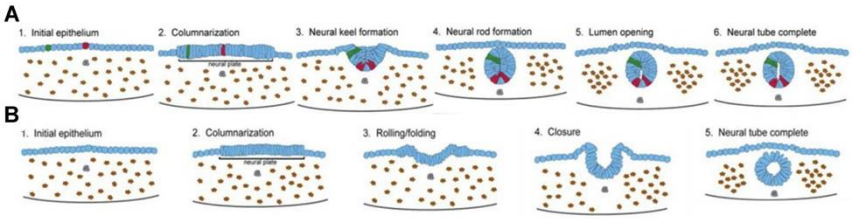

Figure 4. The neural tube is formed by two different mechanisms in teleost and amniotes. A) In teleost an initial epithelium columnarizes to form the neural plate, which then forms a solid neural keel and a tube. The midline of the tube becomes distinct and a lumen opens from ventral to dorsal. The relative position of neural plate cells is maintained during neural tube formation (red and green cells). B) During primary neurulation in amniotes the neural tube is formed by columnarization of an existing epithelium that rolls and folds. The cavitation is formed during the closure of the tube. Modified form Lowery and Sive, 2004.

2.2 Anatomy of the hindbrain

During the process of neurulation the neural tube is regionalized in three different brain vesicles along the AP axis: forebrain, midbrain and hindbrain, and the spinal cord that it develops as a narrow tube.

The forebrain will give rise to telencephalon and diencephalon, the midbrain to the mesencephalon and the hindbrain to the metencephalon and the myelencephalon. The metencephalon will form the cerebellum, and the myelencephalon will give rise to the pons and the medulla oblongata (Fig.5).

The neurons located in the cerebellum generate nerve centers responsible for pain relay to the head and neck, auditory connections, balance control, tongue, neck and eye movement, as well as breathing, gastrointestinal and heart rate control. The cerebellum is an ancient component of the vertebrate brain and its functions derive on it evolutionarily conserved structure and circuitry. A reminiscent of cerebellar structure is found in cartilaginous fist although it differs from the teleost cerebellum (Altman and Bayer, 1997; Butler, 2005; Nieuwenhuys, 1967).

The medulla oblongata is responsible for regulating several basic functions of the autonomic nervous system such as respiration and heartbeat, and contains the so called "bulbar reflexes" (vomiting, coughing, sneezing, and swallowing).

The pons function deals primarily with sleep, respiration, swallowing, bladder control, hearing, equilibrium, taste, eye movement, facial expressions, facial sensation, and posture.

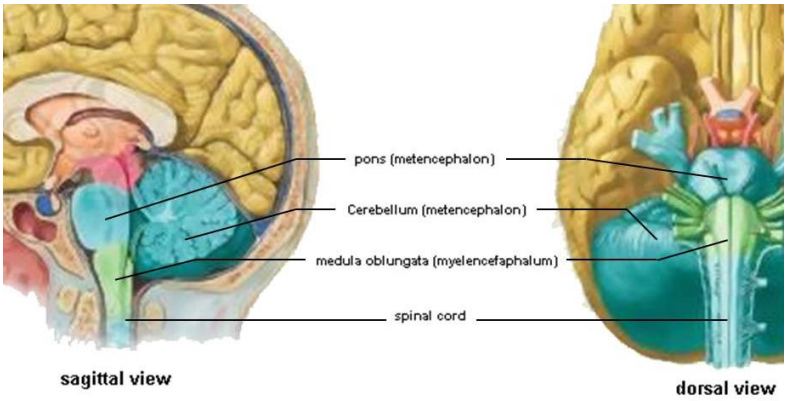

Figure 5: Encephalic trunk of an adult brain. On the left, sagittal view and on the right, dorsal view of an adult human brain. The derived structures from the three brain vesicles are colored in: yellow for forebrain, red and orange for midbrain and blue and green for hindbrain and spinal cord. Pons, cerebellum, medula oblongata and spinal cord are indicated, Adapted from Adult derivatives of the Forebrain, Midbrain and Hindbrain. Elsevier.

2.3 Patterning the hindbrain: the generation of rhombomeres

The hindbrain is segmented along the AP axis in a sequence of 7-8 metameric structures called rhombomeres, visible like a series of bulges in the neuroepithelium (Fig.6). That process is responsible of the juxtaposition of cranial nerves exit points, the correct differentiation of neuronal types, the right migratory stream of neural crest cells and ultimately for the formation of the mature adult structure (Lumsden and Keynes, 1989; Lumsden and Guthrie, 1991 ;Sechrist et al., 1993; Trainor and Krumlauf, 2001).

The segmentation dictates the timing of neuronal differentiation, which is delayed in the odd-rhombomeres, and also its spatial organization: clusters of neurons are present only at the center of the rhombomeres and in the para-boundary territories generating a stereotypic neuronal distribution. Rhombomeric patterning generates the so-called two-segment repeats: one odd- and one even-rhombomere form a unit repeated three times (Fig.6).

The exit points of the motor system are present only in the odd-rhombomeres and the neurons born in the even-rhombomeres project their axons to the exit point of the anterior adjacent rhombomere; in this way the motor nerves are formed in r2 (mV), r4 (mVII) and r6 (mIX) (Lumsden and Keynes, 1989).

Neural cell crest cells (NCCs) of odd- and closest even-rhombomere follow the migratory stream in the same pattern: from r1-2 to branchial arch (BA) 1 (BA1), from r4 to BA2 and from r6-7 to BA3. Rhombomere 3 does not contribute to neural crest at all, and from r5 some NCCs start to migrate and they stop in the posterior-lateral periotic mesenchyme, so they do not follow to the branchial arch (Kulesa et al., 2004; Sechrist et al., 1993).

The hindbrain is also patterned along the DV axis giving rise to different neuronal types according to their position of origin (reviwed in Cordes, 2001). All the motor cranial nerves are contained in the dorsal domain and they are subdivided in three classes, according to their final target: visceral motor nuclei (vm) that innervate parasympathetic ganglia associated with lachrymal and salivary glands, or the neuronal plexus that innervates smooth muscles; somatic motor nuclei (sm) innervating the paraxial and prechordal mesoderm derived-muscles, and branchial motor nuclei (bm) that innervate the muscles in the branchial arches.

The branchiomotor, visceromotor and vestibuloacoustic axons converge on communal exit points in the dorsal domain, while somatic motor neurons leave the neural tube ventrally in small clusters. The ventral part of the

hindbrain is formed by the sensory components of the individual cranial ganglia developed from sensory placodes or derived from neural crest cells. The cell bodies of sensory neurons are positioned outside the neural tube and they project their axons to the brainstem.

A part of sensory and motor neurons the hindbrain is composed also by a population of interneurons, the reticular neurons that are involved in modulation of pain sensation, arousal and rhythmic breathing. They can be classified in 8 different subpopulations depending on their axonal trajectories (Cordes, 2001).

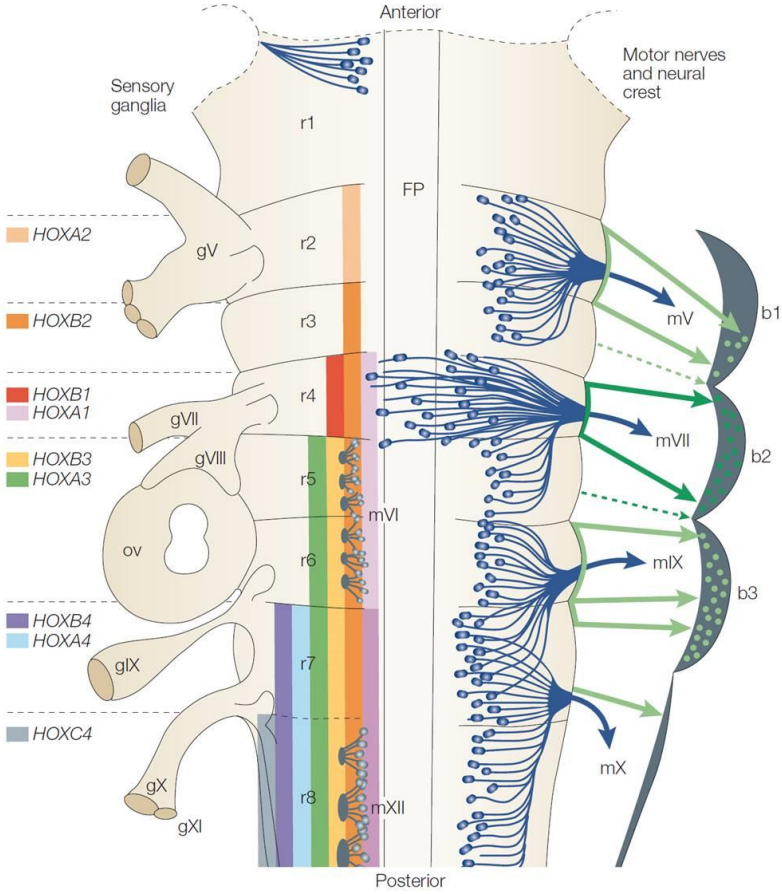

Figure 6. Representation of a chick hindbrain segmentation in a dorsal view. On the right, the formation of motor nuclei (blue) and the exit points of their efferent nerves from rhombomeres 2, 4, 6 and 7. The trigeminal (mV), facial (mVIII) and glossopharyngeal cranial (mIX) nerves project into the first (b1) second (b2) and third (b3) branchial arches (BA). The vagus nerve (mX) innervates a large part of the body. Green arrows represent neural crest cells stream from corresponding rhombomeres migrating to the branchial arches. On the left, the otic vesicle (ov) and the position of the cranial sensory ganglia (gV and gVII-gXI) are indicated, and the segmental expression of *Hox* genes in color-coded. FP: floor plate, mVI, mXII: somatic motor neurons. From Kiecker and Lumsden, 2005.

2.4 Cell lineage restriction of rhombomeric cells

Pioneering work in the chick hindbrain, involving labeling of neuroepithelial cells with a lipophilic dye, identified cell lineage restriction boundaries at the borders between rhombomeres (Fraser et al., 1990), demonstrating that rhombomeres are compartments of cell-lineage (Fig.7). They performed single-cell labeling before and after the appearance of morphological boundaries and showed that the labeled clones were completely restricted to a given rhombomere when the single-cell labeling was done after the appearance of morphological barriers, but surprisingly labeled clones were also confined to a specific rhombomere before the appearance of the boundaries. They speculated that, a part of the barrier generating the morphological boundaries an alternative mechanism for cell restriction had to be present.

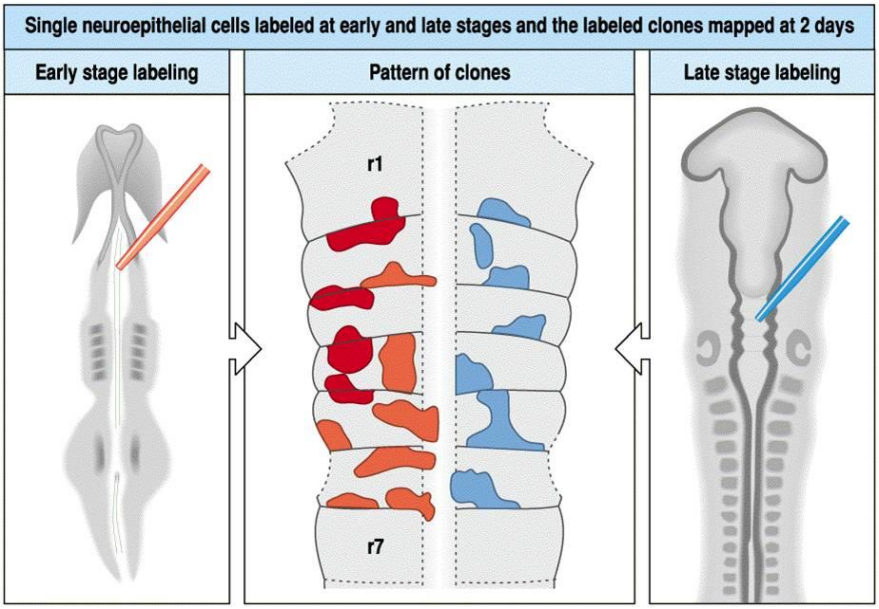

Figure 7. Cell lineage restriction of rhombomeric cells. At the center, representation of a dorsal view of the hindbrain after removal of the roof plate. In the left side of the neural tube, clones generated from single cells marked before the appearance of rhombomeric boundaries (5ss). Red clones do not respect boundaries; orange clones are present in two adjacent rhombomeres. On the right, blue clones generated from single cells traced after morphological boundaries are formed. All clones respect rhombomeric boundaries. Adapted from (Fraser et al., 1990).

Those results were confirmed more recently using genetic-cell tracing (Jimenez-Guri et al., 2010). The strategy was based on the use of knock-in alleles of ubiquitous expression that allowed unrestricted clonal analysis of cell lineage from the two-cell stage to the adult mouse. Combining this analysis with statistical and mathematical tools they showed that there was lineage compartmentalization along the anteroposterior axis from very early stages of mouse embryonic development. (E5.5), indicating that patterning along this axis might involve restrictions of cell dispersion at specific axial positions; probably a cell autonomous mechanism participate to maintain cells separated.

2.5 Boundary refinement leads to correct rhombomere formation

The expression limits of the transcription factors and some of their downstream targets are initially diffuse, but eventually sharpen and prefigure the positions of rhombomeric boundaries. A rhombomere boundary can initially be considered as the interface between adjacent segments; however, a "boundary zone", displaying specific cell types, cell behaviors, histology and gene expression, subsequently develops at particular interfaces between segments (Cooke et al., 2005; Pasini and Wilkinson, 2002). Over the same period, morphological boundaries appear, followed by the expression of boundary-specific markers. How this gradual sharpening of gene-expression occurs, and how boundaries are subsequently maintained, are important questions to our understanding of developmental regionalization.

Sharpening of molecular boundaries can occur mainly by two mechanisms: cells on the "wrong" side of a boundary can switch their identity to that of their neighbors (cell plasticity), or they can move across it by a cell-adhesion based mechanism (cell-sorting) (Cooke and Moens, 2002) (Fig.8).

Cell plasticity

At the beginning of segmentation rhombomeric cells with an initial fate that are located in the boundaries and surrounded by cells of another identity, are able to change their fate due to the contact with the new environment. Several lines of evidence suggest that cell plasticity –the ability of a cell to modulate its segment identity in response to its surroundings- may also play a role. Transplantation or functional experiments have shown that individual cells can readily change their AP identity after transplantation to a different rhombomere (Giudicelli et al., 2001; Schilling and Knight, 2001; Trainor and Krumlauf, 2001; Zhang et al., 2012). In this context the cells stop the expression of one rhombomeric genetic program and switch on another one. This model implies that cells are not fully committed during segmentation and they can change according to their position, via cell-cell interaction or

local signal stimulus. What is the signaling process that drives cells in the wrong segment to change their identity remains to be determined.

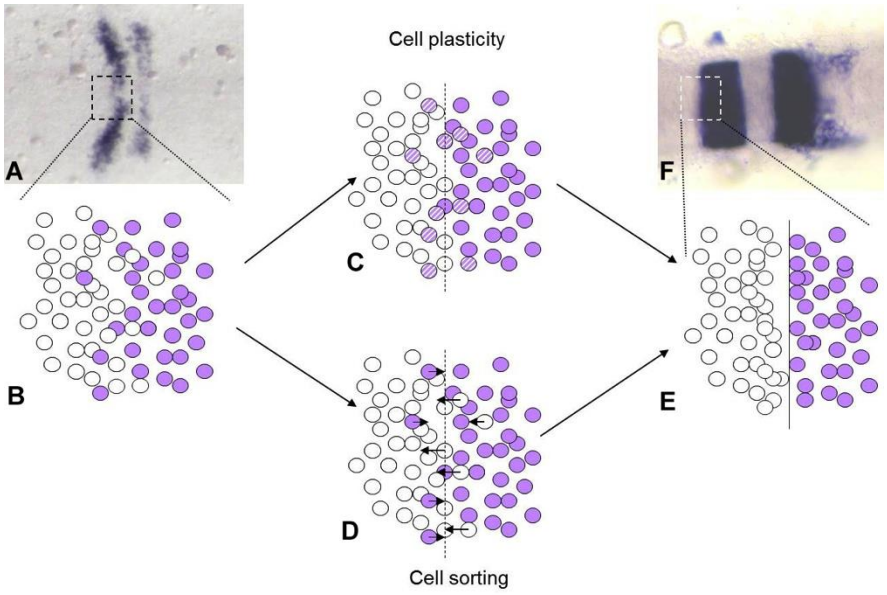

Figure 8. The two proposed models for rhombomeric boundary refinement. In situ hybridization for *krox20* before boundary refinement at 1ss in A), or after at 10ss F), and their windowed parts are schematically represented in B) and E), respectively. Dark violet cells are r3 cells and white cells are r2 cells. C) Cell plasticity, cells of an initial fate influenced by the surrounding territory change their identity: white-r2 cells acquire r3 character and activate *krx20* transcript; dark-violet-r3 cells down-regulate *krx20* gene, both are colored as light violet cells. D) Cell sorting model: cells of specific identity are excluded from the wrong territory and move to the rhombomere where they belong (black arrows). Both models result in a sharped border of rhombomeric-restricted gene expression.

Cell sorting

The other mechanism proposed is based on the cell sorting of rhombomeric cells, meaning that those same cells have the capability to sort out from the territory within cells of another fate. This model involves different cell repulsion/affinity between cells. Eph receptors and their Ephrin ligands are expressed in complementary rhombomere-restricted domains in the hindbrain and interactions between Eph- and Ephrin-expressing cells cause a

repulsive response that is thought to drive cell sorting (Mellitzer et al., 1999; Xu et al., 1999). However, recent results have demonstrated that the main role of EphA4 and EphrinB2 is to promote cell adhesion within the rhombomeres where they are expressed, since cells lacking either protein sort out from cells that express them in mosaic embryos (Cooke et al., 2005; Kemp et al., 2008). How the distinct adhesive and repulsive functions of the Eph/Ephrin system separately contribute to boundary formation is still unknown.

Eph receptors comprise two protein families: EphA and EphB, based on sequence homology and they respectively bind EphrinsA and EphrinsB. Ephrins are transmembrane or GPI-membrane bound ligands, thus Eph/Ephrins signaling requires cell-to-cell interaction.

The EphA receptors bind specifically to Ephrin-A ligands while the EphB receptors bind to Ephrin-B ligands. The only known exception is EphA4 that binds Ephrin-B as well as EphrinA ligands (Cooke et al., 2001).

In the hindbrain *EphA4* is expressed in r3 and r5, *EphB4*a is expressed r2, r3, r5 and r6, while *EphrinB3* is expressed in r2, r4, r6 and *EfnB2* is expressed in r1, r4, r7 (Xu et al., 2000). As seen in Figure 10, the interface between and odd- and even-rhombomeres coincides within the limit of expression of an Eph/Ephrin pair (Fig.9).

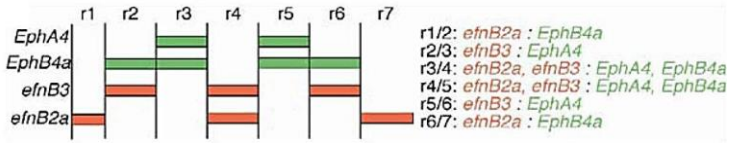

Figure 9. Expression profile of Eph/Ephrin molecules in the hindbrain. Domains of expression of Eph receptors (EphA4 and EphB4a) that bind Ephrin-B types (EphrinB3 and EphrinB2a) in the zebafish hindbrain. Rhombomere boundary is generated at the interface of at least one Eph/Ephrin pair, indicated on the right. From (Cooke et al., 2005).

The role for Eph/Ephrin in boundary formation was initially discovered in *in vitro* assays (Mellitzer et al., 1999; Wizenmann and Lumsden, 1997). Cells of different rhombomeric source (odd- and even-origin) were labeled and mixed in culture, and after a period of incubation even-rhombomeric cells were completely separated from odd-identity ones.

Experiments in zebrafish embryos demonstrated that overexpression of Efnb2 in r3 and r5 causes sorting of these cells to the boundaries (Xu et al., 1999). Moreover, loss-of-function of EphA4 and Efnb2A by morpholinos injection results in unshaped boundaries, incorrect neuronal patterning and loss of boundary cells (Cooke et al., 2005). Cell transplantation experiments showed that EphA4 main role is maintaining the adhesion properties of r3 and r5 (Cooke et al., 2005). Finally, Efnb2A and EphA4 are as well involved in the organization of the neural keel cells during cross-midline cell divisions (Kemp et al., 2009).

3. Genes and morphogenes patterning the AP axis

The segmented rhombomeric structure is the result of gradual patterning. In the neural plate morphogenes released from signaling centers, present in the surrounding tissue and within the neural plate, intervene to instruct the future hindbrain via the activation of specific hindbrain regulatory networks. There is not a restrict hierarchy of functions in this process but it is the mixture of multiple signals that I will try to summarize in this this part.

3.1 Retinoic Acid (RA) is responsible for the initiation of the patterning

Retinoic acid is classical morphogen acting in different cell types and tissues during embryonic development. The source of this morphogen are the tissues expressing the synthetizing enzyme *Raldh1-4* that is released it in the surrounding territories (Duester et al., 2003;Dupe et al., 2003;McCaffery et al., 1991;Niederreither et al., 1997); to counteract that synthesis, members of the RA degradation-*Cyp26* family are expressed in the regions where RA activity has to be inhibited.

Raldh2 is present at somitic stage in the presomitic mesoderm flanking the hindbrain and in the most anterior somites but absent in most caudal region of the embryo; then the *Raldh2*-expressing tissue regresses caudally in the extending vertebrate body axis generating a RA-rostrocaudal dynamic gradient (Begemann et al., 2001;Berggren et al., 1999;Niederreither et al., 1997). Before segmentation all the hindbrain is exposed to that gradient, and as development proceeds only the caudal part is under the influence of RA (Figs.10,12).

In zebrafish a combination of modeling and experimental approaches showed the role of RA gradient during hindbrain development. Implantation of RA-coated beads and cell transplantation in RA-deficient zebrafish embryos demonstrated that RA transmits positional information even at long-range distance (White et al., 2007). It was shown in this work that RA

and FGF synergize to generate a robust patterning, controlling the expression of *Cyp26a1* expression.

Excess to retinoid exposure, before or during neurulation, leads to teratogenic changes in the hindbrain, such as the shortening of the pre-otic region of the hindbrain in the fetus (Morriss, 1972). Similar effects of retinoid exposure, with an apparent loss of the pre-otic hindbrain, were observed in mouse (Morriss-Kay et al., 1991), in *Xenopus* (Durston et al., 1989;Papalopulu et al., 1991) and zebrafish embryos (Holder and Hill, 1991). Retinoid deficiency has the opposite teratogenic effects: in vitamin A deficient (VAD) animal models the posterior hindbrain is anteriorized, but the anterior hindbrain appears normal (Dersch and Zile, 1993;Thompson et al., 1969).*Cyp26* genes are expressed in the anterior hindbrain during development, where they are normally required for patterning. Their depletion causes a posteriorization of the hindbrain, and their overexpression is responsible of the opposite effect (de Roos et al., 1999;Hollemann et al., 1998). Thus, the teratogenic effects of retinoid excess and deficiency seem to be complementary in the hindbrain, targeting predominantly anterior (r1–4) and posterior (r4–8) territories, respectively.

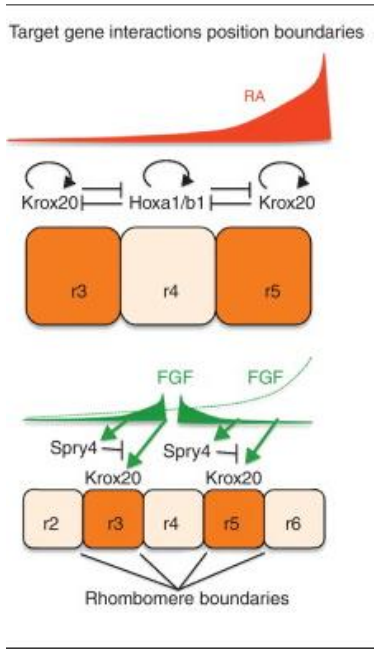

Figure 10. FGFs and RAs gradients in the hindbrain. Models showing the RA gradient (red), cross-inhibition and auto-activation of *Krox20* and *Hoxa1/b1* at boundaries of r3 and r5. This influences the FGF signaling (green), initially from a posterior source and later from r4, and together with Spry4-mediated negative feedback, on *Krox20* induction. From Schilling et al., 2012.

3.2 Fibroblast Growth Factors (FGFs) signaling in the hindbrain

Fibroblast growth factors (FGFs) are another important signaling pathway during hindbrain development.

The principal source of FGFs that instruct the anterior part of hindbrain (r1) is the IsO. The IsO secretes different FGF members (FGF8, FGF17, FGF18) and in particular FGF8 is considered the principal molecule exerting patterning functions (Raible and Brand, 2004). When implanted in rostral mesencephalon or diencephalon embryos FGF-8 coated beads can mimic isthmus effects, by inducing IsO-related genes and generating cerebellar structures (Crossley et al., 1996;Shamim and Mason, 1999). Partial effects are generated when FGF-beads are implanted in the myelencephalon, they can

activate *En2* and *Pax2* related genes but not induce the formation of ectopic structures.

In chick and mouse FGF3 acts alone to instruct the surrounding territory (Lombardo et al., 1998; McKay et al., 1996) and it is dynamically expressed (Mahmood et al., 1995), in chick is initially expressed in pr4-5 (HH9) until the first boundaries are visible (HH15) then it fades in r4 and it is maintained in r5-6; at the same time is started to be expressed in interhombomeric boundaries and once the hindbrain is completely segmented it is maintained in r6 and in all boundaries.

In zebrafish, r4 represents a source of FGFs, since *Fgf3* and *Fgf8* start to be expressed in pr-r4 at the presomitic stage (Maves et al., 2002) and they are maintained until rhombomeric boundaries are visible. *Fgf3* and *Fgf8* pattern the posterior hindbrain and they are involved in inducing and patterning the otic placode (Abello et al., 2010; Kwak et al., 2002; Lecaudey et al., 2007; Leger and Brand, 2002; Maves et al., 2002; Walshe et al., 2002) (Fig.10).

Depletion of only one of the *Fgf* members, analyzing *Fgf3* morphant or *ace* mutant (*Fgf8* hypomorph mutant), does not alter normal hindbrain development; however when both are affected, by co-injection of *Fgf3* and *Fgf8* morpholinos or injection of *Fgf3* morpholino in *ace* mutants, showed defects in rhomboencephalon pattering (Maves et al., 2002). Gain- and loss-of-function approaches for *Fgf3* and *Fgf8* showed requirement of *Fgf8* for expression of *Erm* and *Pea3*, two ETS domain transcription factors that are direct targets of the activity of the FGF pathway (Raible and Brand, 2001).

FGFs are required to specify rhombomeres close to r4, in particular r5 and r6 and also for correct neural development, since their overexpression induces ectopic *Krox20* and *val/Kreisler* (Marin and Charnay, 2000; Maves et al., 2002) and indirectly induce *Hox* genes (Aragon et al., 2005; Aragon and Pujades, 2009).

During development of the hindbrain FGFs activity is progressively restricted to stripes at the centers of the rhombomeres, where it becomes necessary for neural specification of oligodendrocyte progenitors and astroglia through the regulation of *Sox9*, a gliogenic transcription factor the function of which we show to be conserved in the zebrafish hindbrain (Esain et al., 2010) (Fig.10).

3.3 Anteroposterior identity is given by *Hox* genes

Hox proteins are helix-loop-helix transcription factors encoded by related *Hox* family genes organized in different chromosomic clusters. *Hox* genes regulate the specification of AP positional cell identity in different species during embryonic development (Krumlauf, 1994;McGinnis and Krumlauf, 1992).

Their regulation respect the so-called spatial and temporal colinearity: the position of the *Hox* gene within the cluster correlates with the time and the domain of expression in the embryo (Duboule and Dolle, 1989); posterior compartments express more *Hox* genes compared to the anterior ones and that different combination confers AP identity.

In the hindbrain the AP borders of *Hox* gene expression are tightly linked to rhombomeric segments (Figs.11-12) (Keynes and Krumlauf, 1994; Lumsden and Krumlauf, 1996; Maconochie et al., 1996). *Hox* genes within a given paralogous group (PG) generally have the same boundaries of gene expression. Thus, members from *Hox* groups 2, 3, and 4 have anterior borders that map to the r2/r3, r4/r5, and r6/r7 boundaries, respectively.

Loss-of-function of *Hox* genes in vertebrates leads to partial homeotic transformations of the hindbrain, and gain-of-function leads to the opposite effect, thus the caudalization of anterior rhombomeres (Barrow and Capecchi, 1996; Bell et al., 1999; Carpenter et al., 1993; Chisaka and Capecchi, 1991; Chisaka et al., 1992; Gavalas et al., 1997; Gendron-Maguire

et al., 1993; Goddard et al., 1996; Rijli et al., 1993; Studer et al., 1998). These partial effects compared with fully homeotic changes in Drosophila mutants can be explained by the redundancy of *Hox* genes of the same paralogous group expressed in the same rhombomere.

Several evidences demonstrated that the initiation of *Hox* expression implies the RA and FGFs pathways. In support to that, regulatory studies indicate that RA directly activates some *Hox* genes: *Hoxa1*, *Hoxb1*, *Hoxa4*, *Hoxb4*, and *Hoxd4* genes though the RA-Response Elements (RAREs) located in the regulatory regions of the *Hox* genes (Marshall et al., 1994;Packer et al., 1998; Studer et al., 1998; Zhang et al., 2000).

Hox transcription factors interact always with the TALE superfamily cofactors to regulate gene expression. This family include: i) the MEIS subfamily to which belong *Meis* and *Prep* in vertebrates, and *Hth* in Drosophila (Kurant et al., 1998; Moskow et al., 1995; Rieckhof et al., 1997); and ii) Drosophila *Exd* and vertebrate *Pbx1-4*, members of the polycomb superfamily (Monica et al., 1991; Popperl et al., 2000).

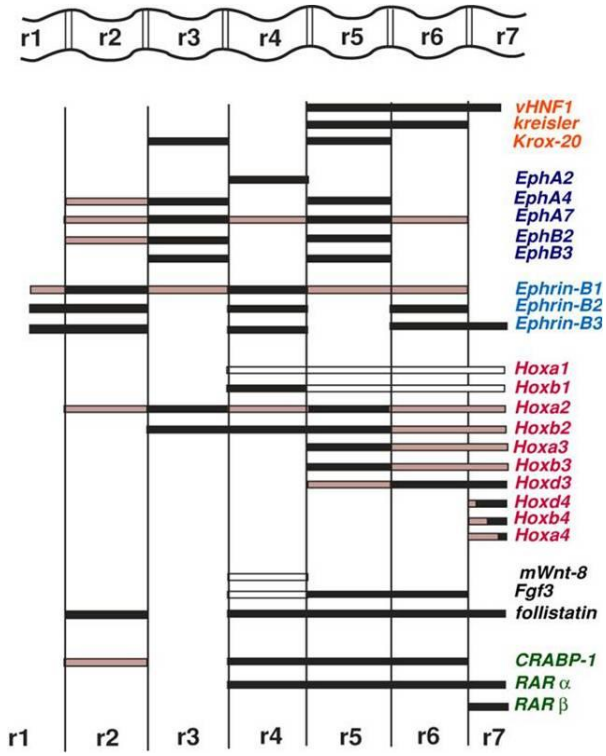

Figure 11. Segmental gene expression in the hindbrain. Rhombomeric boundaries are represented on the top. The shading of the rectangles represents the relative levels of gene expression at 9dpc mouse embryo. Absence of shedding indicates that expression is transient in that region and by this stage it has been down-regulated. On the right the list of the genes segmentally expressed grouped by families or by function. Modified from (Schneider-Maunoury et al., 1998).

3.4 Other transcription factor involved in hindbrain segmentation

3.4.1 *vHnf1* confers caudal character to the hindbrain

vHnf1 (variant hepatocyte nuclear factor is a homeodomain transcription factor transiently expressed in the caudal hindbrain (Aragon et al., 2005) (Figs.11-12). In the zebrafish, FGF and RA signalling activate the expression of *vHnf1* in the presumptive r5 and r6 (Hernandez et al., 2004), through the RARE elements located in the fourth intron of *vHnf1* gene (Pouilhe et al., 2007).

Gain-of-function of *vHnf1* results in activation of r5-r6 specific genes by repressing r4 genes (Aragon et al., 2005; Wiellette and Sive, 2003) and this is done directly through FGF3 MAPK signalling (Aragon and Pujades, 2009). Conversely, depletion of *vHnf1* results in posterior expansion of *hoxb1* whereas *krx20* expression is reduced in r5, and expression of *Kreisler* (*valentino*) in r5 and r6 is abolished (Sun and Hopkins, 2001). Experiments made in mouse have shown that *vHnf1* regulates expression in r5 and r6 by directly binding to the *Kreisler* gene and two *Kreisler*-binding sites are responsible of the *vHnf1* expression in r5 and r6, demonstrating that a direct positive feedback is formed by *Kreisler* and *vHnf1* (Kim et al., 2005).

vHnf1 is involved as well in the establishment of the r4/r5 boundary. r4/r5 boundary is positioned by the complementary expression of two homeobox genes that converge at a common border that is the prospective r4/r5 boundary: a member of the *Iroquois (Irx)* gene family is expressed anterior to r4/r5 boundary while *vHnf1* is expressed posteriorly. In zebrafish, the r4/r5 boundary forms at the interface between the expression territories of *irx7* rostrally and *vhnf1* caudally. Functional experiments demonstrated that these two transcription factors position the boundary by mutual repression (Lecaudey et al., 2004). In mice, the *vHnf1* function is conserved but *Irx3* is the *Irx* gene involved in the establishment of the r4/r5 boundary, and *vHnf1*-/- mutants display a posterior expansion of *Irx3* (Sirbu et al., 2005). *Irx/Hnf1* gene pair responsible for r4/r5 boundary formation was evolutionary conserved in vertebrates, since *IrxA* is expressed in the anterior hindbrain from r1-r4, and *hnf1* is expressed in the posterior hindbrain, in an identical manner to that seen in other vertebrates (Jimenez-Guri and Pujades, 2011).

3.4.2 *MafB/Kreisler* specifies r5-r6

MafB/Kreisler is a member of the MAF leucine zipper-containing transcriptional factors (Kataoka et al., 1994) and its orthologue in zebrafish is called *valentino* (*Val*) (Moens et al., 1996). *MafB/Kreisler* is early expressed in the prospective r5-r6 territory and is maintained in r5 and r6 once these rhombomeres are established (Eichmann et al., 1997) (Figs.11-12).

MafB/kreisler confers caudal identity to r5 and r6 by regulating other AP positional identity genes. Gene regulation analyses showed that *MafB/Kreisler* activates *Hoxa3* and *Hoxb3* in r5 and r6 by directly binding to the their promoters (Krumlauf et al., 1997; Manzanares et al., 1999; Manzanares et al., 2001), in co-operation with *Krox20* (Manzanares et al., 2002). *MafB* mutation in mouse is classically known as *Kreisler* (Cordes and Barsh, 1994) and it is characterized by the lack of morphological segmentation posterior to r3/r4 boundary (McKay et al., 1994). The r5-r6 region is reduced in size and the expression of different rhombomeric-restricted genes is altered (Cordes and Barsh, 1994; McKay et al., 1994). *Krox20* expression is lost while *Hoxb1* is expanded caudally from r4 (Frohman et al., 1993; McKay et al., 1994). Conversely, ectopic expression of *MafB* in r4 results in a *Hoxb1* downregulation, suggesting that in in r5 and r6 *MafB* represses *Hoxb1* (Giudicelli et al., 2003). Inactivation of *val* in zebrafish also leads to loss of segmentation posterior to r3/r4, defects in otic development and a reduced and misspecified r5-r6 territory (Kwak et al., 2002; Moens et al., 1996; Prince et al., 1998).

Ectopic expression of *MafB* in chick demonstrates that *MafB* is able to induce its own expression in a cell-autonomous manner in territories caudal to the r2/r3 boundary, suggesting that once *MafB* is induced it maintains its own expression in the caudal hindbrain (Giudicelli et al., 2003).

Recently, functional analysis of the *vHnf1* regulatory regions in mouse suggested that this gene can be directly regulated by *MafB* (Pouilhe et al.,

2007). *MafB* expression in the caudal hindbrain is dependent on FGF signals and *vHnf1* expression (Aragon et al., 2005; Hernandez et al., 2004; Kim et al., 2005; Marin and Charnay, 2000; Wiellette and Sive, 2003) .

3.4.3 *Krox20* is responsible for the segmentation of r3 and r5

Krox20 is a zinc finger transcription factor expressed early during development in the presumptive r3 and r5 of the hindbrain and then maintained once r3 and r5 are established (Figs.11-12)). The analysis of *Krox20* null mice reveals that those territories are formed but are progressively eliminated, suggesting that this gene is fundamental for r3 and r5 maintenance (Schneider-Maunoury et al., 1997; Voiculescu et al., 2001). The loss of these segments results in the absence of axonal projections and in the adjacent-rhombomere normal development. *Krox20* synergizes with *Hoxa1* to specify r3 character (Helmbacher et al., 1998).

Krox20 confers odd-identity to the hindbrain territories and also directly regulates *Hoxb2*, *Hoxa2* in r3 and r5 and it promotes the expression of *Hoxb3* only in r5 (Maconochie et al., 1996;Nonchev et al., 1996). *Krox20* directly regulates *EphA4*, a member of Eph-receptor family, involved in the adhesion properties of odd-rhombomeres (Manzanares et al., 2002). *Krox20* also acts as a negative regulator and it represses *Hoxb1* expression in r3 (Garcia-Dominguez et al., 2006).

Krox20 activation is the result of the integration of the inputs from different signalling pathways, such as Wnt, RA and FGF, but also from the activity of several transcription factors (Aragon et al., 2005; Chomette et al., 2006; Marin and Charnay, 2000; Wiellette and Sive, 2003).

In zebrafish and chick, FGF signalling is necessary to activate the appropriate onset of *Krox20* expression (Aragon and Pujades, 2009; Walshe et al., 2002), through the action of Sprouty gene 4 (*Spry4*), FGF negative-feedback regulators (Labalette et al., 2011).

In r5, *vHnf1* and *MafB* initiate *Krox20* expression (Wiellette and Sive, 2003) and then it is maintained by an autoregulatory loop (Chomette et al., 2006; Giudicelli et al., 2001). It was shown that both cell-autonomous and non cell-autonomous mechanisms contribute to the recruitment of cells to r3 and r5 (Giudicelli et al., 2001; Voiculescu et al., 2001). *Krox20* is activated by *Hoxb1* in r3-r4 border (Wassef et al., 2008) and also *Hox/Pbx* proteins intervene in its expression (Chomette et al., 2006; Wassef et al., 2008). In zebrafish *Iro7* and *Meis1.1* are responsible for *Krox20* regulation in r3 (Stedman et al., 2009).

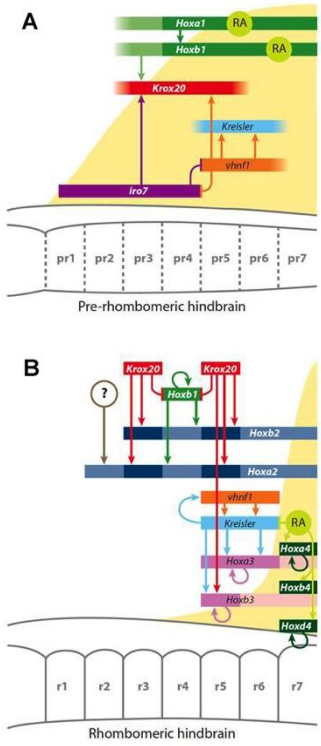

Figure 12. Gene regulatory network involved in the patterning of the hindbrain. A) Before the appearance of the rhombomeres. Retinoic gradient (RA) is represented by yellow background produced by Raldh2 enzyme expressed in the somites flanking caudal hindbrain. *Hoxa1* and *Hoxb1* (green) expression is activated by RA. *Hoxb1* induces *Krox20* (red) expression in the presumptive r3. In zebrafish, mutual repression of *iro7* (purple) and *vhnf1* (orange) divides the anterior and posterior hindbrain. *vhnf1* induces *kreisler* expression and both transcription factors synergize to activate *krox20* in presumptive r5 (pr5). B) Gene regulatory network once rhombomeres appear. Borders of gene expression coincide with segmentation.

Krox20 and *Hoxb1* expression patterns become localized to specific rhombomeres and *Hoxa1* expression is switched off. The expression of *Hox* genes is mediated by a crossregulatory loop: *Hoxb1* regulates group 2 paralogues (dark blue) expression in r4); upstream regulators like *Krox20* and *Kreisler* and in response to RA (group 4 paralogues in dark green). RA domain has been posteriorized. Darker blue shading indicates that several *Hox* genes display higher levels of expression in different rhombomeres: *Hoxb2*, *Hoxa2* in r3 and r5. Different *Hox* genes autoregulate (circular arrows). From (Alexander et al., 2009).

4. Embryonic compartments and boundaries

The generation of a compartment is strictly linked to the formation of boundaries. Two types of boundaries can be described in undifferentiated tissues, depending on what the cells do upon perturbation. Cells can freely move across the borders, adopting the fate of the other compartment so we will refer to **non-lineage boundary** and in this case the fate determination requires continuous external signal that directs cells in changing fate but maintaining the integrity of the boundary and a posterior physical restriction can intervene to restrict cell mixing. Conversely, the cells can inherit the fate and there is no requirement of external instruction, in this cases the cell intermingling and has to be restricted and the boundary has to be maintained by a mechanism present in the undifferentiated tissue to counteract the major deformations that can suffer the tissue: morphogenesis and cell division. This type of **lineage-boundaries**, also called compartment boundaries, was identified in insects by lineage experiments (Garcia-Bellido et al., 1973; Lawrence, 1973). Doing genetic mosaics during early development clones derived from those marked cells never crossed the borderline in the adult structure, and defined the so-called compartment. Subsequently it was demonstrated that gene expression domain defined the compartment (Kornberg et al., 1985).

4.1 Compartments and boundaries in *D. melanogaster*

In *D. melanogaster*, the discovery of compartment boundaries generated the rationale that genes define the territory where they are expressed and that confers identity to the cells belonging to it. They were called 'selector genes' (Garcia-Bellido et al., 1973). Their depletion eliminates that territory and their ectopic expression can give identity to the cells expressing it.

The best example of a selector gene is *Engrailed*, a homeodomain-cointaning transcription factor that is specifically expressed in the posterior segment

both in the embryonic ectoderm and in the imaginal wing disc. Its expression is complementary to *Invected* domain (Garcia-Bellido and Santamaria, 1972) (Fig.13). In the AP boundary region of the wing imaginal disc a cell-lineage restriction boundary population is formed, which is able to instruct the closest territory by the expression of the morphogen Decapentaplegic (dpp) (Capdevila et al., 1994; Lecuit et al., 1996; Nellen et al., 1996).

The wing imaginal disc is compartmentalized also along the DV axis. Hh activity regulates the expression of *wg* and *vein* (*vn*), an EGFR ligand, in a group of cells in the most ventral and the most dorsal part of the A compartment, respectively. *vn* is a morphogene that diffuses and generates a gradient that maintains its own expression and also activates *apterous* (*ap*) (Basler and Struhl, 1994; Simcox et al., 1996). This gene represents another selector gene expressed in the dorsal segment that confers dorsal character and avoids the cell intermingling with ventral cells (Milan et al., 2001).

The dorsal segment of the wing disc expresses *fringe*, a Notch modulator, controlled by Apterous, that in turn activates Notch ligands *delta* (*dl*) and *serrate* (*ser*) respectively in the ventral and the dorsal part of the boundary, via lateral inhibition (de Celis et al., 1996; Diaz-Benjumea and Cohen, 1993). After the establishment of the boundary, boundary cells express another morphogen, wingless (wg), which controls the wing margin patterning (de Celis et al., 1996; Diaz-Benjumea and Cohen, 1993; Micchelli et al., 1997).

Recently*, in silico* and *in vivo* approaches have modeled and tested regulatory network responsible for DV patterning and unveiled a new property for the formation of boundary cells: refractoriness. The cells at the DV border display high levels of Notch pathway that, via Cut protein, makes them become refractory to wg signaling (Buceta et al., 2007; Canela-Xandri et al., 2008). This is necessary for correct formation of DV boundary.

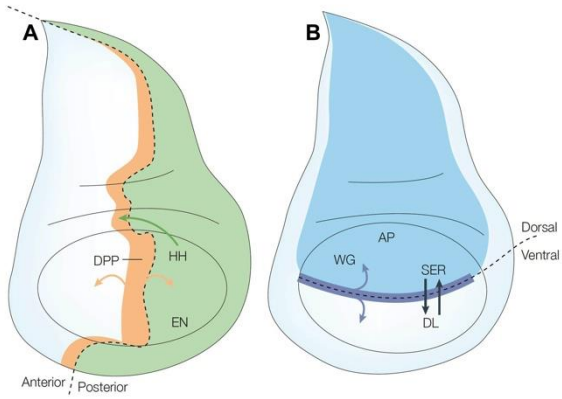

Figure 13. Compartments and local centers in the wing imaginal disc. a) The developing wing is subdivided in AP lineage-restriction boundary expressing Decapentaplegic (DPP, orange). Posterior segment expresses *Engrailed* that activates Hedgehog signaling. HH is responsible of boundary formation. b) Dorsal compartment express *Apterous* (light blue) responsible of the Delta and Serrate Notch-ligands at the DV boundary (dark blue). DV boundary expresses wingless (WG) morphogen that regulates patterning of the wing margin. From (Kiecker and Lumsden, 2005).

4.2 Forebrain boundaries in the vertebrate CNS

Like the hindbrain, the forebrain is characterized by the presence of bulges and constrictions. Analyzing the morphology and the expression profiles of several neural markers it was initially proposed that the forebrain was composed by six lineage-compartments, the prosomeres. The posterior three (p1-p3) form the diencephalon whereas the anterior ones (p4-p6) represent hypothalamus and telencephalon (Reichert, 2002). However, fate-mapping analysis demonstrated that between the three prosomeres cells are able to cross the supposed boundary between the prosomeres showing that there is no cell lineage restriction (Larsen et al., 2001) evidence were published for anteroposterior lineage restriction These results led to the conclusion that the only lineage-boundaries in the forebrain are: the Pallial-Subpallial Boundary (PSB), between the cortex and the lateral ganglionic eminence; the Diencephalon-Midbrain Boundary (DMB); the border between the thalamic and prethalamic primordial called Zona Limitans Intrathalamica (ZLI); and the mid-hindbrain boundary (MHB) (Fig.14).

In particular ZLI is much closer to a compartment than to a boundary (Larsen et al., 2001); the presumptive ZLI (prZLi) territory is characterized by a gap of lunatic fringe (*Lfng*) expression in the forebrain but prZLI is positive for *Wnt8b*, subsequently narrower and it forms the definitive ZLI marked by *Shh* expression (Zeltser et al., 2001).

4.3 Somites are generated by a clock and wavefront mechanism.

In a vertebrate developing embryo, the presomitic mesoderm (PSM) is subdivided in somites, bilaterally blocks of epithelial cells deposited close to the neural tube in the anteroposterior axis. Somites will form skeletal muscle, cartilage, tendons, endothelial cells and dermis (Benazeraf and Pourquie, 2013; Gossler and Hrabe de Angelis, 1998).

The somitogenesis requires a molecular mechanism driven by a molecular oscillator: the 'segmentation clock'. The cells display a periodic expression of Notch-pathway genes, called cyclic-genes; they appear as a wave of transcription sweeping along the PSM in a caudo-rostral progression during the formation of each somite (Cooke, 1981; Dequeant and Pourquie, 2008).

The *Tbx6* transcription factor is homogenously expressed in all PSM anteriorly limited by the previous generated somite and this anterior border represents the wavefront (Oginuma et al., 2008; Yasuhiko et al., 2008). Notch is oscillatory expressed in the PSM and it represents the clock (Maroto and Pourquie, 2001). Once the Notch receptor (*Notch1* and/or *Notch2*) is activated in the posterior half of the prospective somite, the signal is transduced to the ubiquitously expressed RBPJk, which in turn activates the potential bHLH target genes *Mesp1*, *Mesp2* and *Hes5* (Morimoto et al., 2005; Morimoto et al., 2007; Takahashi et al., 2010). Mesp2 is the central transcription factor in new somite formation. During each cycle of somite formation, in the anterior limit of *Tbx6* expression, *Tbx6* and the temporal pulse of Notch activates *Mesp2* that in turn activates *Ripply* (Kawamura et al., 2005; Morimoto et al., 2007; Takahashi et al., 2010), which repress the same

Mesp2 in the forming somite and *Tbx6* in all the forming somite (Takahashi et al., 2010).

In this way the *Tbx6* switch off moves the anterior limit of the wavefront posteriorly, in order to generate a new round of somite formation. *Mesp2* activates *Lfng* in the rostral half of the somite, which in turn suppresses Notch activity and this causes the direct oscillation of this pathway. This gene is also responsible for the activation of *EphA4* (Nakajima et al., 2006; Nomura-Kitabayashi et al., 2002), which is responsible for the appearance of morphological boundaries in the somites. This is done by the interaction with *Ephrin2,* expressed in the caudal half of the anterior somite (Julich et al., 2009). *Mesp2* can be seen as a non-lineage boundary selector gene for the rostral somite

4.4 Boundary cells acting as secondary organizers: the Mid-Hindbrain Boundary (MHB)

The stabilization of signalling centres that instruct surrounding territories is a fundamental feature of compartment boundaries. The boundary between the midbrain and the hindbrain (MHB), plays a central role for the correct development for the midbrain and the cerebellum (Liu and Joyner, 2001; Raible and Brand, 2004; Wurst and Bally-Cuif, 2001). This boundary is also called isthmic organizer (IsO) (Fig.14).

The MHB is established at the interface of the expression domains of the homeobox genes *Otx2,* expressed in presumptive forebrain and midbrain, and *Gbx2* (expressed in the anterior hindbrain). Functional studies demonstrated that *Gbx2/Otx2* mutually repress to establish and maintain the MHB. Cell-tracing experiments combined with gene expression pattern at single-cell level during midbrain and hindbrain segregation demonstrated that MHB consist in a lineage-restricted boundary (Langenberg and Brand, 2005).

MHB was considered to be the only organizer in the developing CNS, since cell transplantation of the MHB into ectopic parts of the neural tube results in the induction of midbrain and cerebellum, and the implantation of beads soaked with FGF8 mimics the effect of the MHB (Crossley et al., 1996). Like the gastrula organizer, the MHB can induce cellular fates in a non-autonomous manner (Sato et al., 2001). Studies made in *Fgf8* mutant mice and zebrafish confirm the essential role of FGF8 in the correct generation of midbrain and hindbrain (Chi et al., 2003; Reifers et al., 1998). Although transplantation experiments showed organizing functions of the MHB, they revealed that the competence to respond to MHB-signals is posterior to the ZLI (Kobayashi et al., 2002).

Wnt1 is another signalling factor that was initially thought to have the same role of FGF8. Its expression is present thought the midbrain and then it becomes restricted to the MHB, overlapping *Fgf8* domain. Dramatic midbrain defects are found in *Wnt1* mutant mice, but the ectopic expression of this gene does not show the effects of FGFs (Liu and Joyner, 2001; Wurst and Bally-Cuif, 2001).

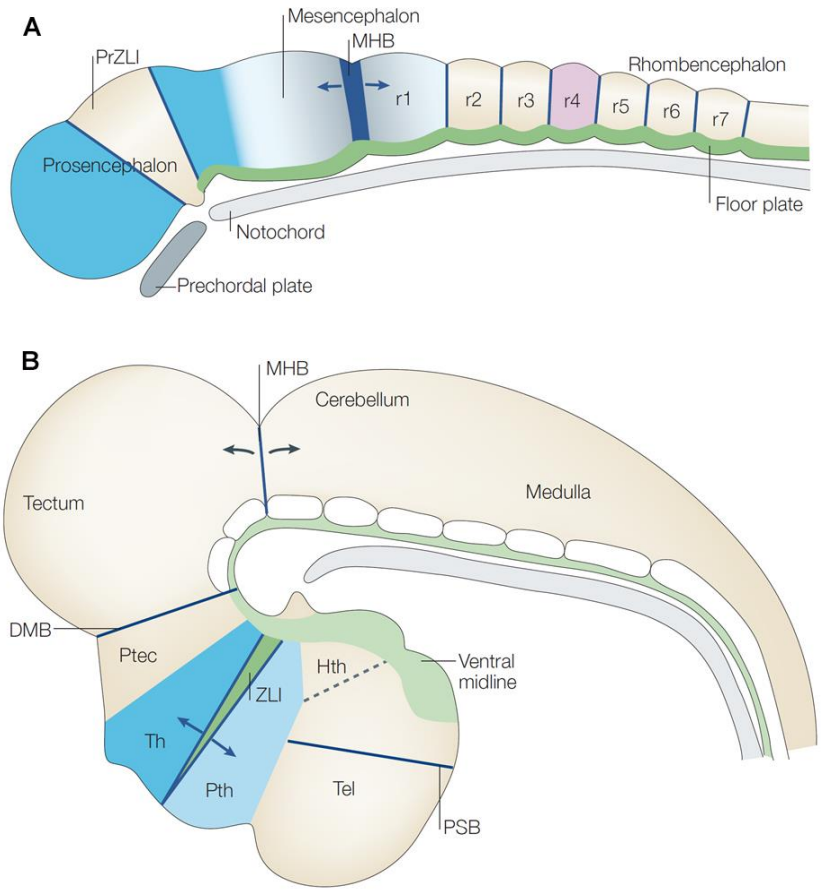

Figure 14. Boundaries and local signaling centers in the developing CNS. Lateral view of chick embryonic brain. a) In HH13 chick embryos are visible: anterior and posterior borders of the presumptive zona limitans intrathalamica (PrZLI), mid-hindbrain boundary (MHB) and interhombomeric boundaries (r1-r7). MHB and r4 and hindbrain boundaries act as signalling centers. b) Stage HH-24 embryo Other compartment boundaries appear: pallial-subpallial boundary (PSB), diencephalon-midbrain boundary (DMB) but interhombomeric boundaries disappeared. Major local signalling centers at this stage are ZLI and MHB. Anterior to the left, dorsal to the top. Arrows represent bidirectional signals. Hth, hypothalamus; Ptec, pretectum; Pth, prethalamus; Tel, telencephalon; Th, thalamus. From Kiecker and Lumsden, 2005.

4.5 Hindbrain boundaries and the boundary cell population

Once the molecular rhombomeric borders are refined and the hindbrain is segmented, a new cell population arises at the interface between adjacent

rhombomeres, the **boundary cell population** (Fig.14a). They showed a characteristic triangular-elongated cell shape and express specific molecular markers such as *Rfng, Foxb1.2* and *Sema2a*, and they are sources of signaling molecules such as *Wnt1* (Amoyel et al., 2005) and signaling centers (Gonzalez-Quevedo et al., 2010; Terriente et al., 2012). However, their fate is still unknown.

It is controversial which is the molecular mechanism responsible for the correct formation of boundary cells: evidences in zebrafish suggested that the Notch pathway is involved in boundary cell affinity and their segregation into the boundaries (Cheng et al., 2004). The Eph/Ephrin system can also have a role in boundary cell generation. Ephs and Ephrins are expressed in complementary rhombomere-restricted domains, each segment boundary forms at the interface between one or more receptor-ligand pair. Interestingly, Epha4/Ephrinb2a-double morphant zebrafish embryos showed the complete absence of *Rfng*-boundary marker (Cooke et al., 2005). The authors suggest that Eph/Ephrin signaling at interhombomeric boundaries can let the cells juxtaposed into the borders differentiate into boundary cells.

Boundary cells have a reduced cell proliferation and reduced interkinetic nuclear migration (INM), which let to conclude that the role of boundary cells can be to stabilize rhombomeric borders (Amoyel et al., 2005; Guthrie and Lumsden, 1991; Guthrie et al., 1991; Heyman et al., 1993; Heyman et al., 1995; Lumsden and Keynes, 1989; Sela-Donenfeld et al., 2009).

An alternative role for boundaries would be the anteroposterior organization of neurogenesis in the hindbrain (Hanneman et al., 1988; Metcalfe et al., 1986; Trevarrow et al., 1990). In fact, primary reticulospinal neurons are generated at rhombomeric centre, glial cells developed close to boundaries, so boundaries can have a role regulating position and cell differentiation acting as signaling centers.

Boundary cells express *Radical fringe* (*Rfng*) a modulator of Notch pathway, which prevents neurogenesis of the same boundary cells and activates *Delta* expression in non-boundary region by lateral induction (Cheng et al., 2004; Qiu et al., 2004). This role it was confirmed recently by other evidences where it was showed that boundaries are able to instruct the fate of surrounding cells by the expression of morphogen wnt1, activating *Rfng* (Cheng et al., 2004). Knock-down of Wnt pathway components by morpholinos showed that Wnt signaling is important for the integrity of the boundaries and neurogenesis patterning of the rhombomeres (Amoyel et al., 2005; Dorsky et al., 2003; Riley et al., 2004).

Recently it was also shown that rhombomeric boundaries express two semaphorins (*Sema3fb* and *Sema3gb*) that are required for maintaining the spatial organization of the entire hindbrain by correctly positioning neuronal populations (Gonzalez-Quevedo et al., 2010), which in turn are fundamental for patterning neurogenesis (Terriente et al., 2012).

5. Molecular mechanisms of boundary refinement

The process of compartmentalization first involves formation of an interface between adjacent segments, and this is followed by the induction of a specialized population of boundary cells at the interface that act as signaling center further patterning the tissue. There has been significant progress in uncovering mechanisms that underlie the segregation of cell populations and formation of boundaries.

Boundary formation can be caused by repulsion of cells of different type, cells that find themselves in another territory actively move to the one where they belong by selectively affinity (Steinberg and Gilbert, 2004). Another situation is the one where the cells display a non-directional movement that enables them to experience several cell-contacts and cell adhesion differences produce forces that generate segregation (Steinberg, 1963). In general this represents the formal difference between cell repulsion and cell affinity; however, both mechanisms can be driven by different molecular pathways.

Independently of which is the cellular mechanism that lead to the generation of the linear and sharp boundary, after hedge refinement the cells are no more freely to cross the borders even changing fate. Thus, it needs to be a mechanism to maintain the boundary upon tissue deformation, which normally are morphogenesis and cell division.

Three are the main mechanisms described in boundary formation and maintenance. The first was already introduced in the previous chapter and is about Eph/Ephrin signaling, the second involves the cadherin-mediated adhesiveness, and the third is based on the cell cortex tension generated by actomyosin contraction.

5.1 Eph/Ephrin signaling

In two adjacent cells Eph/Ephrin interaction activates the bi-directional signal transduction into both the Eph receptor cell (a process called "forward signaling") and the ligand cell ("reverse signaling"), and both of them (Pitulescu and Adams, 2010). The involve phosphorylation of tyrosine sites in the intracellular domain. Forward ephrinBs reverse signal leads to the phosphorylation of the C-terminal PDZ motif, the binding to cytoplasmic adapters and PDZ proteins. This cytoplasmic domain is not present in EphrinAs, which activate the downstram cascade of Src family kinases (SFKs) and phosphoinositide 3-kinase (PI3K), involving the co-receptor transduction (Davy et al., 1999; Davy and Robbins, 2000) (Fig.15b). It has been shown that TrkB and p75 neutrophin receptor act as co-receptors and after cis-interaction with EphrinA they increase their intracellular signal (Marler et al., 2008).

Eph and ephrin molecules can *cis*-interact in the same cell, this type of binding can be linked to interfering with the interaction with ligand presented on adjacent cell (Carvalho et al., 2006). This mechanism has been proposed to be involved in the developing visual system where the establishment of a gradient of signaling-competent receptor can be generated by the partial co-expression of EphAs and EphrinAs (Carvalho et al., 2006; Flanagan, 2006; Hornberger et al., 1999).

Bidirectional signal regulates different biological processes such as: differentiation, proliferation and cell migration. The Eph/Ephrin interaction can lead to repulsive signal that generate segregation of two initially mixed Eph- and ephrin-expressing cells, like previously explained in the case of the hindbrain (Fig.15c).

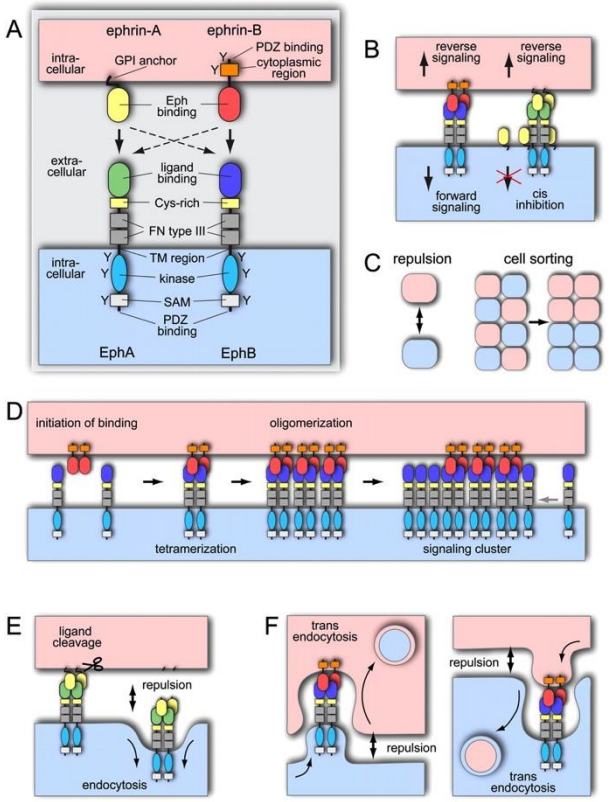

Figure 15. Eph/Ephrin structure, signaling and mechanism of action. A) Structure of Eph-receptors and ephrin-ligands. Cysteine (Cys)-rich, fibronectin (FN) type III, SAM domains, transmembrane (TM) regions and tyrosine phosphorylation sites (Y) are indicated. EphA receptors typically bind ephrin-A (GPI-anchored ligands) and EphB receptors bind ephrin-Bs (arrows). B) Eph/Ephrin interactions: trans-activating bidirectional signal. Cis-interaction impairs transduction of signal. C) Eph/Ephrin interaction result in repulsive signal important for cell migration and cell sorting. D) Eph/Ephrin proteins form heterotetramers to initiate the signal oligomerization, they expands laterally through Eph/Ephrin cis-interaction. E) EphA/ephrinA interaction leads to association of metalloprotease which cleavages the ligand, mediates endocytosis of the complex and end the cell-to-cell interaction. F) Eph/Ephrin can generate repulsion also by trans-endocytosis of the complexes in both forward or reverse directions. From Pitulescu and Adams, 2010.

The role of Eph/Ephrin system in cell segregation *in vivo* has been described in different tissues during development (Gale et al., 1996). Complementary expression of Eph receptor and ephrin ligand is found in other developing tissues where a boundary refinement is discovered, like in somitogenesis

(Barrios et al., 2003; Julich et al., 2009) and limb cell segregation (Compagni et al., 2003; Davy et al., 2004).

Eph and ephrin molecules can undergo *trans*-endocytosis (Fig.15f). This was proposed to mediate cell repulsion of Eph-receptor and Ephrin-cell. After Eph/Ephrin binding of two adjacent cells, the receptor-ligand complex can be internalized into the Eph- or Ephrin-expressing cell and this can result in the ending of the cell-adhesion (Lauterbach and Klein, 2006; Mann et al., 2003; Marston et al., 2003; Zimmer et al., 2003) (Fig.15f).

5.1.1. Eph/Ephrin pathway in integrin clustering and activation during somitogenesis

In the presomitic mesoderm Eph/Ephrin signaling is involved in the epithelialization of mesenchimal cells (Barrios et al., 2003). EphA4 is expressed in the anterior half and EphrinB2 in the posterior half of the generating somites. Within the tissue, interplay between Eph/Ephrin signaling and ligand-independent integrin clustering drives restriction of de novo ECM production to somite boundaries (Julich et al., 2009). The intersomitic boundary is stabilized by an integrin α5-dependent accumulation of fibronectin matrix (Julich et al., 2005; Koshida et al., 2005). The receptor-ligand interaction leads the phosphorylation of cytoplasmic domain of EphA4 and this causes the clustering and activation of Integrin α5 in the surface of contact between the two cell populations. The integrin clustering generates the accumulation and polymerization of fibronectin matrix fibers in the extracellular space that it will behave as physical barrier, avoiding cell intermingling between two different somites (Julich et al., 2009) (Fig.16).

These findings demonstrate that initially Eph/Ephrin interactions refine boundaries and then they recruit extracellular matrix to maintain cell populations segregated.

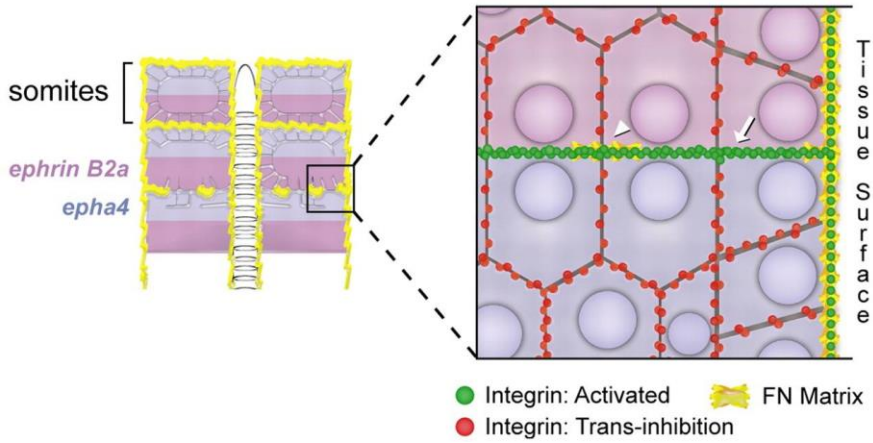

Figure 16. Model of Itgα5 activation and FN matrix assembly along somite borders in zebrafish. Itgα5 is trans-inhibited in a non-cell autonomous way within the cells of the same forming somite (red); but it is activated (green) in the contact surface of two adjacent somites allowing the coating of the paraxial mesoderm with FN matrix (yellow). Itgα5 is activated at the interface of the *Ephrinb2a*- and *EphA4*-expression domains. EphA4 highest activation leads to Itgα5 clustering and subsequent FN matrix assembly (arrowheads). From Julich et al., 2009.

5.1.2 Eph/Ephrin signaling in adhesiveness

Another mechanism by which Eph/Ephrin signaling can drive segregation is that cell repulsion creates differential adhesion between cells of different compartments (Steinberg, 2007) by controlling the subcellular localization of E-cadherin (Cortina et al., 2007) (Fig.17).

EphB receptors interact with E-cadherin and with the metalloproteinase ADAM10 at sites of adhesion. Their activation induces shedding of E-cadherin by ADAM10 at interfaces with EphrinB-expressing cells. This process results in asymmetric localization of E-cadherin and, as a consequence, in differences in cell affinity between EphB-positive and ephrinB-positive cells (Hattori et al., 2000; Janes et al., 2005). Recent studies in epithelial cells revealed a mechanism by which EphB/EphrinB interactions regulate the formation of E-cadherin-based adhesions: when mixing EphB3- and B1-expressing cell populations *in vitro*, upon

EphB3/EphrinB1 binding ADAM10 metalloproteinase is recruited in the contact surface of between the cells of the different populations (Solanas et al., 2011) (Fig.17). ADAM10 is responsible of the cleavage of E-cadherin interacting with the two cells and it causes differential adhesion and contributing to cell segregation of the two cell populations. Moreover the expression of dominant-negative ADAM10 in the intestine causes the mis-positioning of the cells in the stem niche that is normally regulated by EphB3 protein (Solanas et al., 2011).

Figure 17. Model for cell sorting induced by EphB/EphrinB signaling. EphB/EphrinB complex activates ADAM10 locally, which mediates E-cadherin shedding of the contacts between EphB- and EphrinB expressing cell. Asymmetry of E-cadherin interactions decreases affinity between and two populations and results in cell sorting. Adapted from (Solanas et al., 2011)

5.2 Differential adhesion mediated by cadherins

Mechanical forces can contribute to the segregation of cells in the same way that superficial tension is generated contacting oil with water. This theory takes the name of Differential Adhesion Hypothesis (DAH) and it was formulated by Steinberg in the 1963 (Steinberg, 1963).

Cells and tissues minimize their free energy and surface-area by reducing at the minimum cell-cell adhesion interaction and as a result cells with different adhesion do not intermingle and a linear boundary between compartments is generated. This hypothesis involves the role of cadherins, proteins that mediate cell-interaction.

Cells expressing same levels of proteins that mediate cell-interaction interact stronger one with each other than with cells expressing different levels; they

enrich the lowest level of global free energy in which the maximal contact between cells with the higher mutual affinity. In this hypothesis the level of cadherins expressed per cell in both cell populations is a crucial issue.
The genetic modulation of the cadherin levels has been studied during embryonic development: in mouse forebrain they showed a role for R-cadherin and cadherin-6 in cell segregation (Inoue et al., 2001); in *D. melanogaster* follicles the oocyte is correctly located thanks to DE-cadherin (Godt and Tepass, 1998), and the partition of the spinal cord motor neurons is mediated by MN-cadherin (Price et al., 2002).

5.3 Cell cortex tension

Cell segregation can be driven by tension and contraction of cell-surface instead of differential adhesion (Harris, 1976). Using atomic force microscopy (ATM) it was demonstrated that during zebrafish gastrulation different germ layers are segregated by actomyosin-dependent cell-cortex tension (Krieg et al., 2008). Ectodermal cells show less cohesivity compared with mesoendodermal cells but a higher cell-cortex tension regulated by Nodal signaling.

Several works point to actomyosin cables as major players in restricting the intermingling of different cell populations. The local enrichment of contractile elements such as F-actin and Myosin II in boundaries has been reported previously in Drosophila in the parasegment boundaries of the embryonic epidermis (Monier et al., 2010), and in the AP and DV boundaries of the different larval imaginal discs (Becam et al., 2011; Curt et al., 2013; Landsberg et al., 2009; Major and Irvine, 2006). Experiments of laser ablation of cell bonds showed that it generates an approximately 2.5 higher tension compared with non-boundary tissues (Landsberg et al., 2009).

Lately, combination of theory and quantitative experiments helped to understanding the physical mechanisms shaping these imaginal disc boundaries. Vertex models based *in silico* analysis of wing imaginal disc

morphogenesis showed that interplay between cytoskeleton mechanics (actomyosin cable), cell cycle, cell growth and cell signaling is required for correct shaping of DV organizer (Canela-Xandri et al., 2011). In addition, experiments in the same system revealed that the roughness of the DV compartment boundary is dynamic and it decreases during development. This decrease correlates with increased cell bond tension along the boundary (Aliee et al., 2012). Therefore, they proposed that higher cell tension at the boundary, oriented cell division and cell elongation of the tissues are the three variables responsible for the linearity of the boundaries.

It was shown that Notch is involved in DV affinity at the boundaries mainly repressing *Bantam* miRNA activity at the border of the segment. Decreased Notch leads to lower level of *Bantam* at the boundaries, thus in turn drives reduced proliferation rate and an actin accumulation, via Enabled (Ena), an actin regulator. This is required for the establishment of actomyosin cables preventing cell mixing. Later, boundary cells are formed and they activated Notch pathway that induces Cut expression. Cut is required to repress Ena protein and an actomyosin cable is formed at the interface between boundary and non-boundary population (Becam et al., 2011) (Fig.18).

Another work showed that accumulation of non-muscle myosin II in AP and DV compartment boundaries is mediated by *Hox* gene *Ultrabithorax* differentially expressed in the segments, even in the absence of Notch and Hedgehog (Curt et al., 2013).

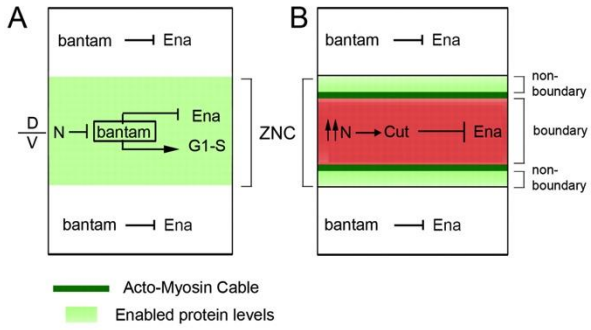

Figure 18. DV affinity boundary is maintained by the role of *bantam* miRNA and Cut. a) In mid third instar (mid-L3) wing imaginal discs, low level of Notch (N) activity (green) reduces the activity of bantam, this causes an accumulation of Ena (light green), a bantam target. Ena decreases proliferation rates at the DV boundary. b) In late third instar (late-L3) boundary population (red) and non-boundary cells are distinguished. High levels of Notch activity induces Cut expression, which in turn represses Ena protein; this establishes actomyosin cables at the border between boundary and non-boundary cells (green). From Becam et al., 2011.

Evidences in the parasegmental ectodermal tissues demonstrated the involvement of Myosin II in the impairment of cell mixing between the anterior and the posterior segment; a sharp boundary is regenerated after cell division that challenges the border. Very elegant experiments by chromophore-assisted laser- inactivation (CALI) of Myosin II specifically at the boundaries, results in cell-mixing of the two segments demonstrating the importance of the tension generated by the actomyosin cable (Monier et al., 2010) (Fig.19).

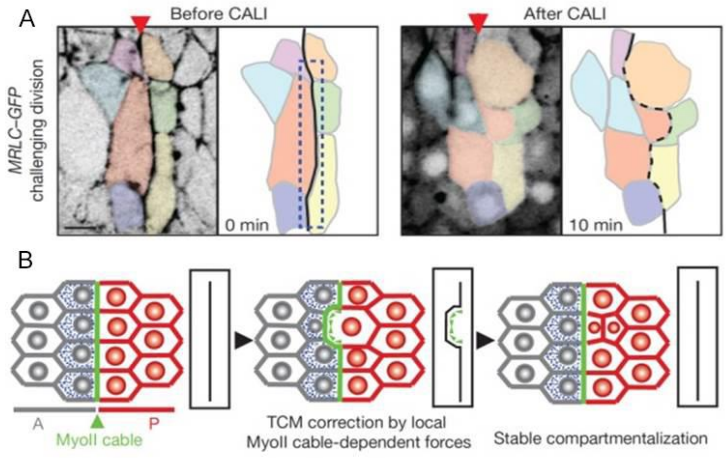

Figure 19. CALI inactivation of the MyoII cable causes cell sorting defects at PS boundaries. A) Movie frames showing results of CALI on the PS boundary (dashed box) in embryos expressing *MRLC–GFP*. In the presence of a dividing anterior boundary cell (colored red), CALI inactivation of MyoII at the cable leads to an irregular PS boundary (dashed line, right panel). After division, one daughter cell invades the posterior compartment. B) Model of cell sorting at *Drosophila* embryonic lineage restriction boundaries. Adapted from Monier et al., 2010.

In general all those evidences support the presence of an alternative adhesion-independent mechanism that plays a central role in cell sorting; moreover different signaling pathway are shown to activate the accumulation of F-actin and non-muscle myosin, like wingless and Notch.

5.4 F-actin and myosin II

Actin is a 42-kDa globular protein (G-actin) that it is arranged in a head-to tail conformation to form filamentous actin (F-actin). The actin filaments or microfilaments are one of the three components of the cytoskeleton and are double-stranded helical polymers of actin with a diameter of 5-9 nm. They appear like flexible structure and they are organized as linear bundles, dispersed throughout the cell but mostly concentrated in the cell-cortex. In response to different stimuli microfilaments are continuously assembled and disassembled in a nucleation and polymerization process. They are involved

in different essential cellular processes like cell motility, cell contraction and cell division and they are generally associated with several actin-binding proteins (ABP) and the most important are myosins.

Myosins are a superfamily of ATP-dependent motor proteins that play a central role in muscle contractility and they are involved in several eukaryotic motility processes. Myosins interact with actin filaments to produce tension (Fig19). This superfamily is composed by different members that differ for functions and structure and among them non-muscle myosin II (NMII) is one of the most interesting. It is composed by three different peptides: two heavy chains two regulatory chains and two essential light chains that stabilize the heavy chain structure. NMII interacts with microfilaments to form actomyosin structures that have a fundamental role in: i) cellular shaping and movement, like cell migration and cell adhesion; ii) epithelial cell polarization, when present in the epithelial cell junction; iii) other developmental processes such as gastrulation, trachea formation, dorsal closure, morphogenesis of the neural tube (reviewed in Vicente-Manzanares et al., 2009).

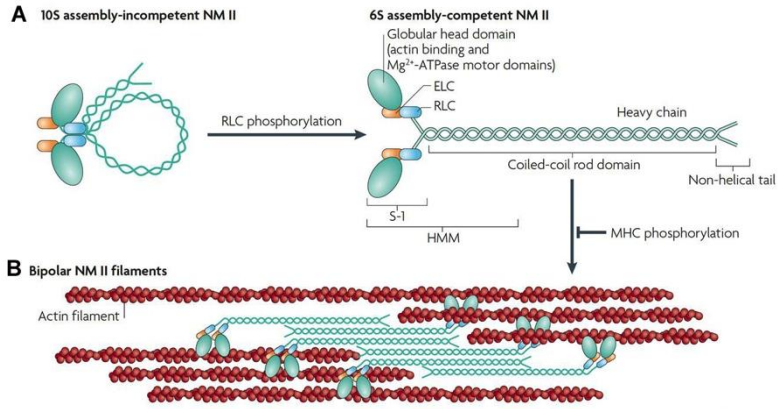

Figure 20. Domain structure of NMII. A) The subunit and domain structure of non-muscle myosin II (NM II), which forms a dimer through interactions between the α-helical coiled-coil rod domains. The globular head domain contains the actin-binding regions and the enzymatic Mg^{2+}-ATPase motor domains. The essential light chains (ELCs) and the regulatory light chains (RLCs) bind to the heavy chains at the

lever arms that link the head and rod domains. In the absence of RLC phosphorylation, NMII forms a compact molecule through a head to tail interaction. This results in an assembly-incompetent form (10S; left) that is unable to associate with other NMII dimers. On RLC phosphorylation, the 10S structure unfolds and becomes an assembly-competent form (6S). S-1 is a fragment of NMII that contains the motor domain and neck but lacks the rod domain and is unable to dimerize. Heavy meromyosin (HMM) is a fragment that contains the motor domain, neck and enough of the rod to effect dimerization. B) NMII molecules assemble into bipolar filaments through interactions between their rod domains. These filaments bind to actin through their head domains and the ATPase activity of the head enables a conformational change that moves actin filaments in an anti-parallel manner. Bipolar myosin filaments link actin filaments together in thick bundles that form cellular structures such as stress fibres. From Vicente-Manzanares et al., 2009.

OBJECTIVES

Objectives

The control of cell movements to generate and maintain the precision of tissue organization is of central importance for the development of the hindbrain and there is consequently much interest in identifying the underlying cellular and molecular mechanisms. The process of compartmentalization first involves formation of an interface between adjacent segments, and this is followed by the induction of a specialized population of boundary cells at the interface that act as signaling center further patterning the tissue. There has been significant progress in uncovering mechanisms that underlie the segregation of cell populations and formation of boundaries in other systems; however in the hindbrain, many questions still remain.

In this thesis we wanted to answer some of these biological questions using zebrafish embryos as model system. Thus, the specific objectives of this work are the following:

a) To comprehend the cellular mechanism responsible of refinement of gene expression in the rhombomeric boundaries.
b) To unveil the mechanism that accounts for rhombomeric cell segregation;
c) To dissect the molecular effectors of the cell sorting;
d) To understand which is the origin of the hindbrain boundary cells and their behavior.

RESULTS

1. Characterization of two *krox20* reporter transgenic lines

1.1 Expression and function of *krox20*

Krox20 encodes a zinc-finger transcription factor (Chavrier et al., 1988) that is involved in both hindbrain patterning and specification of odd rhombomeric identity (Voiculescu et al., 2001). It is expressed specifically in the developing r3 and r5 and it is one of the earliest genes expressed in a segmental pattern (Schneider-Maunoury et al., 1993; Wilkinson et al., 1989).

In zebrafish, *krx20* expression starts at 100%-epiboly/tailbud stage initially in presumptive rhombomere 3 (pre-r3) and at 0-1ss is activated in pre-r5 like two not linear stripes; then the territory of *krx20* expression is expanded in both rhombomeres and first the stripes become more linear and then they convert into two non-adjacent blocks of expression. At 6ss gene expression boundaries start to be refined and at 10ss are completely sharpened, and r3 and r5 look two equal not adjacent squared blocks. *krx20* expression is maintained in r3 and r5 until 30hpf (data not shown), when the expression is downregulated firstly in r3 and later in r5.

Krox20 directly regulates the expression of numerous genes also involved in AP patterning, like *Hox* genes of the paralogous groups 1 to 3, such as *Hoxb1*, *Hoxa2*, *Hoxb2* and *Hoxb3* (Giudicelli et al., 2001; Manzanares et al., 2002;Nonchev et al., 1996; Nonchev et al., 1996; Seitanidou et al., 1997; Vesque et al., 1996) and directly activates the expression of the receptor tyrosine kinase gene EphA4 in r3 and r5, which is involved in the cell sorting (Theil et al., 1998). Krox20 has also been shown to activate both cell-autonomously and non-cell-autonomously its own expression (Giudicelli et al., 2001).

Krox20 knock-out mice showed loss of r3 and r5 territories (Schneider-Maunoury et al., 1993), leading to mis-specification of these segments, and the fate of prospective r3 and r5 cells in mutant mice show that r3 acquires r2 and r4 identity, and r5 acquires r6 identity (Voiculescu et al., 2001).

1.2 Transcriptional reporters of *krx20* expression

Our objective was to search for a transcriptional reporter of *krx20* in order to perform an in vivo tracking of *krx20*-expressing cells. We took advantage from the work done in understanding the regulatory sequences of *krx20* and also the effort in generating enhancer trap screenings, and we selected tg[elA:GFP] and Mü4127 reporter lines (Fig.21). Therefore, we characterized the onset and expression of fluorescent reporters in r3 and r5 in these transgenic fish lines (Fig.22).

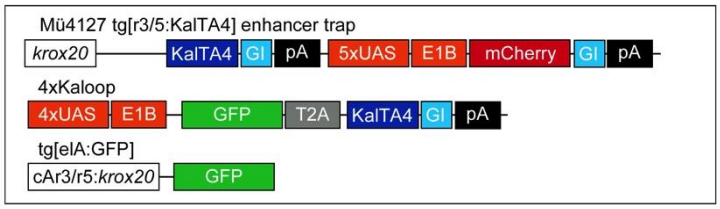

Fig. 21 Scheme of the inserted transgenes in the fish lines. Mü4127 is an enhancer trap inserted in the *krox20* locus. 4xKaloop is a UAS-GFP driver, tg[elA:GFP] expresses GFP under the control of chick element A.

Initially, *krx20* displays a jagged border of expression in r3 and r5 boundaries at 10hpf, but becomes sharply defined at 14hpf (Fig.22A-B, see arrow in C).

tg[elA:GFP]

The expression of *krx20* in the hindbrain is regulated by three enhancer elements (A, B and C) located in very far upstream of the gene (200kb) and conserved between chick, mouse and human. Those elements have different roles: element B is responsible of the initiation of *krx20* expression in r5; element C is responsible of the initiation of the expression both r3 and r5;

and element A is involved in the maintenance of *krx20* expression. The sequence and position of these elements are mainly conserved in different species, although element A in zebrafish is conserved in position and function, but not fully conserved in sequence (Chomette et al., 2006; P Gilardi, personal communication). We obtained tg[elC:GFP] and tg[elA:GFP] stable lines from P Charnay laboratory (Paris, France).

We initially considered to use the tg[elC:GFP]; however after first analyses of GFP expression we observed likeness of the transgene and dropped it for our study (data not shown).

In tg[elA:GFP] the *gfp* transcript is detected by ISH slightly later in respect with endogenous *krx20* (Fig. 22A,K). At 1ss few cells start to express *gfp* in pre-r3 (Fig.20K); this region expands and by 3ss (Fig.22L). By 10ss the territory of *gfp*-expression fully coincides with the endogenous *krx20*, although r5 expresses the transgene at lower level compared with r3 (Fig.22N-O). Double fluorescent in situ hybridization (FISH) for *krx20* and *kalta4* showed that expression border of both endogenous and transgene perfectly overlaps at 14hpf once boundaries are refined (Fig.22N,R). More importantly for our study GFP protein is already detected at 3ss by immune staining at the stage where the boundaries are still jagged (Fig.22Q).

Therefore, tg[elA:GFP] spatially recapitulates *krx20* expression, first in r3 and then in r3 and r5 with a slight delay in time

Mü4127

Enhancer trap screenings offer big opportunities to capture a transcriptional reporter of a gene of interest. The group of RW Koster (Neuherberg, Germany) isolated a *krx20* enhancer trap fish line (Mü4127). They were able to map the insertion of the cassette 3kb downstream of the gene by nested inverse-PCR (Distel et al., 2009).

The enhancer trap construct contains an optimized version of GAL4 for zebrafish (KalTA4GI) controlled by a nothocord specific enhancer (*tw/hh*), followed by 5xUAS copies controlling the expression of KCherryGI (Fig.21).

In Mü4127, the *Kalta4* transgene is activated at 1ss (Fig.22F-G) contemporaneously in pre-r3 and pre-r5, but half-an-hour later compared with endogenous *krx20*. The number of cells expressing *Kalta4* increases with the time and by 10ss *Kalta4* is expressed in full r3 and r5 (Fig.22I-J); by 10ss the *krx20* expression domain corresponded with the expression of the reporter gene (Fig.22J).

The characterization of the two transgenic fish lines revealed that both, *kalta4* and *gfp* reporters mRNA and GFP protein in tg[elA:GFP], display earlier (11hpf) fuzzy boundaries of the expression and then sharp borders by 14hpf, as is the case for *krx20* (Fig.22B,G,L, see arrows in C,H,M and arrows in Q). Thus, even with slight differences in time, tg[eleA:GFP] and Mü4127 are transcriptional reporters of *krx20* and the transgenes are activated during the entire segmentation process.

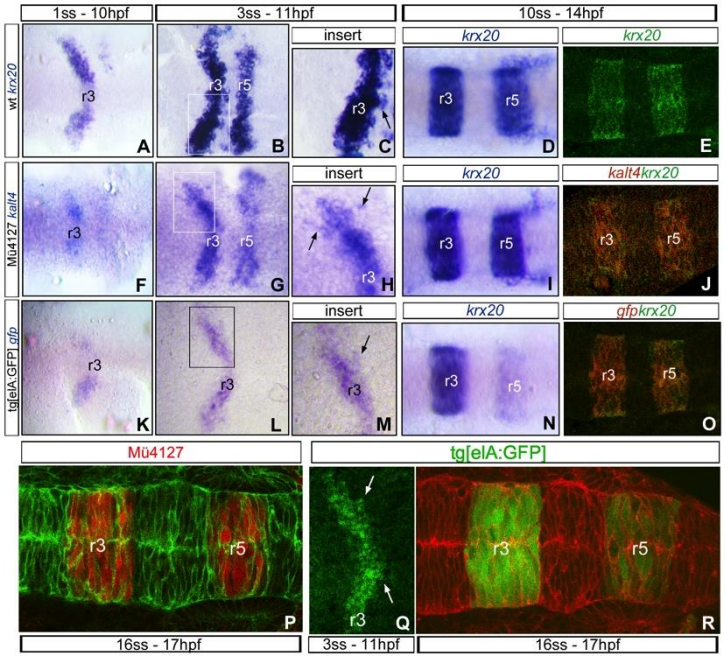

Figure 22. Characterization of the fish transgenic lines used in the study. (A-O) Spatio-temporal characterization of the expression of the transgene (*kalta4*, *gfp*) in the different transgenic lines by in situ hybridization compared with endogenous expression of *krx20* in wt embryos. Note that at early stages of embryonic development in all zebrafish strains, *krx20*, *kalt4* or *gfp*-positive cells are found surrounded by cells of different identity (C,H,M, for magnifications, see arrows); later on, clear and sharp gene-expression domains are generated (D,I,N). (E,J,O) Single-FISH for *krox20* and double-FISH for *krx20* and the reporter in both transgenic lines. (P-R) Spatio-temporal characterization of the reporter fluorescent protein expression in the two different transgenic lines. (P,R) embryos were injected with mRNA driving expression to the plasma membrane such as lyn:GFP and or memb:mCherry. Note that GFP protein expression is activated as early as 3ss (Q) in cells located in ectopic rhombomeres. Dorsal views with anterior to the left.

2. Refinement of molecular boundaries in the hindbrain by cell sorting

The segregation of rhombomeric cell populations involves the formation of a sharp interface between adjacent segments with different identity. The segregation of cells and the formation of well-defined boundaries can be visualized by observing gene expression within the rhombomeres. Initially, *krx20* displays a jagged border of expression in r3 and r5 boundaries at 10hpf (Fig 22B-C, see arrow in C) but becomes sharply defined at 14hpf (Fig 22D-E; (Cooke and Moens, 2002). Gene expression boundary sharpening can occur by a number of possible mechanisms: cells on the "wrong" side of a boundary can move across it by a cell-adhesion/repulsion based mechanism –cell sorting- (Cooke et al., 2005; Kemp et al., 2009; Xu et al., 1999); or they can switch their identity to that of their neighbors –cell plasticity– (Schilling and Knight, 2001; Zhang et al., 2012); however there is no a clear picture about the main mechanism applying. To study deeper how this molecular refinement is generated we analyzed the behavior of cells with different rhombomeric identities during early embryonic development.

Because the two lines recapitulate the dynamics of *krx20* expression next we used them to trace rhombomeric cells using two approaches: i) *in vivo* imaging to follow single cells from different rhombomeres, using tg[elA:GFP] embryos injected with H2B-mCherry; and ii) fake cell-tracing analysis in fixed embryos.

2.1 In vivo time-lapse of tg[elA:GFP] reveals the cell sorting mechanism

Transgenic reporter lines expressing fluorescent proteins offer the possibility to perform in vivo experiments by time-lapse in order to understand how development occurs at tissue level in 3D+time; moreover cellular tracking showed how a single cell behave in a specific-territory. We decided to apply

this approach to our system to comprehend the cellular mechanism involved in the patterning using tg[elA:GFP] since the fluorescent reporter is detected earlier compared with Mü4127.

To explore the behavior of groups of cells in adjacent territories we followed several individual cells by time-lapse analysis during 5h (from 11 to 16hpf). In order to visualize the cell nuclei, we injected 4-8-cell stage embryos with *H2B-mCherry* mRNA. Like this we have a mosaic mCherry expression, and GFP cytoplasm staining in r3 and r5 (n=3). We in vivo imaged the hindbrain of embryos from ~11hpf (3ss) until the end of hindbrain patterning (18hpf=18ss) (Fig.23).

The rational of the experiment is that since we can know the final fate of an individual cell by the expression of GFP, if we back-track the cells we can allocate their origin and therefore see whether cells changed their fate.

Single red nuclei of GFP-positive and GFP-negative cells mainly located in the r3-r6 region (n=43), and at different positions along the rhombomeres (close/far to the boundary) were manually back-tracked. This means that cells that by the end of the movie were located in given positions of the hindbrain were followed back to their original positions at the beginning of the movie.

As shown in Fig. 23 and Movie 1, analysis of several individual cell trajectories indicated that cells that at the beginning of the analysis (11hpf) were in the nearby of their future position but somehow intermingled (Fig.23; see mixed light blue, green and yellow dots in A'-C'), were sorted out from the neighboring territory with distinct molecular identity by the end of the analysis (Fig.23; see segregated light blue, green and yellow dots in D'-F'). In Movie 1 it can be observed that cells do not migrate long distances, but they mainly intermingle. Thus, cells that are early located in the fuzzy boundary region, end up segregated along the sharp boundary of gene expression.

Interestingly, the onset of GFP expression in r5 is during the video recording (~4ss), and all GFP-positive cells switched on the reporter at the same moment and they maintain the expression until the end of the video. On the other hand, GFP-negative cells never switch it on. Cells of all rhombomeres undergo symmetric cell division and the progeny never changes the fate. As expected, all cells maintain their relative position along the AP without further migrations.

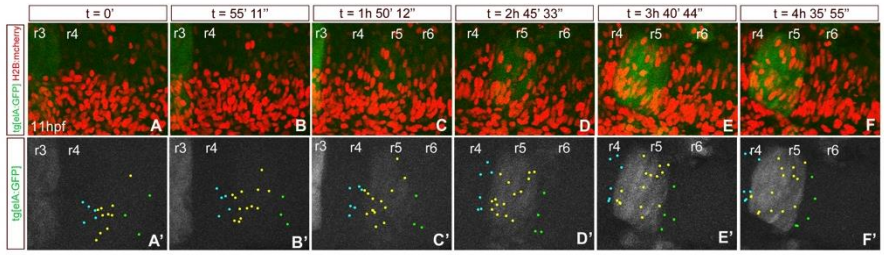

Figure 23. Global cell-tracking shows that rhombomeric cells maintain their fate and relative position. Time-lapse of an embryo at 11hpf where several single cell trajectories within r3-r6 were back-tracked and overlaid; not all the 43 are shown to avoid overlapping of multiple points. Merge of green and red channels, displaying in green the emergence of r3 first and later r5 and in red all labeled cell nuclei; (A'-F') Green channel displayed in white, to observe the appearance of r3 first and then r5, and the position of tracked-cells with colored dots. Blue dots correspond to r4-cells, yellow dots to r5-cells and green dots to r6-cells. See Movie 1 for original data. Note that cells at the boundaries that at the last time point are segregated were mixed at the beginning of the movie. Dorsal views with anterior to the left.

In another set of experiments we focused on detailed cell trajectories in the vicinity of rhombomeric borders and followed *in vivo* single r5 or r6 cells by tracking cell nuclei. We observed that cells located on either side of the r5/r6 boundary did not change their molecular identity (Fig.24, see blue dots for single cells, Movies 2-3). r5 GFP-positive cells were kept into r5 and maintained the GFP during the length of the movie (Fig.24, see blue dot and white arrow for a given example; Movie 2). r6 GFP-negative cells behaved in a similar manner, namely, r6 cells that incurred into the r5 territory were sorted out and never changed their molecular identity even after cell division (Fig.24, see blue dots and white arrows; Movie 3). These results show that

when cells of a given identity are found within an environment of different identity are sorted out.

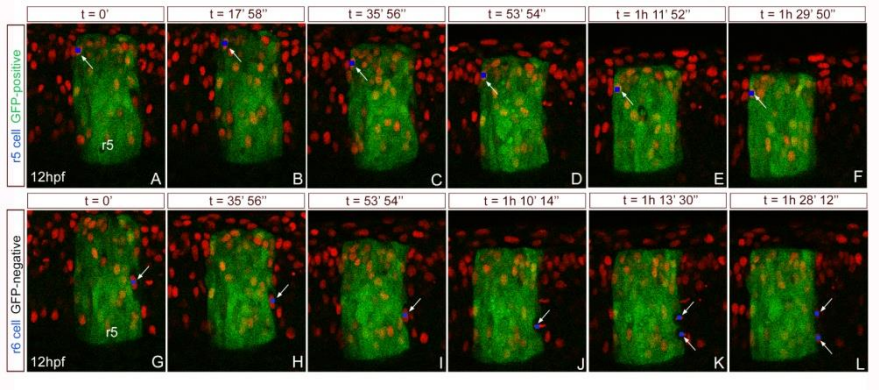

Figure 24. Tracking of single cells shows that rhombomeric cells are sorted out from territories with different rhombomeric identity. In vivo imaging of tg[elA:GFP] embryos injected with H2B-mCherry mRNA at 4-8cell stage. (A-L) Time-lapse of an embryo from 12hpf onwards: (A-F) a single GFP-positive cell from r5 (see blue dot pointed with white arrow); (G-L) a single GFP-negative cell from r6 that divides in two GFP-negative cells (see blue dots pointed with white arrows).

These results support **cell sorting** as the mechanism operating in the refinement of molecular rhombomeric boundaries in zebrafish, independently of the identity of the cell.

2.2 Fake-cell tracing of the two transcriptional reporters

However, to fully support this hypothesis we did a fake cell-tracing analysis in the transgenic zebrafish lines tg[elA:GFP] and Mü4127.

The rationale of the experiment was that cells expressing *krx20* will switch on the reporter gene *mCherry/gfp* and then mCherry/GFP proteins will be synthesized. Since fluorescent proteins are more stable than *krx20* mRNA, we will be able to trace cells that once activated *krx20* by the expression of the fluorescent reporter even at a stage when normally *krx20* gene has already been switched off. If cell plasticity was the cellular mechanism used by the cells to generate the pattern we would find ectopic fluorescent cells in

r2, r4 or r6 that no longer expressed *krx20* mRNA at late developmental stages (18hpf). On the other hand, if cell sorting was the main mechanism accounting for the sharpening of gene expression we should not expect any ectopic fluorescent cells, since *krx20* cells located in the "wrong" side (r2, r4 and r6) would segregate to the "right" side (r3 and r5). Following this hypothesis, we performed fluorescent *in situ* hybridization for *krx20* combined with antibody staining to detect the reporter fluorescent protein followed by confocal analysis (Fig.25).

When expression of *krx20* was analyzed in embryos at 18hpf (once molecular boundaries have been clearly refined), no ectopic *krx20*-cells were found in r2, r4 or r6 in any of the transgenic lines (Fig.25A,D). Moreover, in these same embryos no ectopic GFP-positive cells were observed (Fig.25B,E). Accordingly, the big majority of cells expressing GFP also expressed *krx20* mRNA (Fig.25C,F). To quantify this, we counted the number of cells close to boundary regions that expressed both *krx20* and GFP, and found that over 95% of the cells in any of the rhombomeric boundaries shared both markers (Fig.25J-K). Since we observed jagged expression of *mCherry* and *gfp* at early developmental stages (see arrows in Fig.22H,M,Q), these results strongly suggest that cell sorting plays a major role in the sharpening of *krx20* expression. However, to unveil any possible cell plasticity events that can have a compensatory effect correcting errors or noise but could be masked by the strength of the sorting mechanism, we knocked-down EphA4 function, which plays a known role in cell sorting (Xu et al., 1999). When EphA4 was downregulated, boundaries were jagged but all GFP-positive cells still expressed *krx20* (Fig.25G-I; see white arrow head pointing to an isolated cell expressing both markers). Cells not expressing *krx20*, did not have any GFP either (Fig.25H-I; see white arrows). No changes were detected when different rhombomeric boundaries were analyzed (Fig.25J-K), pointing to cell sorting as the sharpening mechanism in

all hindbrain boundaries -independent of the cell position along the antero-posterior (AP) axis.

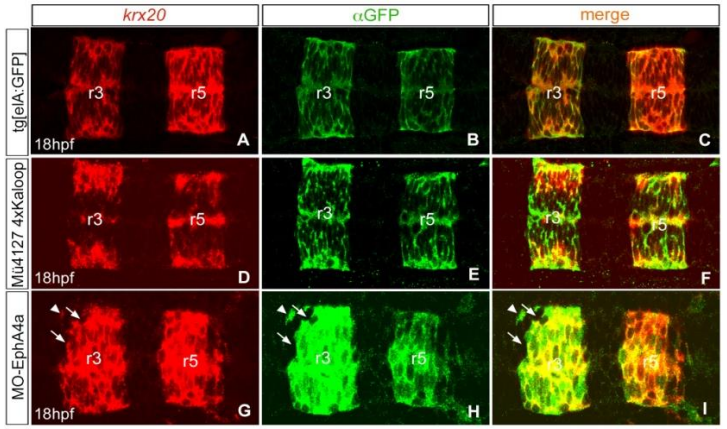

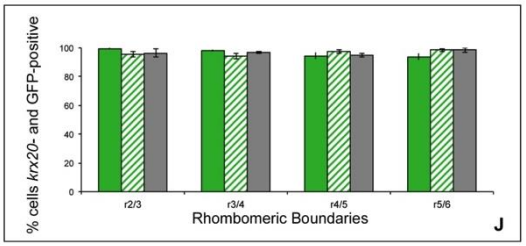

K	r2/r3	r3/r4	r4/r5	r5/r6	n
elA:GFP	99.6±0.2	98.3±0.6	94.3±2.2	94±2.3	8
elA:GFP MO-EphA4	95.4±1.8	94.2±1.9	97.5±1.2	98.6±1.8	5
elA:GFP MO-CTRL	96.5±2.8	96.7±0.5	94.8±1.2	98.5±1.5	3

Figure 25. Cell sorting is the main cellular mechanism involved in molecular boundary refinement. (A-I) Fluorescent *krx20* in situ hybridization (red) followed by anti-GFP immunostaining (green) to detect the expression of the reporter gene under the control of *krx20* in the different transgenic zebrafish lines: (A-C) tg[elA:GFP] and (D-F) double transgenic Mü4127 4xKaloop embryos, which express GFP in r3 and r5; (G-I) tg[elA:GFP] embryos injected with MO-EphA4a. Note that in all cases cells co-express *krx20* (red) and GFP (green). Even when cell sorting is disrupted after morpholino-injection and a given cell is found isolated it expresses either both markers (see white arrow heads), or it expresses none (see white arrows). All images are dorsal views with anterior to the left. (J-K). Quantification of cells expressing *krx20* and GFP in the vicinity of all rhombomeric boundaries. Green bars: tg[elA:GFP] embryos; dashed bars: tg[elA:GFP] embryos injected with MO-EphA4a; grey bars: tg[elA:GFP] embryos injected with MO-CTRL.

3. Unveiling the mechanisms of rhombomeric cell segregation

3.1 Timing of appearance of morphological rhombomeric boundaries

Previous evidences showed that the border of expression of transcription factors prefigures the position of the morphological rhombomeric boundaries (Maves et al., 2002). As shown above, once gene expression domains achieve sharp boundaries due to cell sorting, morphological boundaries are visible as shallow indentations on the outside of the neural tube and cell mixing is restricted between rhombomeres. In zebrafish, hindbrain morphological boundaries are visible around 15hpf (Maves et al., 2002). In addition, we know that cells belonging to different rhombomeres do not intermingle (Fraser et al., 1990;Jimenez-Guri et al., 2010). Thus we decided to investigate when morphological boundaries were firstly visible and how was their order of appearance. We did so by time-lapse analysis by injecting wild type embryos with *lyn-GFP* mRNA to visualize the cell contour and this allow to detect morphological changes of tissues.

In vivo imaging shows constriction in the neuroepithelium starts to be visible from 12ss (Fig.26A). At 13ss and 14ss the rhombomeres are like highly compact bulges of cells (Fig. 26B-C); the contact between boundary cells of different segments is a linear boundary but in their internal side there are verging to the center of the rhombomere, this cause the triangular cell shape characteristic of these cells (Fig.26B'); we defined these changes as formation of morphological boundaries.

Thus three types of cell morphologies are observed: i) rounded cells that are cells undergoing mitosis (purple cell); ii) cells within the rhombomere that are spindle shaped and narrow apically and basally (blue cell), and iii) boundary cells with a characteristic triangular shape (orange cell) (Fig.26B').

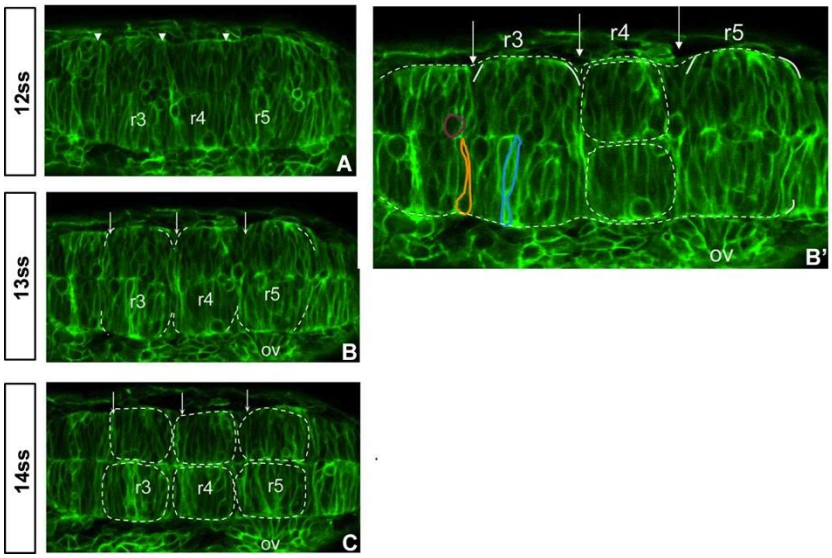

Figure 26. Cell shape changes according to their position within the rhombomere. Dorsal views of time-lapse video of a wt embyo injected with *lyn-GFP* mRNA where three snapshots at 12ss (A), at 13ss (B) and 14ss(C) are shown. Arrows indicate bulge constrictions appearance and dashed lines the borders of the rhombomeres In (B') three type of cell morphologies are highlighted with different colours. Anterior to the left.

3.2 Hindbrain boundaries are challenged by cell division

In the developing neuroepithelium, cells undergo interkinetic nuclear migration, and the nuclei occupy different positions along the apico-basal axis according to the progression in the cell-cycle. Neuroepithelial cells are normally spindle-shaped; when they undergo into mitosis they become rounded, the plasma membrane enfolds the nucleus and cytoplasm previously migrated close to the midline, and contacting the apical part with a linear extension.

We performed live imaging in the proliferating tissue and looked at cell behaviors upon cell division close to the boundaries. tg[Mü4127] embryos were injected with *lyn-GFP* mRNA and imaged during 3 hours (18hpf) (Fig.27, Movie 4). We found that, upon cell division, boundary cells are continuously challenging the rhombomeric boundary deforming it. After cytokinesis the daughter cell closest to the boundary transiently invaded the

neighbouring territory and it is rapidly pushed back to the territory where it belongs restabilising a linear boundary and a new triangle-shaped boundary cell is generated (Fig.27C-D;C'-D' see arrowheads).

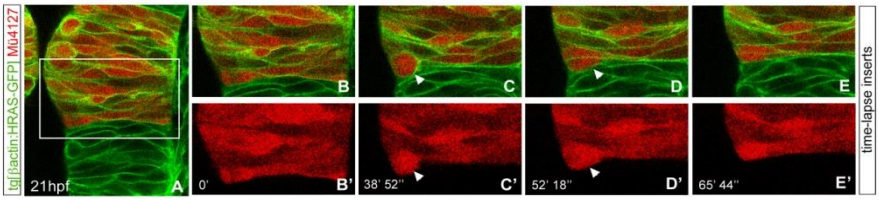

Figure 27. Cell division challenges hindbrain boundaries. (A-E') Dorsal views of time-lapse stacks of rhombomeres 3 (red) and 4 of tg[actin:HRAS-GFP] Mü4127 embryos from 21hpf onwards. (B-E') Inserts of the region framed in (A). Note that cell division challenges the boundary (see white arrow head). Anterior is to the top. See Movie 4 for the original data.

This result suggests that this can be due to the presence of physical barrier in the boundary interfaces that avoid cell mixing, maintaining linear boundary even in the presence cellular movements.

Several mechanisms have been proposed for keeping cells segregated, mainly differential cell adhesion but also extracellular matrix fences (Batlle and Wilkinson, 2012). Thus, we decided to investigate the role of mechanical barriers in maintaining distinct rhombomeric borders or keeping rhombomeric cells segregated, exploring two possible mechanisms: a barrier made of extracellular matrix deposition such as in the embryonic intersomitic boundaries in zebrafish (Julich et al., 2009), or a barrier based in actomyosin fibers as previously described in Drosophila (Aliee et al., 2012; Becam et al., 2011; Major and Irvine, 2005; Major and Irvine, 2006; Monier et al., 2010).

3.3 Absence of FN matrix deposition in interhombomeric boundaries

During somitogenesis, an accumulation of extra cellular matrix (ECM) components in the intersomitic space is responsible for avoiding cell mixing between two adjacent somites.

EphA4 is expressed in the anterior half of a somite and Efnb2a in the posterior half of the somite and, upon EphA4-Ephrin2ba binding in the surface of contact of these two populations in different somites, EphA4 activates its intracellular pathway by autophosphorilation and it recruits a member of integrin family (Itgα5) in the cytoplasmic membrane. Itgα5 is responsible for the assembly of Fibronectin (FN) matrix fibres in the intersomitic space.

Due to similarities in terms of biological processes (patterning) and expression of molecules (EphA4-Ephrinb2a) we decided to test if the mechanisms involved in somitogenesis were also playing a role in the hindbrain.

We investigated any contribution of FN matrix deposition in the interhombomeric boundaries analyzing the presence of FN matrix assembly between rhombomeres. To do so we immunostained tg[elA:GFP] embryos of different stages (18, 24 and 30hpf) for FN and GFP (to label r3 and r5) (Fig.28). When embryos were immunostained, no FN matrix deposition was observed in the hindbrain boundaries although a clear staining was visible at the somites interface (Fig.28, C').

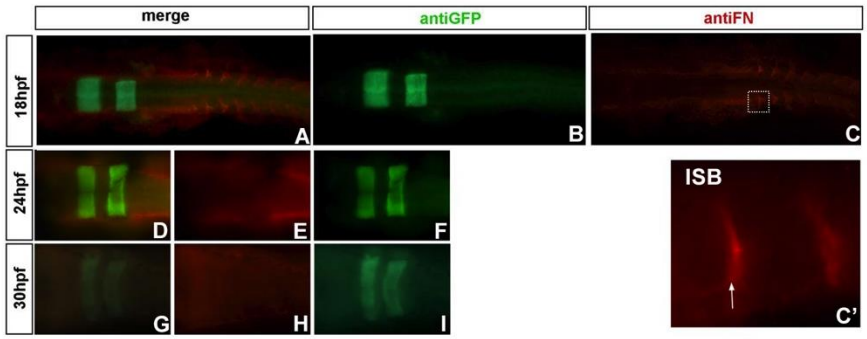

Figure 28. Fibronectin matrix is detected in the somites but not in the interhombomeric boundaries. Dorsal views of tg[elA:GFP] embryos immunostained with anti-FN in three different stages at 18hpf, 24hpf and 30hpf. Note that there is not enrichment of FN in the hindbrain although there is a clear FN-deposition in the intersomitic boundaries (ISB).

Similar results were obtained when we injected embryos with mRNA of the Itgα5, a FN receptor that clusters upon activation (Julich et al., 2009) and assembles FN fibers, (Fig.29). These results show that extracellular matrix does not play a major role in keeping rhombomeric cells apart.

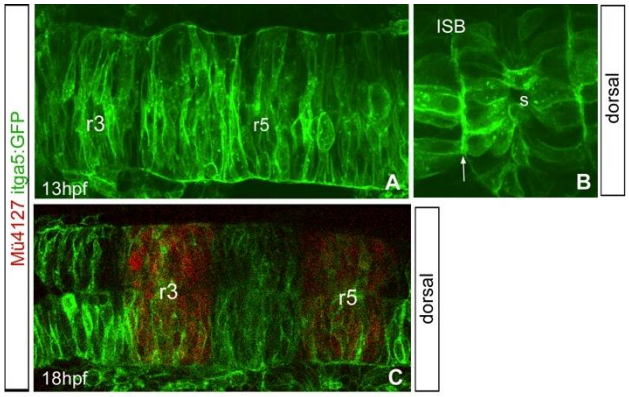

Figure 29. Clustering of Itgα5 is not detected in the interhombomeric boundaries. Mü4127 embryos were injected with itgα5:GFP mRNA in order to visualize the clustering –and therefore the activation- of α5 integrins in the hindbrain boundaries. Note that as FN, no enrichment of itgα5 was found in the hindbrain although it can be clearly observed in the ISB (B).

3.4 Presence of an actomyosin cables in the interhombomeric boundaries

An alternative mechanism to the formation of the physical barrier is the presence of cortical tension that maintain in the cell population of the same segments joint together. Different evidences demonstrated that during embryogenesis of *Drosophila melanogaster,* to maintain separate groups of cells of different compartments, an enrichment of MyosinII and F-actin in the apical cortex of boundary cells is formed (Aliee et al., 2012; Becam et al., 2011; Major and Irvine, 2005; Major and Irvine, 2006;Monier et al., 2010).

We explored the presence of actin-filament structures in the hindbrain at the time when morphological bulges appeared. For this purpose, we used the transgenic lines tg[lifeactin:GFP] and tg[utrophin:GFP] that allow the visualization of F-actin, and tg[myoII:mcherry/GFP], which let us visualize Myosin II when bound to actin filaments (Behrndt et al., 2012;Maitre et al., 2012). Since actomyosin cables are always located at the apical side of the cells, we did analyze the presence of Actin filaments in the hindbrain observing the apical side of the rhombomeric cells, which is located close to the midline (Fig.30B, displays a view of the stacks contained within the orange frame in A). For this we took confocal images of embryos in dorsal views and did Maximal Intensity Projections of only the most apical stacks in a sagittal-like view (see Materials and Methods, and Fig.39). Indeed, an enrichment of Actin cable-like structures was visible from 15hpf, coinciding with the stage where morphological boundaries were already visible (Fig.30 C-H). These cables could not be observed earlier (Fig.30C-D) and were visible at least up to 24hpf (Fig.30E-H; data not shown).

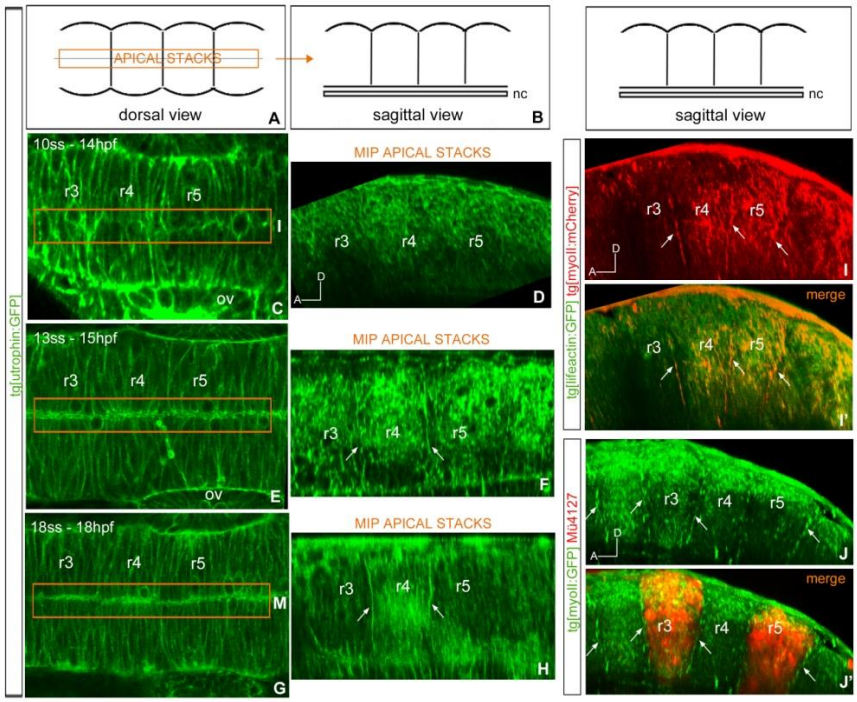

Figure 30. Actomyosin cables are present in the interhombomeric boundaries. (C,E,G) Dorsal views of tg[utrophin:GFP] embryos from 14 to 18hpf. (D,F,H) Sagittal-optical sections of same embryos obtained as Maximal Intensity Projections of the XZ apical planes depicted in (C,E,G) within the orange frame. See scheme in (A,B) for further clarity and Fig.39 for more exhaustive explanations. Arrows point to the enrichment of F-actin. Note that the enrichment of F-actin structures can be observed from 15hpf, once the morphological rhombomeric bulges are visible (Fig.26). Anterior is always to the left. (I-I') Sagittal-optical views obtained as in (B) of double transgenic tg[lifeactin:GFP]/tg[myoII:mCherry] embryos showing that interhombomeric cables are formed by F-actin and Myosin II (see arrows). Myosin II can be seen in red (I), and the merge of F-actin and Myosin II in yellow (I'). (J-J') Sagittal-optical views from double transgenic tg[utrophin:GFP]/Mü4127 embryos where Myosin II cables are located in the interhombomeric boundaries (see arrows). Anterior is always to the left.t.

To demonstrate that these cables were formed by F-actin and Myosin II, we sought the presence of actomyosin fibers by crossing tg[lifeactin:GFP] with tg[myosinII:mCherry] and showed that indeed the rhombomeric cables contained both elements of the actomyosin structures (Fig.30I-I'). Finally, we demonstrated that these cables were specifically located in the interhombomeric boundaries, coinciding with the border of mCherry

expression as a readout of *krx20* in Mü4127/tg[myoII:GFP] embryos (Fig.30J-J').

These data demonstrate the local enrichment of contractile elements such as F-actin and Myosin II in hindbrain boundaries, as reported previously in Drosophila at the parasegment boundaries of the embryonic epidermis (Monier et al., 2010) and the boundaries between compartments in different larval imaginal discs (Becam et al., 2011; Curt et al., 2013; Landsberg et al., 2009; Major and Irvine, 2005; Major and Irvine, 2006). These results point to actomyosin cables as major players in restricting the intermingling of different rhombomeric cells.

3.5.1 Actomyosin cables act as physical barriers avoiding cell-mixing

We wanted to study whether actomyosin cables had any active role in restricting cells of different compartments. When double transgenic Mü4127/tg[utrophin:GFP] embryos were treated with different inhibitors of Myosin II activity, such as Blebbistatin or Rockout, the actomyosin cables in the apical side of the cells were dismantled (compare Fig.31C and D; 76% for Blebbistatin, 90% for Rockout data not shown), and r3 or/and r5 ectopic cells were found in adjacent rhombomeres (Fig.31H, 60%, see white arrows pointing at ectopic cells) when compared with control embryos (Fig 31G, 0%). These results support the idea that actomyosin cables serve as mechanical barriers that restrict cell movement between rhombomeres during hindbrain segmentation. Interestingly, when Myosin II contractility was artificially enhanced exposing embryos to Calyculin A (a compound that overactivates Myosin II inhibiting Myosin phosphatase; (Filas et al., 2012), the morphological bulges were more visible (see the indentations in the neural tube in Fig.31E, 100%). As expected no cell mixing was observed (Fig.31I, 100%), indicating that these actomyosin cables are indeed functional. We have found a clear correlation between the lack/disorganization of the actomyosin cables and the extent of cell

intermingling. These results support the hypothesis that vertebrates have a mechanism based in actomyosin-dependent mechanical barriers to maintain straight interfaces between different cell populations, and therefore to keep them segregated.

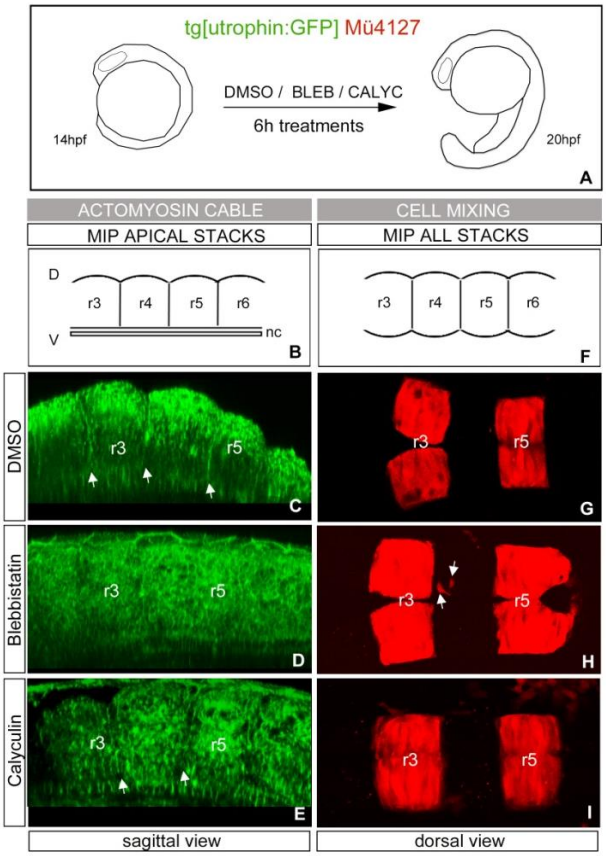

Figure 31. Actomyosin barriers prevent cell intermingling between rhombomeres. (A) Scheme depicting the experiment: double transgenic tg[utrophin:GFP] Mü4127 embryos at 14hpf were treated with different pharmacological agents that modulate the function of the actomyosin cable, such as: (C,G) DMSO as control, (D,H) Blebbistatin and (E-I) Calyculin. (B-E) show the presence/absence of the actomyosin cable in apical sagittal-like views, and (F-I) display dorsal views of r2-r6 region to observe the extent of cell mixing. Note that once the actomyosin cable is disrupted (D), ectopic r3/r5 cells are found in r4 (see white arrows in (H). Anterior is always to the left. (B,F) are schemes to help in the comprehension the 3D-tissue organization.

Rhombomeric cells on both sides of the boundary are perfectly aligned and form a straight interface (Fig.31G, Fig.32A). We quantified the degree of misalignment when compartmentalization was compromised (Fig.31B) using as a readout *krx20*-expression. We measured the Index of Straightness (IS, Fig.39; (Monier et al., 2010) considering that the straighter the boundary, the closer will be IS to 1, which corresponds to a perfect straight line. Quantification of the IS confirmed that interhombomeric interfaces were straighter in control embryos (Fig.32A,D; IS=1.1 n=10) than in Blebbistatin-treated embryos (Fig.32B,D; IS=1.2 n=13), and even straighter boundaries were observed in embryos where Myosin II activity was enhanced by addition of Calyculin A (Fig.32C-D; IS=1.05 n=8). These results support our previous conclusions in that mechanical barriers maintain the straightness of the boundaries.

3.5.2 Myosin-II inhibitors conditions do not affect interkinetic nuclear migration in treated embryos

During development in the neuroepithelia cell nuclei moves in the apical-basal axis depending on the phase of the cell-cycle they are in that moment, this fundamental process is called interkinetic nuclear migration (INM). Mitosis always occurs in the apical side close to the ventricular surface.

Since actomyosin is required for INM (Spear and Erickson, 2012) we wanted to make sure that the observed phenotype –lack of interhombomeric cables- was not due to a secondary effect resulting from the overall changes in morphogenesis and, in particular, to specific basal-to-apical nuclear migration defects in the rhombomeric cells.

To tackle this issue we analyzed the effects of MyoII inhibitors and activators in the Interkinetic Nuclear Migration. For this purpose, we sought the position and number of mitotic cells in the hindbrain (Fig.32E-I), and calculated the Interkinetic Nuclear Migration Ratio (apical nuclei/basal nuclei, see in Material and Methods Fig.40). No differences in the apical

position of the mitotic cell nuclei of embryos treated with DMSO, Blebbistatin, Rockout or Calyculin (Fig.32E-H), or in the total number of pH3-positive cells were observed (Fig.32I). Thus, our experimental conditions did not compromise the overall proliferation of the neural progenitors. On the other hand, when the INM Ratio was assessed, both for Blebbistatin or Calyculin A treated embryos, we consistently observed more cell nuclei in an apical location (Fig.32J). Nevertheless, given that both antagonistic treatments interfere with the basal-to-apical INM, the dismantling of the cable cannot be explained by a disruption in basal-to-apical INM of rhombomeric cell progenitors.

In conclusion, the observed phenotypes are specific to the interhombomeric actomyosin cables because their dismantling in drug-treatments cannot be explained by the disruption of INM in rhombomeric neural progenitors.

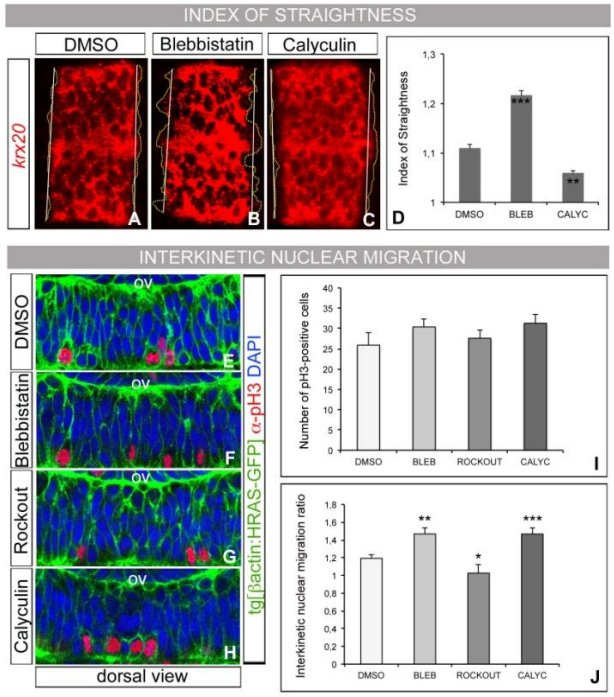

Figure 32. Analysis of the Index of Straightness (IS) within the *krx20*-expression border. (A-C) wt embryos were treated with same pharmacological agents as in previous experiments and assayed for *krx20* situ hybridization. Note

that upon Blebbistatin treatment the border of *krx20*-expression is very fuzzy compared with the sharp border displayed by DMSO or Calyculin treated embryos. Anterior is to the left. (D) Quantification of the Index of Straightness (IS) upon different conditions. IS was measured according to Fig S8B. *** $p<0.001$, **$p<0.005$. (E-J) Effect of the pharmacological treatments on the Interkinetic Nuclear Migration (INM). (E-H) tg[actin:HRAS-GFP] embryos upon different treatments were stained for anti-pH3 to visualize mitotic cells and counterstained with DAPI to singularize cell nuclei. Dorsal views of half-side hindbrains with anterior to the left and apical to the bottom. Images were analyzed according to Fig.40 and the data obtained was plotted as: (I) number of cells undergoing mitosis in the hindbrain (pH3-positive cells), and (R) Interkinetic Nuclear Migration Ratio, which is calculated as the number of nuclei located in the apical side of the cells divided by the number of nuclei located in the basal side of the cells (DAPI-positive cells); ***$p<0.001$ **$p<0.005$.

3.5.3 Mechanical barriers act downstream of EphA/Ephrin signaling to segregate cells from different rhombomeres

Our next question was to address how these mechanical barriers were established. Interestingly, when cell sorting was compromised by EphA4a-MO injections, not only ectopic r3 and/or r5 cells were found outside their territory as expected (Fig.33D 100%, see white arrows; Cooke et al., 2005), but actomyosin cables were highly disrupted (Fig.33H, 100%) when compared with control embryos (Fig.33C,G, respectively). To further support this, when EphA4a-morphants were treated with a Myosin II inhibitor the phenotype was enhanced and the hindbrain boundaries were further jagged, hence displaying a higher IS (Fig.33K,M). Interestingly, when actomyosin filament stability was enhanced treating EphA4-morphants with Calyculin A, no r3/r5 cells were found ectopically (Fig.33E, 100%) and actomyosin cables were partially rescued (Fig.33I, 60%), which strongly suggests that assembly of actomyosin cables is an event downstream of EphA/Ephrin signaling. Accordingly, boundaries were straighter and consequently the IS was closer to 1 (Fig.33L,M). Altogether, these results suggest that mechanical barriers act downstream of EphA/Ephrin signaling to segregate cells from different rhombomeres.

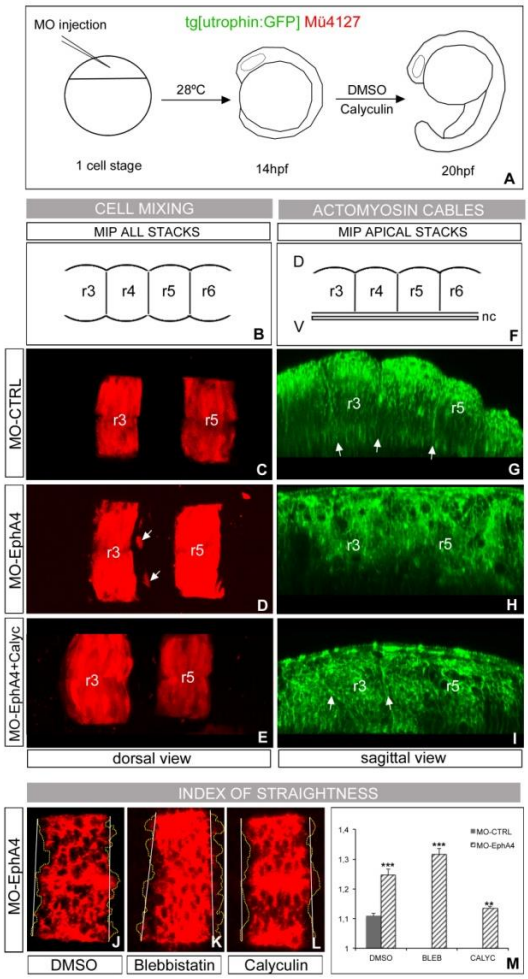

Figure 33. EphA/Ephrin signaling is upstream of the generation of the actomyosin cables. (A) Scheme of the functional experiment: double transgenic embryos Mü4127 tg[utrophin:GFP] injected with CTRL-MO (C,G) or EphA4a-MO (D-E,H-I) at 1-4 cells stage, incubated from 14hpf for 6h with DMSO (C-D,G-H), or Calyculin A (E,I). Afterwards, the degree of cell mixing (C-E) and the presence of actomyosin cables (G-I, see arrows) were assessed. Dorsal views (B-E) and sagittal-optical views of apical stacks (F-I) with anterior to the left. Embryos injected with CTRL-MO behave as control embryos in previous experiments. Note the cell mixing in embryos where the cable was disrupted (D,H, see white arrows), and the partial rescue of the cable in EphA4a-MO embryos treated with Calyculin A (I) resulting in no cell mixing (E). (J-M) Analysis of the Index of Straightness (IS) in wt embryos injected with EphA4-MO at 1-4 cells stage, incubated from 14hpf for 6h with different pharmacological agents and assayed for *krx20* in situ hybridization.

Note that the jagged *krx20*-expression domains upon Blebbistatin treatment, and how this enhances the effect of EphA4a-MO. IS is partially rescued in morphants upon Calyculin treatment. Dorsal views with anterior to the left. (M) Quantification of the IS for embryos in experiment (J-L) (dashed bars), and comparison with control embryos (solid bar).

Altogether, these results suggest that mechanical barriers act downstream of EphA/Ephrin signaling to segregate cells from different rhombomeres.

4. Which is the origin of the hindbrain boundary cell population: cell fate and behavior

The boundary cell population (BCP) is generated at interface between two rhombomeres once morphological boundaries are visible. The BCP display specific markers such *Rfng* and *Foxb1.2*. However, not much is known about this cell population and specifically, which is its origin and to what they five rise to. To study this we performed a detailed spatio-temporal analysis of the expression of a BCP marker such as *Rfng* and of a marker of rhombomeric territory such as *krx20*.

Although up to 16hpf *Rfng* is expressed only in r2 (Fig.34A), there is an onset of *Rfng* expression in the BCP at 18hpf and it is maintained selectively in this population until 30hpf (Fig.34B-C and data not shown).

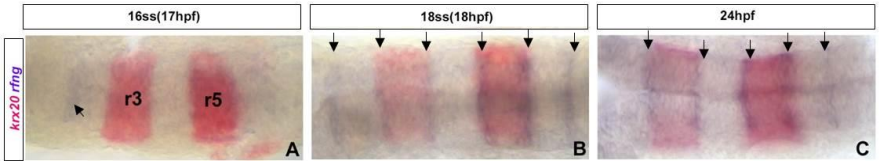

Figure 34. *Rfng* is restricted to hindbrain boundaries by 18 hpf. Double in situ hybridization for *krx20* (pink) and *rfng* (purple) at three different stages. Arrowheads indicate *rfng* expressed initially only in r2 (A) and later in boundary cells (B,C).

Double ISH for specific rhombomeric genes expressed complementarily, like members, showed that at every developmental stage all the cells of the hindbrain belong to one specific rhombomere, with no gap of expression in the interhombomeric boundaries, suggesting that boundary cells belong always to one of the two adjacent rhombomere. Therefore, the question we wanted to answer is whether the BCP is generated from only cells belonging to one rhombomere, or cells from adjacent rhombomeres acquire the boundary cell phenotype.

Boundary cells present a characteristic triangular morphology (Fig.26B') that can be visualized in embryos expressing membrane-tagged fluorescent proteins. We analysed tg[HRAS:GFP] 18hpf embryos that express ubiquitously a membrane-tagged version of GFP with confocal microscopy. As showed in Fig.35A, when focusing at the boundary (in this case r4/r5) we can observe the presence of two boundary cells, by their typical triangular shape. Once we injected tg[Mü4127] with *lyn-GFP* mRNA appears clear that those two cells are juxtaposed in the boundary of mCherry domain, one boundary red cell is contacting one boundary red-negative cell (Fig.35B).

To fully demonstrate that BCP originate from adjacent rhombomeres, we performed a double *in situ* hybridization staining for *krx20*, expressed in r3 and r5, and *Rfng*, a boundary marker. *Rfng* is expressed by one *krx20*-positive cell, which belongs to r5, and by one *krx20*-negative cell that is part of the adjacent rhombomere 4 (Fig.35C). Higher magnification of same analysis in the r3/r4 boundary showed similar results (Fig.35D-F), clearly demonstrating this statement.

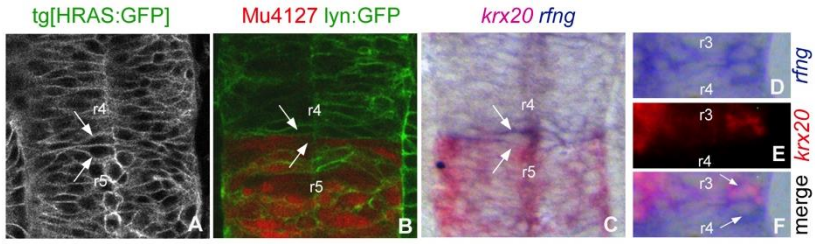

Figure 35. Adjacent rhombomeres contribute to the boundary cell population. (A) b:actin-HRAS-GFP transgenic embryo. (B) Mu4127 embryo injected with lyn-GFP mRNA. (C) Double in situ hybridization for *krx20* and *rfng*, focusing in r4/5 and in (D-F) r3/4 boundary. Dorsal views with anterior to the top. Arrows indicate boundary cells.

This result was confirmed by cellular analysis. Tg[elA:GFP] embryos were assayed for ISH for *Rfng*, followed by GFP immunodetection to label for r3 and r5. After sagittal cryosections we could observe the presence of both

GFP-positive *Rfng*-positive and GFP-negative *Rfng*-positive cells at the boundaries (Fig.36).

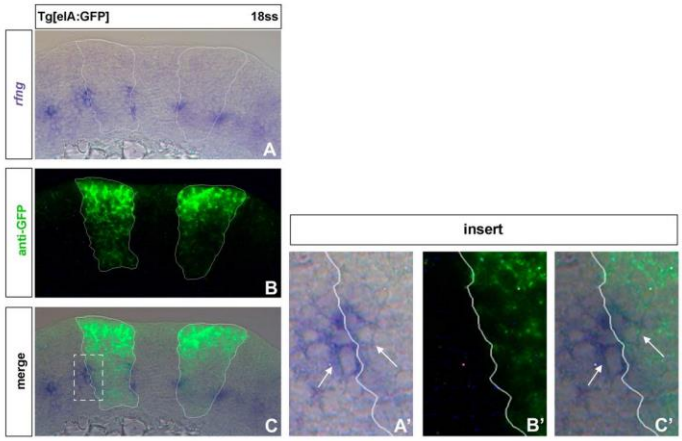

Figure 36. Adjacent rhombomeres contribute to boundary cells. Whole–mount ISH for *rfng* (A) followed by immunostaining for GFP (B) of tg [elA:GFP] embryos at 18hpf. (C) Merge of (A) and (B). (A'-C') insert of r2/3 boundary Arrows indicate cells from both rhombomeres contributiong to the BCP. Solid white line represents the limit of r2/r3.

DISCUSSION

Cell sorting is the main mechanism involved in boundary refinement

Previous evidences showed that events of cell plasticity can occur in the hindbrain and that the cells are able to change their fate. Trainor et al demonstrated that transplantation of rhombomeric cells into another rhombomere leads to the changing of the molecular profile of those cells (Trainor and Krumlauf, 2001). Overexpression of *krox20* is able to induce in an autonomous and non-autonomous manner the autoactivation of this gene, so the r3 and r5 identity (Giudicelli et al., 2001). Further experiments demonstrated that by genetic deletion of *krox20* gene r3 and r5 cells switch to closer rhombomeric fate (Voiculescu et al., 2001). On the other hand, several evidences support the hypothesis of cell sorting as a major mechanism operating in the sharpening of gene expression in rhombomeric boundaries (Cooke et al., 2005; Kemp et al., 2009).

We reasoned that experimental models used to support cell plasticity unveil hypothetical competences of the cells to change their identity. In the *krox20* null mice, r3 and r5 cells do not enter in their fate. Transplantation experiments are also unnatural conditions in which the cells find an unexplored territory and can switch their fate. All these conditions do not represent what occur in the wild type background, they only show the competence for plasticity, the possibility of the cells to reprogram themself but this does not mean that this is what really occurs in the cells at the boundaries.

Knock-in transgenic mice that express reporter cassettes in a given gene locus, allowed to follow the fate of the cells that once expressed the targeted gene. We decided to take a similar approach using zebrafish, by the means of two different transgenic reporter lines: tg[elA:GFP] and tg[Mü4127] that are

reporters of *krx20* transcription and recapitulate *krx20* expression with slight differences in time.

We demonstrate by different approaches that cell sorting is the major mechanism operating in the sharpening of gene expression in rhombomeric boundaries, independently of the cell identity and the position along the AP axis. A recent report suggested that an attenuation mechanism relying on intracellular noise induces cells to switch their identity during r4/r5 boundary sharpening (Zhang et al., 2012). Their model proposes that noise in the Retinoic Acid (RA) morphogen gradient can lead to rough gene expression boundaries initially, and that sharpening is driven by noise in the expression of *hoxb1a* and *krx20*, due to induced switching between expression of one gene and the other (Zhang et al., 2012). However, we observe only cell-sorting events at the rhombomeric boundaries, either by: i) analyzing single cell trajectories and behaviors (such as cell division), ii) cell tracing using stability of fluorescent proteins versus less stability of mRNA, or iii) trying to unveil any possible cell plasticity events downregulating the cell sorting, and we could not find evidences for cell switching. Nevertheless, this difference between our results and theirs might be explained by the fact that the cells undergoing plasticity display very low *krx20*-expression, as they pointed out in their work, which might not be detectable with our transgenic lines.

Interestingly, another difference in our study is that all rhombomeric boundaries behave similarly, regardless of their AP position, meanwhile Zhang et al describe cell switching depending on RA fluctuations mainly in r4/r5. Since r4/r5 is the first rhombomeric boundary to appear (Lecaudey et al., 2004; Maves et al., 2002) and it is evolutionary conserved (Jimenez-Guri and Pujades, 2011) it is possible that r4/r5 is under such evolutionary pressure of being properly regulated that it might undergo dual refining mechanism based in both cell sorting and cell plasticity events, acting with different temporal specificities, since we do not see cells losing *krx20*-expression and changing identity in our temporal frame study.

Another point is not considered in this work is that *hoxb1a* is responsible of *krox20* activation in r3/r4 border in conferring r3 character not only defining r4 identity, they showed a moment in which cells express both genes (Wassef et al., 2008). May be this can be also true for r4/5 border and *krox20*/*hoxb1* co-expression can represent a state in which cells are acquiring *hoxb1*-activated *krox20* character and not a jumping from r4 to r5 identity before taking a decision.

Interestingly, a recent report discovered that the sharply delineated pattern of neural progenitor domains along the DV axis forms through sorting of specified cells. They found that specified progenitors of different fates are spatially mixed and cell sorting rearranges them into sharply bordered domains (Xiong et al., 2013). May be the *krx20* activation is the result of both, interpretation of morphogen concentration and a gene regulatory network, which are spatially inaccurate and a cell-autonomous mechanism (cell sorting) is needed for refinement. Since the formation of spatially distinct domains faces noise at multiple scales, most probably multiple strategies are used to achieve robust patterning.

The link between our results and the models previously proposed where in *krox20*$^{-/-}$ mice r3/r5 cells lose their character (Voiculescu et al., 2001), may suggest that r3 and r5 need *krox20* on top of other transcription factors. In other words, its absence does not mean a change in fate but a lack of character acquisition and this is why they remain positive for *Hoxa2* or *Hoxb1* in r3 and *Kreisler* in r5.

Actomyosin barriers segregate cells at rhombomeric boundaries

The key challenge to rhombomeric boundaries we have detected is the division of the cells at the boundary. Mitotic cells incurring into the adjacent rhombomeres are pushed back to their rhombomere of origin, suggesting a mechanical barrier is involved in keeping different cell populations segregated.

The finding that differential cell adhesion, cortical tension and Eph/Ephrin signaling can each mediate cell segregation suggest that they can be recruited to be used as alternative mechanisms for different boundaries and/or at different stages of development. We wanted to investigate whether these mechanisms may play a alternative or synergistic role in the segregation of different rhombomeric cells.

Here, we provide evidences of the presence of actomyosin cables at the interhombomeric boundaries, and show that Myosin II function is required for restriction of cell intermingling. Our experiments with pharmacological drugs that enhance or decrease the stability of the actomyosin complex in a very precise time window demonstrate that actomyosin cables are functional, and this can be modulated upon specific experimental conditions. Interestingly, it has been reported that Myosin II is active in the hindbrain at 18hpf peaking at 21hpf (Gutzman and Sive, 2010), the period when morphological rhombomeric bulges are visible. In addition, mutants for *mypt1*, a Myosin II phosphatase mutant that display an overactive Myosin II, display similar defects to our experiments with Calyculin A: the neural tube is narrower and indentations in the neural tube are deeper at the morphological boundaries than in control embryos. We have detected actomyosin cables in the apical side of the neuroepithelial cells, although a readout of Myosin II activity, pMRLC (phosphorylated Myosin Regulatory Light Chain), was reported to localize in the basal as well as in the apical side of the neural tube

during lumen formation (Gutzman and Sive, 2010). This is probably due to the fact that Myosin II and Actin have pleiotropic functions: they are important for neuroepithelial cell shape, rhombomere morphogenesis and ventricle expansion from 24hpf onwards (Gutzman and Sive, 2010), and for actomyosin fiber assembly from 15hpf as we show in our report. We demonstrate that actomyosin-based barriers are involved in segregating cells at rhombomeric boundaries and keep them apart, since embryos in which the actomyosin fiber has been dismantled display a certain degree of rhombomeric cell mixing (see Fig.38 for model).

Previous models for cell sorting predicted that boundaries formed as a consequence of different rhombomeric cell types having distinct adhesive properties. They also brought up Eph/Ephrin signaling as an important factor in maintaining the boundaries between adjacent odd- and even-numbered rhombomeres (Batlle and Wilkinson, 2012; Dahmann et al., 2011). Our data helps to understand how the juxtaposition of different rhombomeric cells triggers actomyosin assembly interfaces along rhombomeric boundaries through Eph/Ephrin signaling. We showed that the actomyosin cable is located apically, there is a single cable and that it seems to be in the Ephrin-positive rhombomere. However, because insufficient optical resolution we have been unable to reassure this observation. Nevertheless, upon abrogation of Eph/Ephrin signaling actomyosin cables are perturbed and cells mix with the adjacent rhombomere neighbors. In addition, this phenotype is partially rescued by enhancing Myosin II function, suggesting that these cables, not completely dismantled in the downregulation of the EphA4a, upon favorable conditions can be functionally restored to a wild type phenotype. These evidences suggest that assembly of actomyosin fibers is downstream of Eph/Ephrin signaling, and this is crucial to maintain rhombomere sharpening. Whether this mechanism acts in parallel or downstream to other known roles in cell adhesion/repulsion of Eph/Ephrin signaling remains to be shown. To this

end, one possible molecular mechanism would be that Ephrin-reverse signaling is responsible for recruiting PDZ-domain proteins involved in actomyosin assembly, and therefore the key factor for assembling the mechanical barrier (Klein, 2012). The other option is that Eph receptor upon ligand binding enhances Rock activation, which inhibits F-actin depolymerization and MLCP activity, favoring accumulation of actomyosin cables as shown in a recent work where actomyosin-based contraction is responsible for specific sorting of neuronal auditory projections (Defourny et al., 2013).

We tested whether the other two alternative Eph/Ephrin dependent mechanisms could play a synergistic role with the actomyosin barrier.

Eph receptors and Ephrin ligands are expressed in adjacent somites, very similar to their expression in adjacent rhombomeres. Within the tissue, interplay between Eph/Ephrin signaling and ligand-independent integrin clustering drives restriction of de novo ECM production to somite boundaries (Julich et al., 2009). After analysis of integrin ($\alpha5\beta1$) clustering – and therefore integrin activation- and fibronectin extracellular fences within the interhombomeric boundaries and we did not observe any expression of FN or enrichment of Itgα5:GFP at the rhombomeric boundaries, although we did observe their expression in the intersomitic boundaries. This tells that there are not ECM mechanical barriers in the hindbrain.

With same rational, one mechanism by which Eph/Ephrin signaling can drive segregation is that cell repulsion creates differential adhesion. Recent studies in epithelial cells revealed a mechanism by which EphB/EphrinB interactions regulate the formation of E-cadherin-based adhesions (Solanas et al. 2011). EphB receptors interact with E-cadherin and with the metalloproteinase ADAM10 at sites of adhesion. Their activation induces shedding of E-cadherin by ADAM10 at interfaces with Ephrin-B1-expressing cells. This process results in asymmetric localization of E-

cadherin and, as a consequence, in differences in cell affinity between EphB-positive and EphrinB-positive cells. With this in mind, we liked to investigate the contribution of ADAM activity in the restriction of cell intermingling within rhombomeres. EphA4 is expressed in r3 and r5, and EphrinB3 is expressed in r2, r4 and r6. Our hypothesis was that Eph/Ephrin signaling controled ADAM10 activity in the hindbrain boundaries, and therefore shedding of Cadherin in these boundaries. This would lead to differential adhesion between EphA4-positive cells and EphrinB3-positive cells avoiding cell mixing. To do so we took three different approaches: i) to investigate the expression of cadh2 (N-cadherin) in the hindbrain by immunostaining, or ii) by injection of mRNA (Stockinger et al., 2011), and iii) to make use of the specific ADAM10 inhibitor (Hoettecke et al., 2010). In the two first scenarios we would expect a downregulation of cadh2 expression at the boundaries, and in the second we expected rhombomeric cell intermingling. However, in any of these approaches we got evidences to support the role of this mechanism in rhombomeric cell segregation.

As a summary, the picture that emerges from our results is the existence of a conserved strategy between vertebrates and Drosophila based in actomyosin-driven mechanical forces to sort cells at compartment boundaries. Another relevant aspect of our study, also related to Eph/Ephrin being upstream of actomyosin cable formation, is that this sharpening mechanism can be a common strategy to be used for other boundaries where this signaling pathway is involved, such as gut or somites.

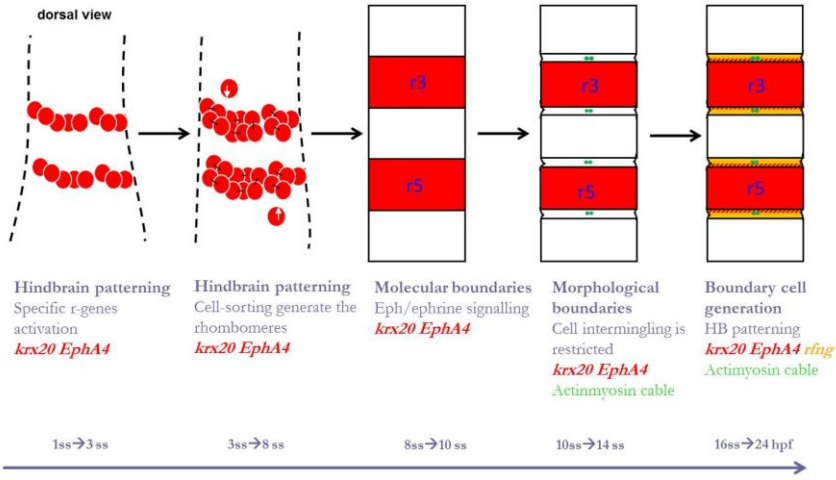

Figure 37. Model of segmentation in zebrafish hindbrain development. During hindbrain patterning cells start to express specific rhombomeric-genes (1-3ss stage). Cell-sorting intervene to generate functional rhombomeres (3-8ss). Eph/Ephrin members are involved in the refinement of molecular boundaries (8-10ss). Formation of actomyosin cable leads to the formation of morphological boundaries that restrict cell intermingling (10-14ss). Both adjacent rhombomeres contribute to the formation of boundary cell population (16ss-24hpf).

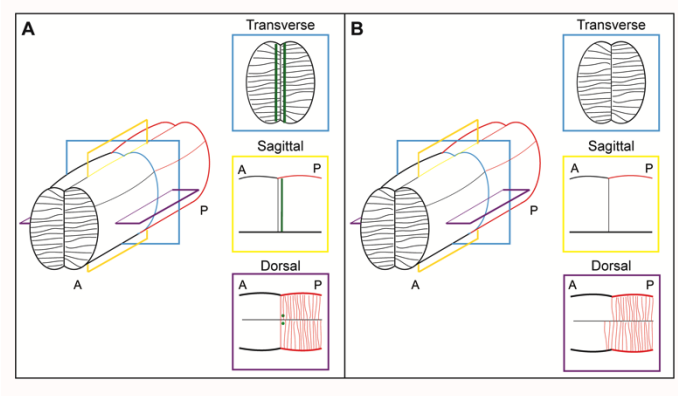

Figure 38. Model for the requirement of actomyosin cables in the interhombomeric boundaries to keep different rhombomeric cell populations segregated. Schematic 3D-representation of a hindbrain territory depicting two adjacent rhombomeres. Three different orthogonal views are taken from this scheme: transverse (blue), sagittal (yellow) and dorsal (purple). Actomyosin cables are represented as green lines in transverse and sagittal views and as green dots in the dorsal view. To help clarity, in the dorsal view cells are represented only for the

posterior rhombomere (red cells). A) DMSO, Calyculin or CRTL-MO embryos. Note the sharp boundary in the dorsal view. B) Blebbistatin, Rockout and EphA4a-MO embryos. Actomyosin cables are dismantled and cells from the posterior compartment cross the boundary to the anterior compartment. AP axis is indicated in the diagram

Future plans

The last part of the work was dedicated to the analysis of boundary cells, where we showed that boundary cells are contributed by adjacent rhombomeric cells (Figs.34-36.).

Evidences showed that boundary cells have an important role in instructing neighbouring cells, via cell-.to-cell contact (Cheng et al., 2004;Qiu et al., 2004) and also acting as organizer emanating signaling molecules that are involved in the correct location of neural progenitors (Gonzalez-Quevedo et al., 2010;Terriente et al., 2012). Old papers have proposed that boundary cells have a reduced rate of proliferation according to BrdU incorporation (Guthrie et al., 1991) and that they do not undergo neurogenesis. Moreover, the size of the boundary cell population does not increase at the same rate that the rhomberes (Fig.34). These evidences pointed out the attractive hypothesis that boundary cell population could represent a stem cell niche, where they could enter in the cell-cycle only in response to specific local stimuli and divide asymmetrically to generate a neural progenitor and a stem cell to renew stem population, or they could have a lower cell cycle rate than rhombomeric cells. This can explain their reduced BrdU incorporation rate and the fact that the size of boundary domain is constant during development while rhombomeres increase in volume. To rule out this, we would like to quantify the cell-cycle length and to perform an in vivo global cell-tracking of the boundary cell population.

1. Measurement of the cell-cycle length in boundary and non-boundary cells

To test our hypothesis we are quantifying the cell-cycle length in boundary cells compared with the rest of rhombomeric cells. To do so, we are performing a double staining for BrdU and IddU, two analogous of the timidine that can be integrated in the DNA in the S-phase cells. Embryos are initially incubated with IddU and after a given period incubated with both BrdU and IddU and then immunostained for both molecules. The cells that exit S-phase during the first incubation are not going to be labeled with anti-BrdU. Respecting the following equation we will obtain the duration of the total cell-cycle (*Tc*), where *Ti* is the interval between Iddu and IddU/BrdU incubation, *Lcells* is the amount of single-labeled cells, which left S-phase during *Ti* (Boehm et al., 2010).

$$T_c = T_i \frac{Total_{cells}}{L_{cells}}$$

Counting single BrdU-positive cells and double BrdU- and IddU-positive cells in the interhomberic boundaries and in a territory of the same size within the rhombomere will know if the rate of proliferation is lower in boundary cell population.

3D+time tracking of boundary cells

A short stay in the lab of Dr. Peyriéras (Institut de Neurobiologie Alfred Fessard, CNRS Gif-sur-Yvette, France) gave me the possibility to carry out a 3D+time tracking of boundary cell population using *in vivo* time-lapse, which represent the best approach in order to understand the behavior of this population during development.

We injected *H2B-mCherry* mRNA in a tg[elA:memb-GFP] embryo , at 4-8-cell stage to get a mosaic red nuclear staining and membrane-staining in r3 and r5. We imaged hindbrain development with 2-Photon microscopy from 18hpf to 42hpf. We obtained several videos that are underoging data

processing using the BioEmergences platform (Gif-sur-Yvette). They developed algorithms that recognize all the cell nuclei in each 3D image and automatically track overtime, detecting also mitosis.

We will use the visualization tool MOVIT, designed by the Peyriéras group, which was specifically designed to visualize and validate the described data. Its validation unit includes the possibility of correcting false positives (removing nuclei), false negatives (adding nuclei) and adjusting nuclei positions. It is also possible to verify cells lineage by validating the links between their temporal trajectories, removing false mitosis, creating new links to manually added nuclei, etc.

Once the data will be available, we are going to visualize boundary cells trajectories and in particular answer whether this population contribute to non-boundary population via asymmetric division or it remain in the interface of two adjacent rhombomeres.

CONCLUSIONS

Conclusions

1. *In vivo* global cell-tracking experiments demonstrate that rhombomeric cells do not present any cell plasticity event, independently of their position along the AP axis;

2. Single-cell tracking showed that rhombomeric cells in that are in "wrong" territory are sorted out to the territory of origin;

3. Fake cell-tracing confirms that there are no cell plasticity events that are unveiled when cell-sorting is abolished;

4. All previous evidences support the hypothesis that cell sorting is the main mechanism in the refinement of molecular boundaries in the vertebrate hindbrain;

5. Analysis of cell divisions close to the hindbrain boundaries showed that boundaries are challenged upon cell division, suggesting the presence of mechanical barrier;

6. FN matrix assembly is not involved in the formation of physical barrier that prevents cell intermingling;

7. An actomyosin cable is present at the interhombomeric boundaries;

8. Pharmacological inhibition of myosin II activity leads to dismantling of the actomyosin cable;
9. Pharmacological inhibition of myosin II activity leads to rhombomeric cell intermingling, suggesting that indeed the actomyosin cable is responsible of the cell segregation;

10. Linearity of the boundary is compromised after myosin II inhibitor treatments;

11. Eph/Ephrin signaling is upstream of the actomyosin cable formation. Downregulation of EphA4 leads to the disappearance of the cable and to rhombomere cell intermingling;

12. Constitutive activation of myosin II in Epha4 morphant embryos results in the rescue of cable assembly and cell segregation. This demonstrates that Eph/Ephrin signaling is controlling the assembly of the actomyosin cable.

13. Cells from both adjacent rhombomeres contribute to the formation of the boundary cell population.

MATERIALS AND METHODS

1. Zebrafish strains and maintenance

Zebrafish (*Danio rerio*) embryos were produced by paired mating of adult fish in the PRBB zebrafish facility by standard methods. Strains were maintained individually as inbred lines. All procedures used have been approved by the institutional animal care and use ethic committee (PRBB–IACUC), and implemented according to national rules and European regulations.

Embryos were grown in 50 mm-rounded petri dishes (Sterlin, Cat#121V) in diluted methylene blue (2 ml of 0.1% methylene blue, to 1 liter of fish water) at 28.5ºC. Staging of the embryos was expressed in hours post fertilization (hpf) or somites formed (ss) is according to the zebrafish book (Westerfield, 2000).

Ttransgenic lines used

Tg[Mü4127] is an enhancer trap line in which the trap cassette containing a modified version of Gal4 (KalT4) and mCherry (KalTA4-UAS-mCherry cassette) was inserted in the 1.5Kb downstream of *krx20* gene (Distel et al., 2009).

4xKaloop is a stable transgenic effector strain that carries a bicistronic 4xUAS effector construct driving GFP expression as a reporter that once activated, continuously maintains its own expression by constantly providing the Gal4 activator (KalT4) in a feedback loop (Distel et al., 2009).

Tg[elA:GFP] is a stable reporter line where chicken element A was cloned upstream of the *gfp* reporter in a modified pTol2 vector (Chomette et al., 2006;Labalette et al., 2011;Stedman et al., 2009).

Tg[lifeactin::GFP] is a stable reporter line that allows the visualization of F-actin. It contains the actin binding protein 140 (Abp140) domain fused with GFP under the control of β-actin promoter (Behrndt et al., 2012).

Tg[utrophin::GFP] is a stable reporter line that allows the visualization of F-actin. The calponin homology domain of utrophin (Utr-CH) has been fused to GFP under the control of β-actin promoter (Behrndt et al., 2012).

Tg[myosinII::mcherry]: MYL9L::mCherry; myosin II (non-cardiac myosin associated to actin filaments) protein fused with mCherry under the control of β-actin promoter (Behrndt et al., 2012;Maitre et al., 2012).

Tg[β-actin:HRAS-EGFP] HRAS subunit fused with GFP under the control of b-actin promoter that homogenously labels cell membranes (Cooper et al., 2005).

2. Detection of gene expression by whole-mount mRNA in situ hybridization (ISH)

In situ hybridization is a technique for detection of specific nucleic acid sequences within tissues. RNA sequences are visualized by hybridization with labelled probes that are complementary to the sequence of interest. Depending on the method of colourization ISH can be chromogenic or fluorescent.

The following steps are the general ones used for chromogenic ISH. In the case that Tyramide Signal Amplification (TSA)-ISH was used, differences are indicated.

2.1 Fixation and permeabilization of the embryos

- Collect embryos at the desired stage in PBT and then fix in 4% PFA/PBT O/N at 4ºC.
- Wash 3X 5min PBT
- Dehydrate the embryos through an increasing MeOH/PBT series: 25%, 50%, 75%, 100%; 5 min each.
- The embryos can be stored at -20ºC in MeOH 100%.
- Rehydratation through 75%, 50%, 25% MeOH/PBT 5 min each.
- Wash 2 X 5min PBT.
- For permeabilization of tissue incubate in 10 μg/μL proteinase K (pK). The time of incubation is approximately according to the stage of the embryos: younger than 2ss no pK is needed, for 2-4ss embryos 3 min pK; for 5-15ss embryos 5 min pK; for 15-18ss 8 min, for 18ss-24hpf 8 min.
- Rinse carefully with PBT.
- Post-Fix for 20min in 4%PFA in PBT
- Wash 3X 5min PBT. and store in PBT at 4ºC

Embryos are now ready for ISH or immunohistochemistry.

2.2 Antisense riboprobe synthesis

cDNAs of the genes of interest are cloned into vectors flanked by T7, T3 or SP6 RNA polymerase promoter sequences. The probes used are the following:

Probe	**Vector**	**Linearization enzyme and RNA polymerase**
Krox20	pBS KS	XbaI/ T3
Kalta4	pCS2	SpeI/T3
gfp	pCS	HindIII/T3
Rfng	pGemT-easy	SpeI/T7

Table 1 Constructs used as templates for *in vitro* transcription reactions

The plasmids need to be linearized before riboprobe in vitro transcription. For linearization incubate 2h at 37ºC the following:

- 1 µg of plasmid DNA
- 1 µL of appropriate restriction enzyme
- 1x restriction enzyme buffer
- H_2O to the final volume of 20ul

2.2.1 Stop the digestion and precipitate the linearized cDNA:

- 1/20th volume 0.5M EDTA
- 1/10th volume of 3M Na Acetate
- 2 volumes of ethanol
- Mix well and precipitate at –20°C for 1h.
- Centrifuge 30 min at 4ºC at 13000 rpm.
- Discard the supernatant
- Add 500 µL of 70% ethanol
- Centrifuge 10 min
- Discard the supernatant

- Dry the pellet 15 min at 37ºC
- Resuspend it in 20 µL H_20
- Run 1 µL of linearized plasmid into a 1% agarose gel/1xTBE to verify the digestion
-

2.2.2 RNA In vitro transcription

To generate antisense probes, the linearized cDNA incubate 3h at 37ºC the following:

- 4 µl of linearized cDNA
- 40U RNAse inhibitor (Takara, Cat# 2313A)
- 40U of adequate RNA-polymerase
- DIG RNA labeling mix, Roche Cat#11277073910;
- FLUO RNA labeling mix Roche Cat#11685619910):
- 1mM Digoxigenin-UTP mix *or Fluorescin-UTP UTP if fluo-probe is required* (0.35mM DIG-UTP *or FLUO*-UTP, 0.65mM UTP, 1mM ATP, 1mM GTP, 1mM CTP)
- Sterile mQ-H_2O to final volume

Purification of riboprobes:

- Increase volume to 50 µL with mQ-H_2O and clean up reaction on a Roche mini Quick Spin RNA column (Roche Cat#11814427001) according to Roche's directions
- Run 1 µl into a 1% agarose gel / 1xTBE
- Keep the riboprobe at -20ºC

2.3 Hybridization

Prehybridize embryos previously fixed and permeabilized for at least 1 hour in 200 µl of pre-hybridatization mix (see in list of solutions) at 70ºC.

- Add 1µl of riboprobe to hybridatization mix and let the hybridize O/N at 70ºC

2.4 Post-hybridization washes

- Pre-warm washing solutions before adding to embryos.
- Wash 5 min in 66% hyb mix, 33% 2 x SSC at 65ºC
- Wash 5 min in 33% hyb mix, 66% 2 x SSC at 65ºC
- Wash 5 min in 2 x SSC at 65ºC
- Wash 1 x 20 min in 0.2 x SSC +0.1% Tween-20 at 65ºC
- Wash 2 x 20 min in 0.1 x SSC+0.1% Tween-20 at 65ºC
- Wash 5 min in 66% 0.2 x SSC, 33% PBT at room temp.
- Wash 5 min in 33% 0.2 x SSC, 66% PBT at RT.
- Wash 5 min in PBST at room temp

Only for TSA-based ISH:

- *Incubate in 2% H_2O_2*
- *Wash x 5 min in PBT*

2.5 Immunostaing with anti-digoxigenin *or anti-fluorescin*

- Incubate washed embryos in blocking solution (PBT plus 2% goat serum, 2 mg/ml BSA) 1 hour at room temp.
- Depending on the technique and the riboprobe, choose the appropriate antibody. Alkaline-phosphatase (AP) conjugated anti-DIG *or anti-FLUO* for chromogenic precipitate using NBT/BCIP or FastRed as AP substrates, Horseradish peroxidase (POD) conjugated anti-DIG *or anti-FLUO* for TSA-based staining.
- Dilute the antibodies in blocking solution according to the following table.

Antibody	**Dilution**	**Supplier**
Anti-DIG-AP Fab fragments (alkaline-phosphatase conjugated anti-DIG)	1:2,000	Roche (Cat#11093274910)
Anti-FLUO-AP Fab fragments (alkaline-phosphatase conjugated anti-FLUO)	1:1,000	Roche (Cat#1426338)

Anti-DIG-POD Fab fragments (Peroxidase-conjugated anti-DIG)	1:250	Roche (Cat.#11093274910)
Anti-FLUO-POD Fab fragments (Peroxidase-conjugated anti-FLUO)	1:500	Roche (Cat#1426346)

Table 2. List of antibodies used for ISH

- Incubate with the antibody overnight at 4ºC or 2h at RT. For GFP staining after ISH the anti-GFP Ab is added at this point (dilution and Ab reference)
- Wash 5 x 15 min in PBT and then wash over day and O/N.

2.6 Development of the staining

The colorization can be chromogenic (NBT/BCIP or FastReed) or fluorescent (TSA- or FastRed-based):

Chromogenic staining

- wash 3 x 5 min in NTMT buffer
- Transfer the embryos from the tube into one well of 24-wells plate
- For blue chromogenic colorization: Dilute 7.5µl of NBT (Roche, Cat#1383213) and 4.5µl BCIP (Roche, Cat#11383221001) for blue/purple colorization into 1ml of NTMT buffer
- add 500µl of this mix to embryos after removal of the last NTMT wash and let them develop until desired step

Fluorescent staining

Fast-Red based:

- wash 3 x 5 min in Fast-Red buffer, (pH 8.2)
- Dissolve one Fast Red tablet (Roche, Cat#1496549) into this buffer and then filter it.
- Transfer the embryos from the same tube in one well of 24-wells plate
- add 500µl of this mix to embryos after removal of the last wash and wait for the colorization

TSA-based:

- Incubate in Tyramide-Cy3 *or Tyramide-fluo* 1:100 in 1X Amplification Diluent (PerkinElmer) for 30-60 min.
- Inactivate peroxidase with 2% H_2O_2
- Wash several times and then in case of double ISH follow with procedure explained in section 2.6

Check every 10 minutes if the colorization because the time of incubation is always empiric and it only depends on the riboprobe.

- Once the precipitate is formed stop reaction by washing embryos 2-4x in sterile water
- In the case of double is situ follow with the next part, otherwise:
- store at 4°C in the dark in low-pH (5.5) PBS; 1mM EDTA
- If GFP staining is required follow with secondary Ab incubation (see section 3.)

After colorization the embryos can be stored at 4ºC in acid PBS or mounted for direct visualization or for criosectioning, depending on the experiment

2.7 Double *in situ* hybridizations

Double *in situ* hybridizations can be performed by hybridizing embryos with DIG- and FLUO-labelled probes at the same time in step described in section 2.2., and then detecting the DIG and the FLUO with sequential alkaline reactions using different chromogenic or fluorescent substrates.

- Directly after stopping the first coloration reaction with sterile water washes, incubate embryos in 500µl 0.1M Glycine pH2.2 for 10 minutes
- Wash 4x 5 min in PBST
- Incubate in blocking solution (PBT plus 2% goat serum, 2 mg/ml BSA) 1 hour at room temp.
- Prepare second antibody (anti-FLUO-AP) by diluting it in blocking solution; 1:2,000.

- Incubate with the antibody for 2 hours shaking at room temp, or overnight at 4C.
- Wash 5x 15 min in PBT *(you can leave it in one of the later PBT washes at 4°C overnight)*

Wash 4x 5 min in NTMT (recipe at the end) and from this point the same procedure as in section 2.5 is followed)

2.8 Glycerol passages

After whole-mount ISH or immunohistochemistry pass the embryos in an increasing concentration of glycerol

- Wash in 25% glycerol/ 75% PBT for about 15min.
- Wash in 50% glycerol/ 50% PBT for about 15min.
- Wash in 75% glycerol/ 25% PBT
- Wash in 100% glycerol.

The embryos can be stored at 4ºC, directly flat-mounted, or prepared for cryosectioning.

2.9 Flat-mounting in slides

- Deyolk multiple embryos in a 10mm-rounded plate (Nocken, Cat#821135)
- Transfer 10 embryos one by one and lined up into a slide with 4 "posts" of high vacuum grease,
- Orient them to have the dorsal part up and then place a coverslip (18x18 mm, Menzel-Glaser Cat#BB018018A1) on top and gently press down until the embryo is flattened
- fill to the edges with in 50% glycerol/ 50% PBT

The embryos are ready to be visualized in the microscope.

2.10 Cryosectioning

Before cryosectioning, embryonic tissue needs to be cryoprotected. For this:

- Keep embryos in 15% sucrose O/N 4ºC.

- Change to 7.5% gelatin 15% sucrose in PBS 2h 37ºC.
- Transfer embryos embedded in 15%sucrose/7.5%gelatine in PBS to cryomold and orientate them for proper transverse, sagittal or coronal sections.
- Dip block into -80ºC pre-cooled 2-methil-butane 1 min.
- Keep blocks at -20ºC until use.
- Before sectioning keep blocks in the cryostat chamber 15 min.
- Adhere blocks to the cryostat sectioning support with OCT compound (Tissue-Tek, Cat#4583).
- Make 20 um cryostat sections.
- Collect sections in Superfrost slides, from this moment maintain the slides frost or wet at RT, avoid drying.
- Treatment of the slides
- Rinse the slides in PBT and then they can be processed for image analysis, ISH or immunohistochemistry.

To mount slides with sections, add 200 µL of Mowiol (Calbiochem, Cat#3475904) on the slide and put on the top the coverslips (24x60 mm, Menzel-Glaser Cat#BB024060A1).

3. Whole-mount immunohistochemistry

- Wash embryos 3x 15 min in PBT fixed and permeabilized them ()
- Block in 5%GS PBT at least for 1 hour
- Incubate O/N with Primary Ab (see table)
- Wash 3x 15 min in PBT
- Incubate 2h or O/N with secondary Ab (see table).
- Wash extensively.

Embryos can be passed to glycerol (see section 2.9) and stored or they can be prepared for: flat-mounting or cryosectioning, depending on the experiment

Primary antibodies	**origin**	**Dilution**	**Supplier**
anti-GFP	Rabbit	1:400	Torrey Pines Biolabs (Cat.#TP401)
Anti-HumanFN	Rabbit	1:200	Cat#F3648(Sigma)
Anti-DsRed	Rabbit	1:1,000	Clontech (Cat#632496)

Table 3. List of primary antibodies for immune staining

Secondary antibodies	**origin**	**Dilution**	**Supplier**
Alexa Fluor 488 anti-Rabbit IgG	Donkey	**1:200**	Invitrogen(Cat.#A21206)
Alexa Fluor 594 anti-Rabbit IgG	Goat	1:200	Invitrogen(Cat.#A11012)
Alexa Fluor 488 anti-mouse IgG	Donkey	1:200	Invitrogen(Cat.#A21202)
Alexa Fluor 594 anti-mouse IgG	Goat	1:200	Invitrogen(Cat.#A11005)

Table 4. List of primary antibodies for immune staining

4.Functional experiments

4.1 Loss of function (LOF) using morpholino injection.

Morpholinos are antisense oligomeres, designed to bind specific RNA by complementary sequence blocking either splicing or translation of the transcript.

Morpholino (Genetools, Virgina) are resuspended in water and maintained at -20ºC. In all the experiments EphA4-MO is used at 5-10 ng/nl and co-injected with p53-MO or injected in *p53*-/- mutant embryos to avoid off-target expression caused by toxicity (Gerety and Wilkinson, 2011).

Morpholino	Sequence	Reference
EphA4)	5'-AACACAAGCGCAGCCATTGGTGTC-3	(Cooke et al., 2005)
p53MO	5'-GCGCCATTGCTTTGCAAGAATTG-3'	(Robu et al., 2007)

Table 5. List of morpholinos used in this work

Embryos were injected at 1 cell-stage and let to develop at 28C until desired stages.

4.2 Gain of Function (GOF) by mRNA injection

4.2.1 mRNAs preparation

Capped mRNAs are synthesized with mMESSAGE mMACHINE (Ambion, Cat#AM1340) and resuspended in nuclease-free water.

The part of linearization and purification of the plasmid are identical as in section 2.1.1

4.2.2 In vitro capped-mRNA transcription

Mix and incubate 3h at 37°C the following:

- 10 µl 2X NTP/CAP
- 2 µl 10X Reaction Buffer
- 0.1–1 µg linear template DNA
- 2 µl Enzyme Mix

Purification of the capped mRNA

- Stop the reaction by adding 30µl
- Nuclease-free Water and 30µl LiCl Precipitation Solution.
- Mix thoroughly. Chill for 30min at –20°C.
- Centrifuge at 4°C for 30' at 13,000 rpm to pellet the RNA.
- Wash the pellet once with ~1ml
- 70% ethanol, and re-centrifuge at 13000 rpm.
- Remove the supernatant, let the pellet dry and resuspend it in 20µl of nuclease-free H2O
- Run 1 µL in a 1% agarose gel / 1xTAE
- Measure the concentration of the capped mRNA.
- Aliquot and store at -80°C

The day of injection defrost an aliquot and dilute to the desired concentration of injection. (see the table)

insert	Injection concentration (ng/µL)	Vector	Linearization enzyme and RNA polymerase	references
Lyn-GFP	25	pCSII	NotI/SP6	(Koster and Fraser, 2001)
itga5:GFP	100	pCSII	NotI/SP6	(Julich et al., 2009)

Table 6. cDNA containing full-lenght mRNAs used in this work

4.2.3 Preparation of the needles for injection

- Pull glass-capillary with this puller (Narishige, Model#PC-10) 1mmOD glass-capillary, then backload with 3 µl of injection material.
- Insert the needles in the microinjector.
- Break the needle tip gently pushing it against metal forceps.

- Adjust the volume of injection regulating the air pressure and test it in a mineral oil drop.

4.2.4 Preparation of injection-plate

- Spill 5ml of 1% agarose into a 150mm Petri dish and an ad-hoc designed mold is used to create parallel grooves on it.
- The groove has to have the right size of chorionated embryos
- Once the agarose is solidified the embryos are deposited in line within the groove to remain immobilized.

The embryos can be injected with 1nl of solution. Injection of both morpholinos and mRNAs are performed usually at 1-cell stage.

5. Confocal imaging and in vivo time-lapse

Confocal laser scanning images are acquired in the UPF-CRG Advanced Light Microscopy Unit, located in the PRBB and also in the Institut de Neurobiologie Alfred Fessard, CNRS Gif-sur-Yvette, France. For all the experiments we use inverted SP5 Leica systems.

Anesthetized live embryos of the indicated stage and genotype were embedded in 1% low-melting point agarose (LMA, Ecogen, Cat#AG-400) with tricaine, hindbrain was oriented close to the glass-bottom in a petri dish in order to obtain dorsal view in a inverted objective.

Single nuclei tracing was performed using tg[elA:GFP] embryos injected with *H2B-mcherry* mRNA at 4-8cell stage, in order to have a mosaic expression. Embryos were let them grow until 11hpf and then were, mounted for time-lapse imaging. Dimensions of the video showed in Fig. are the following:

Videos

3. voxel dimension (nm): **x** 387.5 **y** 378.8 **z** 1510.6, time frame: 90s; total time: 2h21 min; pinhole: 60.6 μm; zoom: 2; Obj.: 20x dry; NA: 0.70.
2) voxel dimension (nm): **x** 378.8 **y** 378.8 **z** 1531.4, time frame: 154.7s; total time: 4h36 min; pinhole: 66.7 μm; zoom: 2; Obj.: 20x imm; NA: 0.70.

Back-tracking of red nuclei of GFP+ and GFP-cells was repeated in three independent experiments and several cells were tracked (exp1→ n=41; exp2→ n=43; exp3→n=54) in tg[elA:GFP] embryos was performed in three independent experiment s. Cells were tracked manually from different DV level using ImageJ software.

6. Assessment of cable-like structures in live embryos and pharmacological treatments

6.1. Analysis of Cable-like structures

Anesthetized live embryos embryos at indicated stage were mounted as described in section 5

Once the LMA is solidified, the petri-dish is filled with E3 medium with tricaine in the presence or absence of the desired pharmacological drug.

Images were acquired in dorsal view with 0.6µm z distance, resliced to generate YZ confocal cross-sections and finally a maximal projection in XZ of the sections corresponding to the midline of the neural tube (where the actomyosin cable was visible) was done.

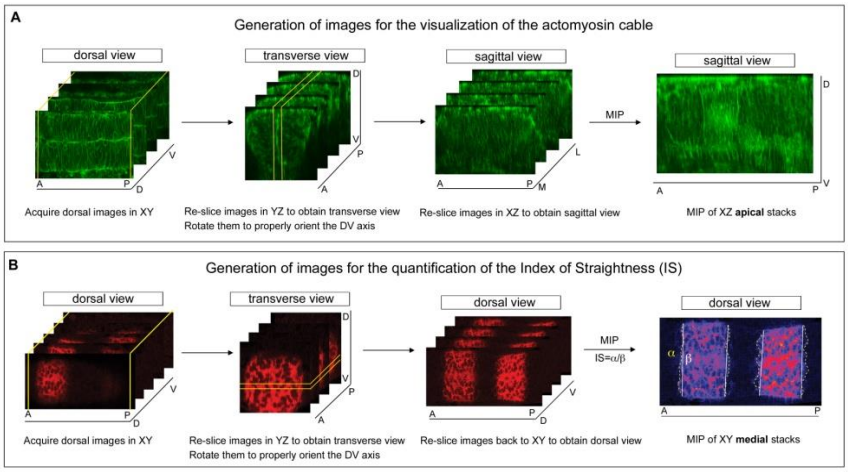

Figure 39. Scheme depicting the processing of the samples to obtain: (A) sagittal-like optical sections to observe actomyosin-cables in the apical side of the cells; and (B) dorsal view images to calculate the IS. (A) Embryos were mounted and dorsal images in XY are acquired in the confocal microscope. Using ImageJ/FIJI, all dorsal images are re-sliced in YZ and rotated if need to have a perfect DV orientation. Afterwards, re-slice all images in XZ to obtain sagittal views and select the apical XZ stacks to MIP. (B) Embryos were mounted and dorsal images in XY are acquired in the confocal microscope. Using ImageJ/FIJI, all dorsal images are re-sliced in YZ and rotated if need to have a perfect DV orientation. Then, re-slice images back to XY and select the stacks from the medial part of the neural tube to MIP.

6.2 Pharmacological treatments

Embryos of indicated stage and genotype are enzymatically dechorionated with pronase (Roche, Cat#11459643001) for 5min at RT. After getting rid of the pronase, they are washed and treated with the corresponding pharmacological agent diluted in E3 medium with tricaine (Sigma, Cat#A5040). As a negative control embryos are treated in 0.1% DMSO (Sigma, Cat#D2650) diluted in E3.

Live embryos were mounted, imaged and analysed as explained in section 5

Generally the treatments are made from 14hpf to 18-20 hpf.

Compound	Concentration used	Supplier
Blebbistatin	25 μM	Calbiochem (Cat# 203390)
Rockout (Rho Kinase Inhibitor III)	50 nM	Calbiochem (Cat# 555553)
Calyculin A	100 nM	Calbiochem (Cat# 208851)

7. Quantification of the Index of Straightness (IS)

The quantification of the Index of Straightness was based in the sharpness of the border of *krx20* expression. Whole-mount *in situ* hybridization for *krx20* was performed on 18hpf fixed embryos from the same batch, after different experimental conditions: control embryos, CTRL-MO or EphA4a-MO injected embryos treated with DMSO, Blebbistatin or Calyculin A. Confocal images were acquired in dorsal view of flat-mounted hindbrains covering the r3-r5 region with 1µm z distance. Images were then re-sliced to generate YZ confocal cross-sections to properly orient the embryos along the DV axis, and finally the same 5µm DV portion in every embryo was selected and re-sliced back to XY to obtain dorsal views. These stacks were then projected into a single dorsal view image (Fig.39B). Once images were obtained, we addressed the index of straightness (IS) of the *krx20* expression border doing the following: longitudes of the *krx20* expression border for r2/r3, r3/r4, r4/5 and r5/r6 boundaries were calculated with FIJI (yellow dotted line, □; Fig 37B), and also the theoretical straight distance of the *krx20*-expression border (white dotted line, □; Fig.39B). The IS is the ratio between □ and □. Since IS=1 would represent a completely straight boundary we plotted the values as a deviation from 1, representing a better indication of the deviation from straightness. In the plots SEM was used and the significance of results was assessed using the two-tailed Student's *t*-test.

8. Quantification of the Interkinetic Nuclear Migration (INM) Ratio

Tg[βactin:HRAS-EGFP] embryos at 18hpf after different pharmacological treatments were immunostained with: i) anti-pH3 to analyse the cells undergoing mitosis, ii) anti-GFP to visualize the plasma membranes and therefore singularize the cells, and iii) DAPI to position cell nuclei. Confocal image stacks with 1µm z and identical zoom were taken in the hindbrain region extending from r2 to r6. Then, an identical XY frame covering half of the neural tube from apical to basal side of the neuroepithelial cells was selected for each embryo (Fig.40B). Channels were split and green channel was subtracted from both blue channel and red channel to help to segment the cell nuclei (Fig.40B-D). Finally, we divided our chosen frame in two halves, one apical and one basal, and counted the number of nuclei located in both sides (Fig.40B'). To assess the Interkinetic Nuclear Migration Ratio we divided the number of apical and basal nuclei. The total number of pH3-positive cells was used as a readout of mitotic cells (Fig.40D'). Results were plotted in, SEM was used and the significance of the results was assessed using the two-tailed Student's *t*-test.

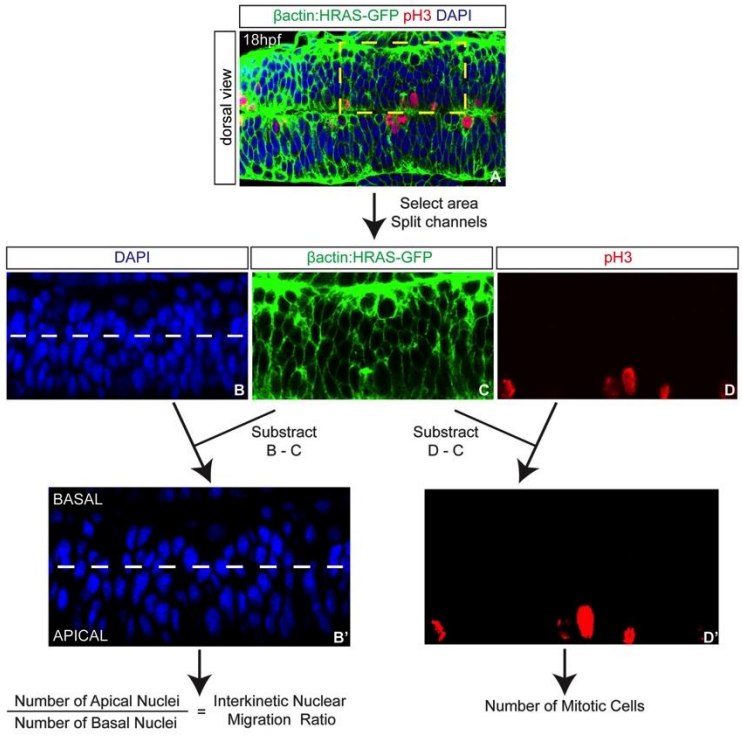

Figure 40. Scheme depicting the processing of the samples for the quantification of the Interkinetic Nuclear Migration Ratio and the number and position of mitotic cells. Tg[actin:HRAS-GFP] embryos were stained for anti-pH3 (red) and DAPI (blue) at 18hpf. To clearly singularize the cell nuclei, the intensity of GFP labeling the plasma membrane (C) was subtracted from the blue channel and the red channel (D). Then, either nuclei (DAPI-staining) or pH3-positive cells were counted in the desired regions.

List of solutions used

Hybridization Solution

- 50% formamide (Sigma, Cat#F7503)
- 5 x SSC
- 50 μg/ml heparin (Sigma, Cat#H3393)
- 500 μg/ml tRNA (Sigma, Cat#R6625)
- 0.1% Tween-20 (Sigma, Cat#P1379)

Adjust to adjust pH to 6.0

NTMT

- 100 mM Tris-Hcl, pH9.5
- 50 mM MgCl2
- 100 mM NaCl
- 0.1% Tween-20

Fastred buffer:

- 100 mM Tris Hcl, pH 9.5
- 400 mM HCl

E3 medium

- 5 mM NaCl
- 0.17 mM KCl
- 0.33 mM $CaCl_2$
- 0.33 mM $MgSO_4$

REFERENCES

References

Abello, G., Khatri, S., Radosevic, M., Scotting, P. J., Giraldez, F. and Alsina, B. (2010). Independent Regulation of Sox3 and Lmx1b by FGF and BMP Signaling Influences the Neurogenic and Non-Neurogenic Domains in the Chick Otic Placode. *Dev. Biol.* 339, 166-178.

Affolter, M. and Caussinus, E. (2008). Tracheal Branching Morphogenesis in Drosophila: New Insights into Cell Behaviour and Organ Architecture. *Development* 135, 2055-2064.

Akam, M. (1987). The Molecular Basis for Metameric Pattern in the Drosophila Embryo. *Development* 101, 1-22.

Alexander, T., Nolte, C. and Krumlauf, R. (2009). Hox Genes and Segmentation of the Hindbrain and Axial Skeleton. *Annu. Rev. Cell Dev. Biol.* 25, 431-456.

Aliee, M., Roper, J. C., Landsberg, K. P., Pentzold, C., Widmann, T. J., Julicher, F. and Dahmann, C. (2012). Physical Mechanisms Shaping the Drosophila Dorsoventral Compartment Boundary. *Curr. Biol.* 22, 967-976.

Altman, J. and Bayer, S. A. (1997). *Development of the Cerebellar System: In Relation to its Evolution, Structure, and Functions*, pp. 783. Boca Raton: CRC Press.

Amoyel, M., Cheng, Y. C., Jiang, Y. J. and Wilkinson, D. G. (2005). Wnt1 Regulates Neurogenesis and Mediates Lateral Inhibition of Boundary Cell Specification in the Zebrafish Hindbrain. *Development* 132, 775-785.

Aragon, F. and Pujades, C. (2009). FGF Signaling Controls Caudal Hindbrain Specification through Ras-ERK1/2 Pathway. *BMC Dev. Biol.* 9, 61.

Aragon, F., Vazquez-Echeverria, C., Ulloa, E., Reber, M., Cereghini, S., Alsina, B., Giraldez, F. and Pujades, C. (2005). vHnf1 Regulates Specification of Caudal Rhombomere Identity in the Chick Hindbrain. *Dev. Dyn.* 234, 567-576.

Artavanis-Tsakonas, S., Rand, M. D. and Lake, R. J. (1999). Notch Signaling: Cell Fate Control and Signal Integration in Development. *Science* 284, 770-776.

Barrios, A., Poole, R. J., Durbin, L., Brennan, C., Holder, N. and Wilson, S. W. (2003). Eph/Ephrin Signaling Regulates the Mesenchymal-to-Epithelial Transition of the Paraxial Mesoderm during Somite Morphogenesis. *Curr. Biol.* 13, 1571-1582.

Barrow, J. R. and Capecchi, M. R. (1996). Targeted Disruption of the Hoxb-2 Locus in Mice Interferes with Expression of Hoxb-1 and Hoxb-4. *Development* 122, 3817-3828.

Basler, K. and Struhl, G. (1994). Compartment Boundaries and the Control of Drosophila Limb Pattern by Hedgehog Protein. *Nature* 368, 208-214.

Batlle, E. and Wilkinson, D. G. (2012). Molecular Mechanisms of Cell Segregation and Boundary Formation in Development and Tumorigenesis. *Cold Spring Harb Perspect. Biol.* 4, 10.1101/cshperspect.a008227.

Becam, I., Rafel, N., Hong, X., Cohen, S. M. and Milan, M. (2011). Notch-Mediated Repression of Bantam miRNA Contributes to Boundary Formation in the Drosophila Wing. *Development* 138, 3781-3789.

Begemann, G., Schilling, T. F., Rauch, G. J., Geisler, R. and Ingham, P. W. (2001). The Zebrafish Neckless Mutation Reveals a Requirement for Raldh2 in Mesodermal Signals that Pattern the Hindbrain. *Development* 128, 3081-3094.

Behrndt, M., Salbreux, G., Campinho, P., Hauschild, R., Oswald, F., Roensch, J., Grill, S. W. and Heisenberg, C. P. (2012). Forces Driving Epithelial Spreading in Zebrafish Gastrulation. *Science* 338, 257-260.

Bell, E., Wingate, R. J. and Lumsden, A. (1999). Homeotic Transformation of Rhombomere Identity After Localized Hoxb1 Misexpression. *Science* 284, 2168-2171.

Benazeraf, B. and Pourquie, O. (2013). Formation and Segmentation of the Vertebrate Body Axis. *Annu. Rev. Cell Dev. Biol.*

Berggren, K., McCaffery, P., Drager, U. and Forehand, C. J. (1999). Differential Distribution of Retinoic Acid Synthesis in the Chicken Embryo as Determined by Immunolocalization of the Retinoic Acid Synthetic Enzyme, RALDH-2. *Dev. Biol.* 210, 288-304.

Boehm, B., Westerberg, H., Lesnicar-Pucko, G., Raja, S., Rautschka, M., Cotterell, J., Swoger, J. and Sharpe, J. (2010). The Role of Spatially Controlled Cell Proliferation in Limb Bud Morphogenesis. *PLoS Biol.* 8, e1000420.

Bossinger, O. and Cowan, C. R. (2012). Methods in Cell Biology: Analysis of Cell Polarity in C. Elegans Embryos. *Methods Cell Biol.* 107, 207-238.

Buceta, J., Herranz, H., Canela-Xandri, O., Reigada, R., Sagues, F. and Milan, M. (2007). Robustness and Stability of the Gene Regulatory Network Involved in DV Boundary Formation in the Drosophila Wing. *PLoS One* 2, e602.

Butler, A. B. (2005). *Comparative Vertebrate Neuroanatomy : Evolution and Adaptation*. Hoboken, N.J.; Chichester: Wiley-Liss; John Wiley distributor.

Canela-Xandri, O., Sagues, F., Casademunt, J. and Buceta, J. (2011). Dynamics and Mechanical Stability of the Developing Dorsoventral Organizer of the Wing Imaginal Disc. *PLoS Comput. Biol.* 7, e1002153.

Canela-Xandri, O., Sagues, F., Reigada, R. and Buceta, J. (2008). A Spatial Toggle Switch Drives Boundary Formation in Development. *Biophys. J.* 95, 5111-5120.

Capdevila, J., Pariente, F., Sampedro, J., Alonso, J. L. and Guerrero, I. (1994). Subcellular Localization of the Segment Polarity Protein Patched Suggests an

Interaction with the Wingless Reception Complex in Drosophila Embryos. *Development* 120, 987-998.

Carpenter, E. M., Goddard, J. M., Chisaka, O., Manley, N. R. and Capecchi, M. R. (1993). Loss of Hox-A1 (Hox-1.6) Function Results in the Reorganization of the Murine Hindbrain. *Development* 118, 1063-1075.

Carroll, S. B. (2005). *From DNA to Diversity : Molecular Genetics and the Evolution of Animal Design*. Oxford: Blackwell.

Carvalho, R. F., Beutler, M., Marler, K. J., Knoll, B., Becker-Barroso, E., Heintzmann, R., Ng, T. and Drescher, U. (2006). Silencing of EphA3 through a Cis Interaction with ephrinA5. *Nat. Neurosci.* 9, 322-330.

Chen, Y. and Zhao, X. (1998). Shaping Limbs by Apoptosis. *J. Exp. Zool.* 282, 691-702.

Cheng, Y. C., Amoyel, M., Qiu, X., Jiang, Y. J., Xu, Q. and Wilkinson, D. G. (2004). Notch Activation Regulates the Segregation and Differentiation of Rhombomere Boundary Cells in the Zebrafish Hindbrain. *Dev. Cell.* 6, 539-550.

Chi, C. L., Martinez, S., Wurst, W. and Martin, G. R. (2003). The Isthmic Organizer Signal FGF8 is Required for Cell Survival in the Prospective Midbrain and Cerebellum. *Development* 130, 2633-2644.

Chisaka, O. and Capecchi, M. R. (1991). Regionally Restricted Developmental Defects Resulting from Targeted Disruption of the Mouse Homeobox Gene Hox-1.5. *Nature* 350, 473-479.

Chisaka, O., Musci, T. S. and Capecchi, M. R. (1992). Developmental Defects of the Ear, Cranial Nerves and Hindbrain Resulting from Targeted Disruption of the Mouse Homeobox Gene Hox-1.6. *Nature* 355, 516-520.

Chomette, D., Frain, M., Cereghini, S., Charnay, P. and Ghislain, J. (2006). Krox20 Hindbrain Cis-Regulatory Landscape: Interplay between Multiple Long-Range Initiation and Autoregulatory Elements. *Development* 133, 1253-1262.

Clarke, J. (2009). Role of Polarized Cell Divisions in Zebrafish Neural Tube Formation. *Curr. Opin. Neurobiol.* 19, 134-138.

Compagni, A., Logan, M., Klein, R. and Adams, R. H. (2003). Control of Skeletal Patterning by ephrinB1-EphB Interactions. *Dev. Cell.* 5, 217-230.

Cooke, J. (1981). The Problem of Periodic Patterns in Embryos. *Philos. Trans. R. Soc. Lond. B. Biol. Sci.* 295, 509-524.

Cooke, J., Moens, C., Roth, L., Durbin, L., Shiomi, K., Brennan, C., Kimmel, C., Wilson, S. and Holder, N. (2001). Eph Signalling Functions Downstream of Val to Regulate Cell Sorting and Boundary Formation in the Caudal Hindbrain. *Development* 128, 571-580.

Cooke, J. E., Kemp, H. A. and Moens, C. B. (2005). EphA4 is Required for Cell Adhesion and Rhombomere-Boundary Formation in the Zebrafish. *Curr. Biol.* 15, 536-542.

Cooke, J. E. and Moens, C. B. (2002). Boundary Formation in the Hindbrain: Eph Only it were Simple. *Trends Neurosci.* 25, 260-267.

Cooper, M. S., Szeto, D. P., Sommers-Herivel, G., Topczewski, J., Solnica-Krezel, L., Kang, H. C., Johnson, I. and Kimelman, D. (2005). Visualizing Morphogenesis in Transgenic Zebrafish Embryos using BODIPY TR Methyl Ester Dye as a Vital Counterstain for GFP. *Dev. Dyn.* 232, 359-368.

Cordes, S. P. (2001). Molecular Genetics of Cranial Nerve Development in Mouse. *Nat. Rev. Neurosci.* 2, 611-623.

Cordes, S. P. and Barsh, G. S. (1994). The Mouse Segmentation Gene Kr Encodes a Novel Basic Domain-Leucine Zipper Transcription Factor. *Cell* 79, 1025-1034.

Cortina, C., Palomo-Ponce, S., Iglesias, M., Fernandez-Masip, J. L., Vivancos, A., Whissell, G., Huma, M., Peiro, N., Gallego, L., Jonkheer, S. et al. (2007). EphB-Ephrin-B Interactions Suppress Colorectal Cancer Progression by Compartmentalizing Tumor Cells. *Nat. Genet.* 39, 1376-1383.

Crossley, P. H., Martinez, S. and Martin, G. R. (1996). Midbrain Development Induced by FGF8 in the Chick Embryo. *Nature* 380, 66-68.

Curt, J. R., de Navas, L. F. and Sanchez-Herrero, E. (2013). Differential Activity of Drosophila Hox Genes Induces Myosin Expression and can Maintain Compartment Boundaries. *PLoS One* 8, e57159.

Dahmann, C., Oates, A. C. and Brand, M. (2011). Boundary Formation and Maintenance in Tissue Development. *Nat. Rev. Genet.* 12, 43-55.

Davy, A., Aubin, J. and Soriano, P. (2004). Ephrin-B1 Forward and Reverse Signaling are Required during Mouse Development. *Genes Dev.* 18, 572-583.

Davy, A., Gale, N. W., Murray, E. W., Klinghoffer, R. A., Soriano, P., Feuerstein, C. and Robbins, S. M. (1999). Compartmentalized Signaling by GPI-Anchored Ephrin-A5 Requires the Fyn Tyrosine Kinase to Regulate Cellular Adhesion. *Genes Dev.* 13, 3125-3135.

Davy, A. and Robbins, S. M. (2000). Ephrin-A5 Modulates Cell Adhesion and Morphology in an Integrin-Dependent Manner. *EMBO J.* 19, 5396-5405.

de Celis, J. F., Barrio, R. and Kafatos, F. C. (1996). A Gene Complex Acting Downstream of Dpp in Drosophila Wing Morphogenesis. *Nature* 381, 421-424.

de Roos, K., Sonneveld, E., Compaan, B., ten Berge, D., Durston, A. J. and van der Saag, P. T. (1999). Expression of Retinoic Acid 4-Hydroxylase (CYP26) during Mouse and Xenopus Laevis Embryogenesis. *Mech. Dev.* 82, 205-211.

Defourny, J., Poirrier, A. L., Lallemend, F., Mateo Sanchez, S., Neef, J., Vanderhaeghen, P., Soriano, E., Peuckert, C., Kullander, K., Fritzsch, B. et al. (2013). Ephrin-A5/EphA4 Signalling Controls Specific Afferent Targeting to Cochlear Hair Cells. *Nat. Commun.* 4, 1438.

Dequeant, M. L. and Pourquie, O. (2008). Segmental Patterning of the Vertebrate Embryonic Axis. *Nat. Rev. Genet.* 9, 370-382.

Dersch, H. and Zile, M. H. (1993). Induction of Normal Cardiovascular Development in the Vitamin A-Deprived Quail Embryo by Natural Retinoids. *Dev. Biol.* 160, 424-433.

Diaz-Benjumea, F. J. and Cohen, S. M. (1993). Interaction between Dorsal and Ventral Cells in the Imaginal Disc Directs Wing Development in Drosophila. *Cell* 75, 741-752.

Distel, M., Wullimann, M. F. and Koster, R. W. (2009). Optimized Gal4 Genetics for Permanent Gene Expression Mapping in Zebrafish. *Proc. Natl. Acad. Sci. U. S. A.* 106, 13365-13370.

Doe, C. Q. and Bowerman, B. (2001). Asymmetric Cell Division: Fly Neuroblast Meets Worm Zygote. *Curr. Opin. Cell Biol.* 13, 68-75.

Dorsky, R. I., Itoh, M., Moon, R. T. and Chitnis, A. (2003). Two Tcf3 Genes Cooperate to Pattern the Zebrafish Brain. *Development* 130, 1937-1947.

Duboule, D. and Dolle, P. (1989). The Structural and Functional Organization of the Murine HOX Gene Family Resembles that of Drosophila Homeotic Genes. *EMBO J.* 8, 1497-1505.

Duester, G., Mic, F. A. and Molotkov, A. (2003). Cytosolic Retinoid Dehydrogenases Govern Ubiquitous Metabolism of Retinol to Retinaldehyde Followed by Tissue-Specific Metabolism to Retinoic Acid. *Chem. Biol. Interact.* 143-144, 201-210.

Dupe, V., Matt, N., Garnier, J. M., Chambon, P., Mark, M. and Ghyselinck, N. B. (2003). A Newborn Lethal Defect due to Inactivation of Retinaldehyde Dehydrogenase Type 3 is Prevented by Maternal Retinoic Acid Treatment. *Proc. Natl. Acad. Sci. U. S. A.* 100, 14036-14041.

Durston, A. J., Timmermans, J. P., Hage, W. J., Hendriks, H. F., de Vries, N. J., Heideveld, M. and Nieuwkoop, P. D. (1989). Retinoic Acid Causes an Anteroposterior Transformation in the Developing Central Nervous System. *Nature* 340, 140-144.

Eichmann, A., Grapin-Botton, A., Kelly, L., Graf, T., Le Douarin, N. M. and Sieweke, M. (1997). The Expression Pattern of the mafB/Kr Gene in Birds and Mice Reveals that the Kreisler Phenotype does Not Represent a Null Mutant. *Mech. Dev.* 65, 111-122.

Erickson, C. A. (1988). Control of Pathfinding by the Avian Trunk Neural Crest. *Development* 103 Suppl, 63-80.

Filas, B. A., Oltean, A., Majidi, S., Bayly, P. V., Beebe, D. C. and Taber, L. A. (2012). Regional Differences in Actomyosin Contraction Shape the Primary Vesicles in the Embryonic Chicken Brain. *Phys. Biol.* 9, 066007-3975/9/6/066007. Epub 2012 Nov 16.

Flanagan, J. G. (2006). Neural Map Specification by Gradients. *Curr. Opin. Neurobiol.* 16, 59-66.

Fraser, S., Keynes, R. and Lumsden, A. (1990). Segmentation in the Chick Embryo Hindbrain is Defined by Cell Lineage Restrictions. *Nature* 344, 431-435.

Freeman, G. (1976). The Effects of Altering the Position of Cleavage Planes on the Process of Localization of Developmental Potential in Ctenophores. *Dev. Biol.* 51, 332-337.

Frohman, M. A., Martin, G. R., Cordes, S. P., Halamek, L. P. and Barsh, G. S. (1993). Altered Rhombomere-Specific Gene Expression and Hyoid Bone Differentiation in the Mouse Segmentation Mutant, Kreisler (Kr). *Development* 117, 925-936.

Gale, N. W., Holland, S. J., Valenzuela, D. M., Flenniken, A., Pan, L., Ryan, T. E., Henkemeyer, M., Strebhardt, K., Hirai, H., Wilkinson, D. G. et al. (1996). Eph Receptors and Ligands Comprise Two Major Specificity Subclasses and are Reciprocally Compartmentalized during Embryogenesis. *Neuron* 17, 9-19.

Garcia-Bellido, A., Ripoll, P. and Morata, G. (1973). Developmental Compartmentalisation of the Wing Disk of Drosophila. *Nat. New Biol.* 245, 251-253.

Garcia-Bellido, A. and Santamaria, P. (1972). Developmental Analysis of the Wing Disc in the Mutant Engrailed of Drosophila Melanogaster. *Genetics* 72, 87-104.

Garcia-Dominguez, M., Gilardi-Hebenstreit, P. and Charnay, P. (2006). PIASxbeta Acts as an Activator of Hoxb1 and is Antagonized by Krox20 during Hindbrain Segmentation. *EMBO J.* 25, 2432-2442.

Gavalas, A., Davenne, M., Lumsden, A., Chambon, P. and Rijli, F. M. (1997). Role of Hoxa-2 in Axon Pathfinding and Rostral Hindbrain Patterning. *Development* 124, 3693-3702.

Gendron-Maguire, M., Mallo, M., Zhang, M. and Gridley, T. (1993). Hoxa-2 Mutant Mice Exhibit Homeotic Transformation of Skeletal Elements Derived from Cranial Neural Crest. *Cell* 75, 1317-1331.

Gerety, S. S. and Wilkinson, D. G. (2011). Morpholino Artifacts Provide Pitfalls and Reveal a Novel Role for Pro-Apoptotic Genes in Hindbrain Boundary Development. *Dev. Biol.* 350, 279-289.

Giudicelli, F., Gilardi-Hebenstreit, P., Mechta-Grigoriou, F., Poquet, C. and Charnay, P. (2003). Novel Activities of Mafb Underlie its Dual Role in Hindbrain Segmentation and Regional Specification. *Dev. Biol.* 253, 150-162.

Giudicelli, F., Taillebourg, E., Charnay, P. and Gilardi-Hebenstreit, P. (2001). Krox-20 Patterns the Hindbrain through both Cell-Autonomous and Non Cell-Autonomous Mechanisms. *Genes Dev.* 15, 567-580.

Goddard, J. M., Rossel, M., Manley, N. R. and Capecchi, M. R. (1996). Mice with Targeted Disruption of Hoxb-1 Fail to Form the Motor Nucleus of the VIIth Nerve. *Development* 122, 3217-3228.

Godt, D. and Tepass, U. (1998). Drosophila Oocyte Localization is Mediated by Differential Cadherin-Based Adhesion. *Nature* 395, 387-391.

Gonzalez-Quevedo, R., Lee, Y., Poss, K. D. and Wilkinson, D. G. (2010). Neuronal Regulation of the Spatial Patterning of Neurogenesis. *Dev. Cell.* 18, 136-147.

Gonzalez-Quevedo, R., Lee, Y., Poss, K. D. and Wilkinson, D. G. (2010). Neuronal Regulation of the Spatial Patterning of Neurogenesis. *Dev. Cell.* 18, 136-147.

Gossler, A. and Hrabe de Angelis, M. (1998). Somitogenesis. *Curr. Top. Dev. Biol.* 38, 225-287.

Guthrie, S., Butcher, M. and Lumsden, A. (1991). Patterns of Cell Division and Interkinetic Nuclear Migration in the Chick Embryo Hindbrain. *J. Neurobiol.* 22, 742-754.

Guthrie, S., Butcher, M. and Lumsden, A. (1991). Patterns of Cell Division and Interkinetic Nuclear Migration in the Chick Embryo Hindbrain. *J. Neurobiol.* 22, 742-754.

Guthrie, S. and Lumsden, A. (1991). Formation and Regeneration of Rhombomere Boundaries in the Developing Chick Hindbrain. *Development* 112, 221-229.

Gutzman, J. H. and Sive, H. (2010). Epithelial Relaxation Mediated by the Myosin Phosphatase Regulator Mypt1 is Required for Brain Ventricle Lumen Expansion and Hindbrain Morphogenesis. *Development* 137, 795-804.

Hanneman, E., Trevarrow, B., Metcalfe, W. K., Kimmel, C. B. and Westerfield, M. (1988). Segmental Pattern of Development of the Hindbrain and Spinal Cord of the Zebrafish Embryo. *Development* 103, 49-58.

Harris, A. K. (1976). Is Cell Sorting Caused by Differences in the Work of Intercellular Adhesion? A Critique of the Steinberg Hypothesis. *J. Theor. Biol.* 61, 267-285.

Hattori, M., Osterfield, M. and Flanagan, J. G. (2000). Regulated Cleavage of a Contact-Mediated Axon Repellent. *Science* 289, 1360-1365.

Helmbacher, F., Pujades, C., Desmarquet, C., Frain, M., Rijli, F. M., Chambon, P. and Charnay, P. (1998). Hoxa1 and Krox-20 Synergize to Control the Development of Rhombomere 3. *Development* 125, 4739-4748.

Hernandez, R. E., Rikhof, H. A., Bachmann, R. and Moens, C. B. (2004). Vhnf1 Integrates Global RA Patterning and Local FGF Signals to Direct Posterior Hindbrain Development in Zebrafish. *Development* 131, 4511-4520.

Hernandez, R. E., Rikhof, H. A., Bachmann, R. and Moens, C. B. (2004). Vhnf1 Integrates Global RA Patterning and Local FGF Signals to Direct Posterior Hindbrain Development in Zebrafish. *Development* 131, 4511-4520.

Heyman, I., Faissner, A. and Lumsden, A. (1995). Cell and Matrix Specialisations of Rhombomere Boundaries. *Dev. Dyn.* 204, 301-315.

Heyman, I., Kent, A. and Lumsden, A. (1993). Cellular Morphology and Extracellular Space at Rhombomere Boundaries in the Chick Embryo Hindbrain. *Dev. Dyn.* 198, 241-253.

Hoettecke, N., Ludwig, A., Foro, S. and Schmidt, B. (2010). Improved Synthesis of ADAM10 Inhibitor GI254023X. *Neurodegener Dis.* 7, 232-238.

Holder, N. and Hill, J. (1991). Retinoic Acid Modifies Development of the Midbrain-Hindbrain Border and Affects Cranial Ganglion Formation in Zebrafish Embryos. *Development* 113, 1159-1170.

Hollemann, T., Chen, Y., Grunz, H. and Pieler, T. (1998). Regionalized Metabolic Activity Establishes Boundaries of Retinoic Acid Signalling. *EMBO J.* 17, 7361-7372.

Hornberger, M. R., Dutting, D., Ciossek, T., Yamada, T., Handwerker, C., Lang, S., Weth, F., Huf, J., Wessel, R., Logan, C. et al. (1999). Modulation of EphA Receptor Function by Coexpressed ephrinA Ligands on Retinal Ganglion Cell Axons. *Neuron* 22, 731-742.

Inoue, T., Tanaka, T., Takeichi, M., Chisaka, O., Nakamura, S. and Osumi, N. (2001). Role of Cadherins in Maintaining the Compartment Boundary between the Cortex and Striatum during Development. *Development* 128, 561-569.

Janes, P. W., Saha, N., Barton, W. A., Kolev, M. V., Wimmer-Kleikamp, S. H., Nievergall, E., Blobel, C. P., Himanen, J. P., Lackmann, M. and Nikolov, D. B. (2005). Adam Meets Eph: An ADAM Substrate Recognition Module Acts as a Molecular Switch for Ephrin Cleavage in Trans. *Cell* 123, 291-304.

Jimenez-Guri, E. and Pujades, C. (2011). An Ancient Mechanism of Hindbrain Patterning has been Conserved in Vertebrate Evolution. *Evol. Dev.* 13, 38-46.

Jimenez-Guri, E., Udina, F., Colas, J. F., Sharpe, J., Padron-Barthe, L., Torres, M. and Pujades, C. (2010). Clonal Analysis in Mice Underlines the Importance of Rhombomeric Boundaries in Cell Movement Restriction during Hindbrain Segmentation. *PLoS One* 5, e10112.

Joubin, K. and Stern, C. D. (2001). Formation and Maintenance of the Organizer among the Vertebrates. *Int. J. Dev. Biol.* 45, 165-175.

Julich, D., Geisler, R., Holley, S. A. and Tubingen 2000 Screen Consortium. (2005). Integrinalpha5 and Delta/Notch Signaling have Complementary Spatiotemporal Requirements during Zebrafish Somitogenesis. *Dev. Cell.* 8, 575-586.

Julich, D., Mould, A. P., Koper, E. and Holley, S. A. (2009). Control of Extracellular Matrix Assembly Along Tissue Boundaries Via Integrin and Eph/Ephrin Signaling. *Development* 136, 2913-2921.

Kataoka, K., Fujiwara, K. T., Noda, M. and Nishizawa, M. (1994). MafB, a New Maf Family Transcription Activator that can Associate with Maf and Fos but Not with Jun. *Mol. Cell. Biol.* 14, 7581-7591.

Kawamura, A., Koshida, S., Hijikata, H., Sakaguchi, T., Kondoh, H. and Takada, S. (2005). Zebrafish Hairy/Enhancer of Split Protein Links FGF Signaling to Cyclic Gene Expression in the Periodic Segmentation of Somites. *Genes Dev.* 19, 1156-1161.

Kemp, H. A., Cooke, J. E. and Moens, C. B. (2008). EphA4 and EfnB2a Maintain Rhombomere Coherence by Independently Regulating Intercalation of Progenitor Cells in the Zebrafish Neural Keel. *Dev. Biol.*

Kemp, H. A., Cooke, J. E. and Moens, C. B. (2009). EphA4 and EfnB2a Maintain Rhombomere Coherence by Independently Regulating Intercalation of Progenitor Cells in the Zebrafish Neural Keel. *Dev. Biol.* 327, 313-326.

Keynes, R. and Krumlauf, R. (1994). Hox Genes and Regionalization of the Nervous System. *Annu. Rev. Neurosci.* 17, 109-132.

Kiecker, C. and Lumsden, A. (2005). Compartments and their Boundaries in Vertebrate Brain Development. *Nat. Rev. Neurosci.* 6, 553-564.

Kiecker, C. and Lumsden, A. (2005). Compartments and their Boundaries in Vertebrate Brain Development. *Nat. Rev. Neurosci.* 6, 553-564.

Kim, F. A., Sing, l. A., Kaneko, T., Bieman, M., Stallwood, N., Sadl, V. S. and Cordes, S. P. (2005). The vHNF1 Homeodomain Protein Establishes Early Rhombomere Identity by Direct Regulation of Kreisler Expression. *Mech. Dev.* 122, 1300-1309.

Klein, R. (2012). Eph/Ephrin Signalling during Development. *Development* 139, 4105-4109.

Kobayashi, D., Kobayashi, M., Matsumoto, K., Ogura, T., Nakafuku, M. and Shimamura, K. (2002). Early Subdivisions in the Neural Plate Define Distinct Competence for Inductive Signals. *Development* 129, 83-93.

Kornberg, T., Siden, I., O'Farrell, P. and Simon, M. (1985). The Engrailed Locus of Drosophila: In Situ Localization of Transcripts Reveals Compartment-Specific Expression. *Cell* 40, 45-53.

Koshida, S., Kishimoto, Y., Ustumi, H., Shimizu, T., Furutani-Seiki, M., Kondoh, H. and Takada, S. (2005). Integrinalpha5-Dependent Fibronectin Accumulation for Maintenance of Somite Boundaries in Zebrafish Embryos. *Dev. Cell.* 8, 587-598.

Koster, R. W. and Fraser, S. E. (2001). Tracing Transgene Expression in Living Zebrafish Embryos. *Dev. Biol.* 233, 329-346.

Krieg, M., Arboleda-Estudillo, Y., Puech, P. H., Kafer, J., Graner, F., Muller, D. J. and Heisenberg, C. P. (2008). Tensile Forces Govern Germ-Layer Organization in Zebrafish. *Nat. Cell Biol.* 10, 429-436.

Krumlauf, R. (1994). Hox Genes in Vertebrate Development. *Cell* 78, 191-201.

Krumlauf, R., Manzanares, M., Nonchev, S., Maconochie, M., Gould, A., Morrison, A., Popperl, H., Studer, M., Cordes, S. and Barsh, G. (1997). Conserved Mechanisms in the Regulation of Hindbrain Segmentation in Vertebrates. *J. Neurochem.* 69, S55-S55.

Kuan, C. Y., Flavell, R. A. and Rakic, P. (2000). Programmed Cell Death in Mouse Brain Development. *Results Probl. Cell Differ.* 30, 145-162.

Kubota, Y. and Ito, K. (2000). Chemotactic Migration of Mesencephalic Neural Crest Cells in the Mouse. *Dev. Dyn.* 217, 170-179.

Kulesa, P., Ellies, D. L. and Trainor, P. A. (2004). Comparative Analysis of Neural Crest Cell Death, Migration, and Function during Vertebrate Embryogenesis. *Dev. Dyn.* 229, 14-29.

Kurant, E., Pai, C. Y., Sharf, R., Halachmi, N., Sun, Y. H. and Salzberg, A. (1998). Dorsotonals/Homothorax, the Drosophila Homologue of Meis1, Interacts with Extradenticle in Patterning of the Embryonic PNS. *Development* 125, 1037-1048.

Kwak, S. J., Phillips, B. T., Heck, R. and Riley, B. B. (2002). An Expanded Domain of Fgf3 Expression in the Hindbrain of Zebrafish Valentino Mutants Results in Mis-Patterning of the Otic Vesicle. *Development* 129, 5279-5287.

Kwak, S. J., Phillips, B. T., Heck, R. and Riley, B. B. (2002). An Expanded Domain of Fgf3 Expression in the Hindbrain of Zebrafish Valentino Mutants Results in Mis-Patterning of the Otic Vesicle. *Development* 129, 5279-5287.

Labalette, C., Bouchoucha, Y. X., Wassef, M. A., Gongal, P. A., Le Men, J., Becker, T., Gilardi-Hebenstreit, P. and Charnay, P. (2011). Hindbrain Patterning Requires Fine-Tuning of Early krox20 Transcription by Sprouty 4. *Development* 138, 317-326.

Landsberg, K. P., Farhadifar, R., Ranft, J., Umetsu, D., Widmann, T. J., Bittig, T., Said, A., Julicher, F. and Dahmann, C. (2009). Increased Cell Bond Tension Governs

Cell Sorting at the Drosophila Anteroposterior Compartment Boundary. *Curr. Biol.* 19, 1950-1955.

Landsberg, K. P., Farhadifar, R., Ranft, J., Umetsu, D., Widmann, T. J., Bittig, T., Said, A., Julicher, F. and Dahmann, C. (2009). Increased Cell Bond Tension Governs Cell Sorting at the Drosophila Anteroposterior Compartment Boundary. *Curr. Biol.* 19, 1950-1955.

Langdon, Y. G. and Mullins, M. C. (2011). Maternal and Zygotic Control of Zebrafish Dorsoventral Axial Patterning. *Annu. Rev. Genet.* 45, 357-377.

Langenberg, T. and Brand, M. (2005). Lineage Restriction Maintains a Stable Organizer Cell Population at the Zebrafish Midbrain-Hindbrain Boundary. *Development* 132, 3209-3216.

Larsen, C. W., Zeltser, L. M. and Lumsden, A. (2001). Boundary Formation and Compartition in the Avian Diencephalon. *J. Neurosci.* 21, 4699-4711.

Larsen, C. W., Zeltser, L. M. and Lumsden, A. (2001). Boundary Formation and Compartition in the Avian Diencephalon. *J. Neurosci.* 21, 4699-4711.

Lauterbach, J. and Klein, R. (2006). Release of Full-Length EphB2 Receptors from Hippocampal Neurons to Cocultured Glial Cells. *J. Neurosci.* 26, 11575-11581.

Lawrence, P. A. (1973). A Clonal Analysis of Segment Development in Oncopeltus (Hemiptera). *J. Embryol. Exp. Morphol.* 30, 681-699.

Lecaudey, V., Anselme, I., Rosa, F. and Schneider-Maunoury, S. (2004). The Zebrafish Iroquois Gene Iro7 Positions the R4/R5 Boundary and Controls Neurogenesis in the Rostral Hindbrain. *Development* 131, 3121-3131.

Lecaudey, V., Cakan-Akdogan, G., Norton, W. H. and Gilmour, D. (2008). Dynamic Fgf Signaling Couples Morphogenesis and Migration in the Zebrafish Lateral Line Primordium. *Development* 135, 2695-2705.

Lecaudey, V., Ulloa, E., Anselme, I., Stedman, A., Schneider-Maunoury, S. and Pujades, C. (2007). Role of the Hindbrain in Patterning the Otic Vesicle: A Study of the Zebrafish Vhnf1 Mutant. *Dev. Biol.* 303, 134-143.

Lecuit, T., Brook, W. J., Ng, M., Calleja, M., Sun, H. and Cohen, S. M. (1996). Two Distinct Mechanisms for Long-Range Patterning by Decapentaplegic in the Drosophila Wing. *Nature* 381, 387-393.

Leger, S. and Brand, M. (2002). Fgf8 and Fgf3 are Required for Zebrafish Ear Placode Induction, Maintenance and Inner Ear Patterning. *Mech. Dev.* 119, 91-108.

Lepage, S. E. and Bruce, A. E. (2010). Zebrafish Epiboly: Mechanics and Mechanisms. *Int. J. Dev. Biol.* 54, 1213-1228.

Liu, A. and Joyner, A. L. (2001). Early Anterior/Posterior Patterning of the Midbrain and Cerebellum. *Annu. Rev. Neurosci.* 24, 869-896.

Liu, A. and Joyner, A. L. (2001). EN and GBX2 Play Essential Roles Downstream of FGF8 in Patterning the Mouse Mid/Hindbrain Region. *Development* 128, 181-191.

Lombardo, A., Isaacs, H. V. and Slack, J. M. (1998). Expression and Functions of FGF-3 in Xenopus Development. *Int. J. Dev. Biol.* 42, 1101-1107.

Lowery, L. A. and Sive, H. (2004). Strategies of Vertebrate Neurulation and a Re-Evaluation of Teleost Neural Tube Formation. *Mech. Dev.* 121, 1189-1197.

Lumsden, A. and Guthrie, S. (1991). Alternating Patterns of Cell Surface Properties and Neural Crest Cell Migration during Segmentation of the Chick Hindbrain. *Development* Suppl 2, 9-15.

Lumsden, A. and Keynes, R. (1989). Segmental Patterns of Neuronal Development in the Chick Hindbrain. *Nature* 337, 424-428.

Lumsden, A. and Krumlauf, R. (1996). Patterning the Vertebrate Neuraxis. *Science* 274, 1109-1115.

Maconochie, M., Nonchev, S., Morrison, A. and Krumlauf, R. (1996). Paralogous Hox Genes: Function and Regulation. *Annu. Rev. Genet.* 30, 529-556.

Mahmood, R., Kiefer, P., Guthrie, S., Dickson, C. and Mason, I. (1995). Multiple Roles for FGF-3 during Cranial Neural Development in the Chicken. *Development* 121, 1399-1410.

Maitre, J. L., Berthoumieux, H., Krens, S. F., Salbreux, G., Julicher, F., Paluch, E. and Heisenberg, C. P. (2012). Adhesion Functions in Cell Sorting by Mechanically Coupling the Cortices of Adhering Cells. *Science* 338, 253-256.

Major, R. J. and Irvine, K. D. (2005). Influence of Notch on Dorsoventral Compartmentalization and Actin Organization in the Drosophila Wing. *Development* 132, 3823-3833.

Major, R. J. and Irvine, K. D. (2006). Localization and Requirement for Myosin II at the Dorsal-Ventral Compartment Boundary of the Drosophila Wing. *Dev. Dyn.* 235, 3051-3058.

Mann, F., Miranda, E., Weinl, C., Harmer, E. and Holt, C. E. (2003). B-Type Eph Receptors and Ephrins Induce Growth Cone Collapse through Distinct Intracellular Pathways. *J. Neurobiol.* 57, 323-336.

Manzanares, M., Bel-Vialar, S., Ariza-McNaughton, L., Ferretti, E., Marshall, H., Maconochie, M. M., Blasi, F. and Krumlauf, R. (2001). Independent Regulation of Initiation and Maintenance Phases of Hoxa3 Expression in the Vertebrate Hindbrain Involve Auto- and Cross-Regulatory Mechanisms. *Development* 128, 3595-3607.

Manzanares, M., Cordes, S., Ariza-McNaughton, L., Sadl, V., Maruthainar, K., Barsh, G. and Krumlauf, R. (1999). Conserved and Distinct Roles of Kreisler in Regulation of the Paralogous Hoxa3 and Hoxb3 Genes. *Development* 126, 759-769.

Manzanares, M., Nardelli, J., Gilardi-Hebenstreit, P., Marshall, H., Giudicelli, F., Martinez-Pastor, M. T., Krumlauf, R. and Charnay, P. (2002). Krox20 and Kreisler Co-Operate in the Transcriptional Control of Segmental Expression of Hoxb3 in the Developing Hindbrain. *EMBO J.* 21, 365-376.

Marcon, L. and Sharpe, J. (2012). Turing Patterns in Development: What about the Horse Part? *Curr. Opin. Genet. Dev.* 22, 578-584.

Marin, F. and Charnay, P. (2000). Hindbrain Patterning: FGFs Regulate Krox20 and mafB/Kr Expression in the Otic/Preotic Region. *Development* 127, 4925-4935.

Marin, F. and Charnay, P. (2000). Positional Regulation of Krox-20 and mafB/Kr Expression in the Developing Hindbrain: Potentialities of Prospective Rhombomeres. *Dev. Biol.* 218, 220-234.

Marler, K. J., Becker-Barroso, E., Martinez, A., Llovera, M., Wentzel, C., Poopalasundaram, S., Hindges, R., Soriano, E., Comella, J. and Drescher, U. (2008). A TrkB/EphrinA Interaction Controls Retinal Axon Branching and Synaptogenesis. *J. Neurosci.* 28, 12700-12712.

Maroto, M. and Pourquie, O. (2001). A Molecular Clock Involved in Somite Segmentation. *Curr. Top. Dev. Biol.* 51, 221-248.

Marshall, H., Studer, M., Popperl, H., Aparicio, S., Kuroiwa, A., Brenner, S. and Krumlauf, R. (1994). A Conserved Retinoic Acid Response Element Required for Early Expression of the Homeobox Gene Hoxb-1. *Nature* 370, 567-571.

Marston, D. J., Dickinson, S. and Nobes, C. D. (2003). Rac-Dependent Trans-Endocytosis of ephrinBs Regulates Eph-Ephrin Contact Repulsion. *Nat. Cell Biol.* 5, 879-888.

Maves, L., Jackman, W. and Kimmel, C. B. (2002). FGF3 and FGF8 Mediate a Rhombomere 4 Signaling Activity in the Zebrafish Hindbrain. *Development* 129, 3825-3837.

McCaffery, P., Tempst, P., Lara, G. and Drager, U. C. (1991). Aldehyde Dehydrogenase is a Positional Marker in the Retina. *Development* 112, 693-702.

McGinnis, W. and Krumlauf, R. (1992). Homeobox Genes and Axial Patterning. *Cell* 68, 283-302.

McKay, I. J., Lewis, J. and Lumsden, A. (1996). The Role of FGF-3 in Early Inner Ear Development: An Analysis in Normal and Kreisler Mutant Mice. *Dev. Biol.* 174, 370-378.

McKay, I. J., Muchamore, I., Krumlauf, R., Maden, M., Lumsden, A. and Lewis, J. (1994). The Kreisler Mouse: A Hindbrain Segmentation Mutant that Lacks Two Rhombomeres. *Development* 120, 2199-2211.

Mellitzer, G., Xu, Q. and Wilkinson, D. G. (1999). Eph Receptors and Ephrins Restrict Cell Intermingling and Communication. *Nature* 400, 77-81.

Metcalfe, W. K., Mendelson, B. and Kimmel, C. B. (1986). Segmental Homologies among Reticulospinal Neurons in the Hindbrain of the Zebrafish Larva. *J. Comp. Neurol.* 251, 147-159.

Micchelli, C. A., Rulifson, E. J. and Blair, S. S. (1997). The Function and Regulation of Cut Expression on the Wing Margin of Drosophila: Notch, Wingless and a Dominant Negative Role for Delta and Serrate. *Development* 124, 1485-1495.

Milan, M., Weihe, U., Tiong, S., Bender, W. and Cohen, S. M. (2001). Msh Specifies Dorsal Cell Fate in the Drosophila Wing. *Development* 128, 3263-3268.

Moens, C. B., Yan, Y. L., Appel, B., Force, A. G. and Kimmel, C. B. (1996). Valentino: A Zebrafish Gene Required for Normal Hindbrain Segmentation. *Development* 122, 3981-3990.

Monica, K., Galili, N., Nourse, J., Saltman, D. and Cleary, M. L. (1991). PBX2 and PBX3, New Homeobox Genes with Extensive Homology to the Human Proto-Oncogene PBX1. *Mol. Cell. Biol.* 11, 6149-6157.

Monier, B., Pelissier-Monier, A., Brand, A. H. and Sanson, B. (2010). An Actomyosin-Based Barrier Inhibits Cell Mixing at Compartmental Boundaries in Drosophila Embryos. *Nat. Cell Biol.* 12, 60-5; sup pp 1-9.

Morimoto, M., Sasaki, N., Oginuma, M., Kiso, M., Igarashi, K., Aizaki, K., Kanno, J. and Saga, Y. (2007). The Negative Regulation of Mesp2 by Mouse Ripply2 is Required to Establish the Rostro-Caudal Patterning within a Somite. *Development* 134, 1561-1569.

Morimoto, M., Takahashi, Y., Endo, M. and Saga, Y. (2005). The Mesp2 Transcription Factor Establishes Segmental Borders by Suppressing Notch Activity. *Nature* 435, 354-359.

Morriss, G. M. (1972). Morphogenesis of the Malformations Induced in Rat Embryos by Maternal Hypervitaminosis A. *J. Anat.* 113, 241-250.

Morriss-Kay, G. M., Murphy, P., Hill, R. E. and Davidson, D. R. (1991). Effects of Retinoic Acid Excess on Expression of Hox-2.9 and Krox-20 and on Morphological Segmentation in the Hindbrain of Mouse Embryos. *EMBO J.* 10, 2985-2995.

Moskow, J. J., Bullrich, F., Huebner, K., Daar, I. O. and Buchberg, A. M. (1995). Meis1, a PBX1-Related Homeobox Gene Involved in Myeloid Leukemia in BXH-2 Mice. *Mol. Cell. Biol.* 15, 5434-5443.

Nakajima, Y., Morimoto, M., Takahashi, Y., Koseki, H. and Saga, Y. (2006). Identification of Epha4 Enhancer Required for Segmental Expression and the Regulation by Mesp2. *Development* 133, 2517-2525.

Nellen, D., Burke, R., Struhl, G. and Basler, K. (1996). Direct and Long-Range Action of a DPP Morphogen Gradient. *Cell* 85, 357-368.

Niederreither, K., McCaffery, P., Drager, U. C., Chambon, P. and Dolle, P. (1997). Restricted Expression and Retinoic Acid-Induced Downregulation of the Retinaldehyde Dehydrogenase Type 2 (RALDH-2) Gene during Mouse Development. *Mech. Dev.* 62, 67-78.

Nieuwenhuys, R. (1967). Comparative Anatomy of the Cerebellum. *Prog. Brain Res.* 25, 1-93.

Nomura-Kitabayashi, A., Takahashi, Y., Kitajima, S., Inoue, T., Takeda, H. and Saga, Y. (2002). Hypomorphic Mesp Allele Distinguishes Establishment of Rostrocaudal Polarity and Segment Border Formation in Somitogenesis. *Development* 129, 2473-2481.

Nonchev, S., Maconochie, M., Vesque, C., Aparicio, S., ArizaMcNaughton, L., Manzanares, M., Maruthainar, K., Kuroiwa, A., Brenner, S., Charnay, P. et al. (1996). The Conserved Role of Krox-20 in Directing Hox Gene Expression during Vertebrate Hindbrain Segmentation. *Proc. Natl. Acad. Sci. U. S. A.* 93, 9339-9345.

Nonchev, S., Vesque, C., Maconochie, M., Seitanidou, T., Ariza-McNaughton, L., Frain, M., Marshall, H., Sham, M. H., Krumlauf, R. and Charnay, P. (1996). Segmental Expression of Hoxa-2 in the Hindbrain is Directly Regulated by Krox-20. *Development* 122, 543-554.

Nonchev, S., Vesque, C., Maconochie, M., Seitanidou, T., Ariza-McNaughton, L., Frain, M., Marshall, H., Sham, M. H., Krumlauf, R. and Charnay, P. (1996). Segmental Expression of Hoxa-2 in the Hindbrain is Directly Regulated by Krox-20. *Development* 122, 543-554.

Oginuma, M., Niwa, Y., Chapman, D. L. and Saga, Y. (2008). Mesp2 and Tbx6 Cooperatively Create Periodic Patterns Coupled with the Clock Machinery during Mouse Somitogenesis. *Development* 135, 2555-2562.

Packer, A. I., Crotty, D. A., Elwell, V. A. and Wolgemuth, D. J. (1998). Expression of the Murine Hoxa4 Gene Requires both Autoregulation and a Conserved Retinoic Acid Response Element. *Development* 125, 1991-1998.

Papalopulu, N., Clarke, J. D., Bradley, L., Wilkinson, D., Krumlauf, R. and Holder, N. (1991). Retinoic Acid Causes Abnormal Development and Segmental Patterning of the Anterior Hindbrain in Xenopus Embryos. *Development* 113, 1145-1158.

Parng, C., Anderson, N., Ton, C. and McGrath, P. (2004). Zebrafish Apoptosis Assays for Drug Discovery. *Methods Cell Biol.* 76, 75-85.

Pasini, A. and Wilkinson, D. G. (2002). Stabilizing the Regionalisation of the Developing Vertebrate Central Nervous System. *Bioessays* 24, 427-438.

Pitulescu, M. E. and Adams, R. H. (2010). Eph/Ephrin Molecules--a Hub for Signaling and Endocytosis. *Genes Dev.* 24, 2480-2492.

Poelmann, R. E., Molin, D., Wisse, L. J. and Gittenberger-de Groot, A. C. (2000). Apoptosis in Cardiac Development. *Cell Tissue Res.* 301, 43-52.

Popperl, H., Rikhof, H., Chang, H., Haffter, P., Kimmel, C. B. and Moens, C. B. (2000). Lazarus is a Novel Pbx Gene that Globally Mediates Hox Gene Function in Zebrafish. *Mol. Cell* 6, 255-267.

Pouilhe, M., Gilardi-Hebenstreit, P., Desmarquet-TrinDinh, C. and Charnay, P. (2007). Direct Regulation of vHnf1 by Retinoic Acid Signaling and MAF-Related Factors in the Neural Tube. *Developmental Biology* 309, 344-357.

Price, S. R., De Marco Garcia, N. V., Ranscht, B. and Jessell, T. M. (2002). Regulation of Motor Neuron Pool Sorting by Differential Expression of Type II Cadherins. *Cell* 109, 205-216.

Prince, V. E., Moens, C. B., Kimmel, C. B. and Ho, R. K. (1998). Zebrafish Hox Genes: Expression in the Hindbrain Region of Wild-Type and Mutants of the Segmentation Gene, Valentino. *Development* 125, 393-406.

Puelles, L. and Rubenstein, J. L. (2003). Forebrain Gene Expression Domains and the Evolving Prosomeric Model. *Trends Neurosci.* 26, 469-476.

Qiu, X., Xu, H., Haddon, C., Lewis, J. and Jiang, Y. J. (2004). Sequence and Embryonic Expression of Three Zebrafish Fringe Genes: Lunatic Fringe, Radical Fringe, and Manic Fringe. *Dev. Dyn.* 231, 621-630.

Raible, F. and Brand, M. (2001). Tight Transcriptional Control of the ETS Domain Factors Erm and Pea3 by Fgf Signaling during Early Zebrafish Development. *Mech. Dev.* 107, 105-117.

Raible, F. and Brand, M. (2004). Divide Et Impera--the Midbrain-Hindbrain Boundary and its Organizer. *Trends Neurosci.* 27, 727-734.

Reichert, H. (2002). Conserved Genetic Mechanisms for Embryonic Brain Patterning. *Int. J. Dev. Biol.* 46, 81-87.

Reifers, F., Bohli, H., Walsh, E. C., Crossley, P. H., Stainier, D. Y. and Brand, M. (1998). Fgf8 is Mutated in Zebrafish Acerebellar (Ace) Mutants and is Required for Maintenance of Midbrain-Hindbrain Boundary Development and Somitogenesis. *Development* 125, 2381-2395.

Rieckhof, G. E., Casares, F., Ryoo, H. D., Abu-Shaar, M. and Mann, R. S. (1997). Nuclear Translocation of Extradenticle Requires Homothorax, which Encodes an Extradenticle-Related Homeodomain Protein. *Cell* 91, 171-183.

Rijli, F. M., Mark, M., Lakkaraju, S., Dierich, A., Dolle, P. and Chambon, P. (1993). A Homeotic Transformation is Generated in the Rostral Branchial Region of the Head by Disruption of Hoxa-2, which Acts as a Selector Gene. *Cell* 75, 1333-1349.

Riley, B. B., Chiang, M. Y., Storch, E. M., Heck, R., Buckles, G. R. and Lekven, A. C. (2004). Rhombomere Boundaries are Wnt Signaling Centers that Regulate Metameric Patterning in the Zebrafish Hindbrain. *Dev. Dyn.* 231, 278-291.

Robu, M. E., Larson, J. D., Nasevicius, A., Beiraghi, S., Brenner, C., Farber, S. A. and Ekker, S. C. (2007). P53 Activation by Knockdown Technologies. *PLoS Genet.* 3, e78.

Salazar-Ciudad, I., Garcia-Fernandez, J. and Sole, R. V. (2000). Gene Networks Capable of Pattern Formation: From Induction to Reaction-Diffusion. *J. Theor. Biol.* 205, 587-603.

Salazar-Ciudad, I., Jernvall, J. and Newman, S. A. (2003). Mechanisms of Pattern Formation in Development and Evolution. *Development* 130, 2027-2037.

Sandell, L. J. and Adler, P. (1999). Developmental Patterns of Cartilage. *Front. Biosci.* 4, D731-42.

Sato, T., Araki, I. and Nakamura, H. (2001). Inductive Signal and Tissue Responsiveness Defining the Tectum and the Cerebellum. *Development* 128, 2461-2469.

Sawa, H. (2012). Control of Cell Polarity and Asymmetric Division in C. Elegans. *Curr. Top. Dev. Biol.* 101, 55-76.

Schilling, T. F. and Knight, R. D. (2001). Origins of Anteroposterior Patterning and Hox Gene Regulation during Chordate Evolution. *Philos. Trans. R. Soc. Lond. B. Biol. Sci.* 356, 1599-1613.

Schilling, T. F., Nie, Q. and Lander, A. D. (2012). Dynamics and Precision in Retinoic Acid Morphogen Gradients. *Curr. Opin. Genet. Dev.* 22, 562-569.

Schneider-Maunoury, S., Gilardi-Hebenstreit, P. and Charnay, P. (1998). How to Build a Vertebrate Hindbrain. Lessons from Genetics. *C. R. Acad. Sci. III* 321, 819-834.

Schneider-Maunoury, S., Seitanidou, T., Topilko, P., Vesque, C., Frain, M., Gilardi-Hebenstreit, P. and Charnay, P. (1997). [Role of the Krox-20 Gene in the Development of Rhombencephalon]. *C. R. Seances Soc. Biol. Fil.* 191, 91-94.

Schneider-Maunoury, S., Topilko, P., Seitandou, T., Levi, G., Cohen-Tannoudji, M., Pournin, S., Babinet, C. and Charnay, P. (1993). Disruption of Krox-20 Results in Alteration of Rhombomeres 3 and 5 in the Developing Hindbrain. *Cell* 75, 1199-1214.

Sechrist, J., Serbedzija, G. N., Scherson, T., Fraser, S. E. and Bronner-Fraser, M. (1993). Segmental Migration of the Hindbrain Neural Crest does Not Arise from its Segmental Generation. *Development* 118, 691-703.

Seitanidou, T., Schneider-Maunoury, S., Desmarquet, C., Wilkinson, D. G. and Charnay, P. (1997). Krox-20 is a Key Regulator of Rhombomere-Specific Gene Expression in the Developing Hindbrain. *Mech. Dev.* 65, 31-42.

Sela-Donenfeld, D., Kayam, G. and Wilkinson, D. G. (2009). Boundary Cells Regulate a Switch in the Expression of FGF3 in Hindbrain Rhombomeres. *BMC Dev. Biol.* 9, 16-213X-9-16.

Shamim, H. and Mason, I. (1999). Expression of Fgf4 during Early Development of the Chick Embryo. *Mech. Dev.* 85, 189-192.

Shimamura, K., Hartigan, D. J., Martinez, S., Puelles, L. and Rubenstein, J. L. (1995). Longitudinal Organization of the Anterior Neural Plate and Neural Tube. *Development* 121, 3923-3933.

Simcox, A. A., Grumbling, G., Schnepp, B., Bennington-Mathias, C., Hersperger, E. and Shearn, A. (1996). Molecular, Phenotypic, and Expression Analysis of Vein, a Gene Required for Growth of the Drosophila Wing Disc. *Dev. Biol.* 177, 475-489.

Sirbu, I. O., Gresh, L., Barra, J. and Duester, G. (2005). Shifting Boundaries of Retinoic Acid Activity Control Hindbrain Segmental Gene Expression. *Development* 132, 2611-2622.

Solanas, G., Cortina, C., Sevillano, M. and Batlle, E. (2011). Cleavage of E-Cadherin by ADAM10 Mediates Epithelial Cell Sorting Downstream of EphB Signalling. *Nat. Cell Biol.* 13, 1100-1107.

Sousa-Nunes, R. and Somers, W. G. (2013). Mechanisms of Asymmetric Progenitor Divisions in the Drosophila Central Nervous System. *Adv. Exp. Med. Biol.* 786, 79-102.

Spear, P. C. and Erickson, C. A. (2012). Interkinetic Nuclear Migration: A Mysterious Process in Search of a Function. *Dev. Growth Differ.* 54, 306-316.

Stedman, A., Lecaudey, V., Havis, E., Anselme, I., Wassef, M., Gilardi-Hebenstreit, P. and Schneider-Maunoury, S. (2009). A Functional Interaction between Irx and Meis Patterns the Anterior Hindbrain and Activates krox20 Expression in Rhombomere 3. *Dev. Biol.* 327, 566-577.

Steinberg, M. (2007). Differential Adhesion in Morphogenesis: A Modern View. *Curr. Opin. Genet. Dev.* 17, 281-286.

Steinberg, M. S. (1963). Reconstruction of Tissues by Dissociated Cells. some Morphogenetic Tissue Movements and the Sorting Out of Embryonic Cells may have a Common Explanation. *Science* 141, 401-408.

Steinberg, M. S. and Gilbert, S. F. (2004). Townes and Holtfreter (1955): Directed Movements and Selective Adhesion of Embryonic Amphibian Cells. *J. Exp. Zool. A. Comp. Exp. Biol.* 301, 701-706.

Stockinger, P., Maitre, J. L. and Heisenberg, C. P. (2011). Defective Neuroepithelial Cell Cohesion Affects Tangential Branchiomotor Neuron Migration in the Zebrafish Neural Tube. *Development* 138, 4673-4683.

Studer, M., Gavalas, A., Marshall, H., Ariza-McNaughton, L., Rijli, F. M., Chambon, P. and Krumlauf, R. (1998). Genetic Interactions between Hoxa1 and Hoxb1 Reveal New Roles in Regulation of Early Hindbrain Patterning. *Development* 125, 1025-1036.

Sun, Z. and Hopkins, N. (2001). Vhnf1, the MODY5 and Familial GCKD-Associated Gene, Regulates Regional Specification of the Zebrafish Gut, Pronephros, and Hindbrain. *Genes Dev.* 15, 3217-3229.

Takahashi, J., Ohbayashi, A., Oginuma, M., Saito, D., Mochizuki, A., Saga, Y. and Takada, S. (2010). Analysis of Ripply1/2-Deficient Mouse Embryos Reveals a Mechanism Underlying the Rostro-Caudal Patterning within a Somite. *Dev. Biol.* 342, 134-145.

Tawk, M., Araya, C., Lyons, D. A., Reugels, A. M., Girdler, G. C., Bayley, P. R., Hyde, D. R., Tada, M. and Clarke, J. D. (2007). A Mirror-Symmetric Cell Division that Orchestrates Neuroepithelial Morphogenesis. *Nature* 446, 797-800.

Terriente, J., Gerety, S. S., Watanabe-Asaka, T., Gonzalez-Quevedo, R. and Wilkinson, D. G. (2012). Signalling from Hindbrain Boundaries Regulates Neuronal Clustering that Patterns Neurogenesis. *Development* 139, 2978-2987.

Theil, T., Frain, M., Gilardi-Hebenstreit, P., Flenniken, A., Charnay, P. and Wilkinson, D. G. (1998). Segmental Expression of the EphA4 (Sek-1) Receptor Tyrosine Kinase in the Hindbrain is Under Direct Transcriptional Control of Krox-20. *Development* 125, 443-452.

Thompson, J. N., Howell, J. M., Pitt, G. A. and McLaughlin, C. I. (1969). The Biological Activity of Retinoic Acid in the Domestic Fowl and the Effects of Vitamin A Deficiency on the Chick Embryo. *Br. J. Nutr.* 23, 471-490.

Trainor, P. A. and Krumlauf, R. (2001). Hox Genes, Neural Crest Cells and Branchial Arch Patterning. *Curr. Opin. Cell Biol.* 13, 698-705.

Trainor, P. A. and Krumlauf, R. (2001). Hox Genes, Neural Crest Cells and Branchial Arch Patterning. *Curr. Opin. Cell Biol.* 13, 698-705.

Trevarrow, B., Marks, D. L. and Kimmel, C. B. (1990). Organization of Hindbrain Segments in the Zebrafish Embryo. *Neuron* 4, 669-679.

Vesque, C., Maconochie, M., Nonchev, S., Ariza-McNaughton, L., Kuroiwa, A., Charnay, P. and Krumlauf, R. (1996). Hoxb-2 Transcriptional Activation in

Rhombomeres 3 and 5 Requires an Evolutionarily Conserved Cis-Acting Element in Addition to the Krox-20 Binding Site. *EMBO J.* 15, 5383-5396.

Vicente-Manzanares, M., Ma, X., Adelstein, R. S. and Horwitz, A. R. (2009). Non-Muscle Myosin II Takes Centre Stage in Cell Adhesion and Migration. *Nat. Rev. Mol. Cell Biol.* 10, 778-790.

Voiculescu, O., Taillebourg, E., Pujades, C., Kress, C., Buart, S., Charnay, P. and Schneider-Maunoury, S. (2001). Hindbrain Patterning: Krox20 Couples Segmentation and Specification of Regional Identity. *Development* 128, 4967-4978.

Walshe, J., Maroon, H., McGonnell, I. M., Dickson, C. and Mason, I. (2002). Establishment of Hindbrain Segmental Identity Requires Signaling by FGF3 and FGF8. *Curr. Biol.* 12, 1117-1123.

Walshe, J., Maroon, H., McGonnell, I. M., Dickson, C. and Mason, I. (2002). Establishment of Hindbrain Segmental Identity Requires Signaling by FGF3 and FGF8. *Curr. Biol.* 12, 1117-1123.

Wassef, M. A., Chomette, D., Pouilhe, M., Stedman, A., Havis, E., Desmarquet-Trin Dinh, C., Schneider-Maunoury, S., Gilardi-Hebenstreit, P., Charnay, P. and Ghislain, J. (2008). Rostral Hindbrain Patterning Involves the Direct Activation of a Krox20 Transcriptional Enhancer by Hox/Pbx and Meis Factors. *Development* 135, 3369-3378.

White, R. J., Nie, Q., Lander, A. D. and Schilling, T. F. (2007). Complex Regulation of cyp26a1 Creates a Robust Retinoic Acid Gradient in the Zebrafish Embryo. *PLoS Biol.* 5, e304.

Wiellette, E. L. and Sive, H. (2003). Vhnf1 and Fgf Signals Synergize to Specify Rhombomere Identity in the Zebrafish Hindbrain. *Development* 130, 3821-3829.

Wilkinson, D. G., Bhatt, S. and McMahon, A. P. (1989). Expression Pattern of the FGF-Related Proto-Oncogene Int-2 Suggests Multiple Roles in Fetal Development. *Development* 105, 131-136.

Wizenmann, A. and Lumsden, A. (1997). Segregation of Rhombomeres by Differential Chemoaffinity. *Mol. Cell. Neurosci.* 9, 448-459.

Wurst, W. and Bally-Cuif, L. (2001). Neural Plate Patterning: Upstream and Downstream of the Isthmic Organizer. *Nat. Rev. Neurosci.* 2, 99-108.

Xiong, F., Tentner, A. R., Huang, P., Gelas, A., Mosaliganti, K. R., Souhait, L., Rannou, N., Swinburne, I. A., Obholzer, N. D., Cowgill, P. D. et al. (2013). Specified Neural Progenitors Sort to Form Sharp Domains After Noisy Shh Signaling. *Cell* 153, 550-561.

Xu, Q., Mellitzer, G., Robinson, V. and Wilkinson, D. G. (1999). In Vivo Cell Sorting in Complementary Segmental Domains Mediated by Eph Receptors and Ephrins. *Nature* 399, 267-271.

Xu, Q., Mellitzer, G., Robinson, V. and Wilkinson, D. G. (1999). In Vivo Cell Sorting in Complementary Segmental Domains Mediated by Eph Receptors and Ephrins. *Nature* 399, 267-271.

Xu, Q., Mellitzer, G. and Wilkinson, D. G. (2000). Roles of Eph Receptors and Ephrins in Segmental Patterning. *Philos. Trans. R. Soc. Lond. B. Biol. Sci.* 355, 993-1002.

Yasuhiko, Y., Kitajima, S., Takahashi, Y., Oginuma, M., Kagiwada, H., Kanno, J. and Saga, Y. (2008). Functional Importance of Evolutionally Conserved Tbx6 Binding Sites in the Presomitic Mesoderm-Specific Enhancer of Mesp2. *Development* 135, 3511-3519.

Zeltser, L. M., Larsen, C. W. and Lumsden, A. (2001). A New Developmental Compartment in the Forebrain Regulated by Lunatic Fringe. *Nat. Neurosci.* 4, 683-684.

Zhang, F., Nagy Kovacs, E. and Featherstone, M. S. (2000). Murine Hoxd4 Expression in the CNS Requires Multiple Elements Including a Retinoic Acid Response Element. *Mech. Dev.* 96, 79-89.

Zhang, L., Radtke, K., Zheng, L., Cai, A. Q., Schilling, T. F. and Nie, Q. (2012). Noise Drives Sharpening of Gene Expression Boundaries in the Zebrafish Hindbrain. *Mol. Syst. Biol.* 8, 613.

Zimmer, M., Palmer, A., Kohler, J. and Klein, R. (2003). EphB-ephrinB Bi-Directional Endocytosis Terminates Adhesion Allowing Contact Mediated Repulsion. *Nat. Cell Biol.* 5, 869-878.

ANNEX

Cell segregation in the vertebrate hindbrain relies on actomyosin cables located at the interhombomeric boundaries

Simone Calzolari+, Javier Terriente+ and Cristina Pujades*
Department of Experimental and Health Sciences, Universitat Pompeu Fabra,
Parc de Recerca Biomèdica de Barcelona, PRBB, 08003 Barcelona, Spain

+ These authors contributed equally to this work
*Corresponding author: cristina.pujades@upf.edu

Corresponding author:
Cristina Pujades, PhD
Department of Experimental and Health Sciences
Universitat Pompeu Fabra
PRBB, Dr Aiguader 88
08003 Barcelona, Spain
Tel. +34.933160839
cristina.pujades@upf.edu

Running title: Cell sorting hindbrain boundaries actomyosin cable

ABSTRACT

Segregating cells into compartments during embryonic development is essential for growth and pattern formation. The physical mechanisms shaping compartment boundaries were recently explored in Drosophila, where actomyosin-based barriers were revealed to be important for keeping cells apart. In vertebrates, interhombomeric boundaries are straight interfaces, which often serve as signaling centers that pattern the surrounding tissue. Here we demonstrate that in the hindbrain of zebrafish embryos cell sorting drives sharpening of molecular boundaries and, once borders are straight, actomyosin barriers are key to keeping rhombomeric cells segregated. Actomyosin cytoskeletal components are enriched at interhombomeric boundaries, forming cable-like structures in the apical side of the neuroepithelial cells by the time morphological boundaries are visible. When Myosin II function is inhibited cable structures do not form, leading to rhombomeric cell mixing. When EphA4a is downregulated, actomyosin cables are compromised and cells with different rhombomeric identity intermingle. This phenotype is rescued in the EphA4a-morphants when the contractility of the actomyosin cable is enhanced, suggesting that mechanical barriers act downstream of Ephrin-EphA signaling to segregate cells from different rhombomeres.

Keywords: actomyosin cable / cell sorting / compartments / rhombomeric boundaries / segmentation

INTRODUCTION

During embryonic development, cells are partitioned into distinct groups or compartments separated by sharp boundaries. Cells do not intermingle across compartment boundaries, ensuring that their fates and/or positional information remain segregated as they proliferate and move. Thus, the establishment of these interfaces is critical to embryonic pattern formation and tissue differentiation, and importantly, tissue interface deregulation plays a key role during tumor formation and metastasis (Dahmann et al, 2011; Batlle and Wilkinson, 2012).

In Drosophila and vertebrates, cell sorting between compartments is governed both by transcription factors that confer compartment-specific identities and by signaling centers localized to the boundaries, such as EphA/Ephrin, Hedgehog or Notch signaling (for review see Dahmann et al, 2011). Downstream of these factors, several mechanisms have been proposed for cell sorting, mainly differential adhesion, regulation of the cytoskeleton, control of cell proliferation or formation of extracellular matrix fences, although the causal relationship among them has not been unveiled. Recently, it has been shown that local regulation of actomyosin contractility and mechanical tension are the primary mechanisms for sorting cells at some compartmental boundaries in Drosophila (Monier et al, 2010; Aliee et al, 2012). However, *in vivo* support for these hypotheses in vertebrates is scarce and the molecular and cellular mechanisms responsible of maintaining sharp boundaries during growth and morphogenesis are not fully explored.

Here, we investigate this question in the embryonic zebrafish hindbrain, which undergoes a segmentation process leading to the formation of seven morphological compartments called rhombomeres (r). These segments are visible transiently during development as a series of bulges in the neuroepithelium. The appearance of morphologically visible rhombomeres

requires the segment-restricted expression of transcription factors. The expression in boundaries of these genes and some of their downstream targets is initially diffuse and jagged but eventually sharpen, and prefigure the positions of rhombomeric boundaries. Over the same period, morphological boundaries appear, followed by the expression of boundary-specific markers (for review see Moens and Prince, 2002). Cell mixing is restricted across rhombomere boundaries (Fraser et al, 1990; Jimenez-Guri et al, 2010) and several works have stressed the importance of EphA/Ephrin signaling in rhombomeric cell segregation. In zebrafish, two mechanisms have been proposed to operate in parallel: i) repulsive interactions between EphrinB-expressing and EphA4-expressing cells at rhombomeric boundaries (Xu et al, 1995; 1999); and adhesive interactions between cells of the same cohort (Cooke et al, 2005; Kemp et al, 2009). We wanted to determine whether multiple mechanisms were additionally required to achieve cell segregation, such as the interplay between adhesion and physical mechanisms.

We demonstrate that in the hindbrain of zebrafish embryos, once gene expression domains have achieved sharp boundaries due to cell sorting, actomyosin cytoskeletal components are enriched at interhombomeric boundaries. These actomyosin-based barriers stop cells from invading neighboring compartments especially upon cell division; when the formation of the actomyosin cable is compromised, rhombomeric cell mixing can occur. Interestingly, the EphA/Ephrin signaling pathway plays an important role in cable stabilization because downregulation of EphA4a results in the disruption of actomyosin cables and cell intermingling. We propose that actomyosin cables at the interhombomeric boundaries act downstream of EphA/Ephrin signaling to segregate cells from different rhombomeres and therefore prevent cell mixing.

RESULTS

The refinement of molecular boundaries in the hindbrain is achieved by cell sorting

The segregation of rhombomeric cell populations involves the formation of a sharp interface between adjacent segments with different identity. The segregation of cells and the formation of well-defined boundaries can be visualized by observing gene expression within the rhombomeres. Initially, *krx20* displays a jagged border of expression in r3 and r5 boundaries at 10hpf (Fig 1B-D, see arrow in D) but becomes sharply defined at 14hpf (Fig 1E-F; Cooke and Moens, 2002). Gene expression boundary sharpening can occur by a number of possible mechanisms: cells on the "wrong" side of a boundary can move across it by a cell-adhesion/repulsion based mechanism –cell sorting– (Xu et al, 1999; Cooke et al, 2005; Kemp et al, 2009); or they can switch their identity to that of their neighbors –cell plasticity– (Schilling et al, 2001; Zhang et al, 2012), however there is no a clear picture about the main mechanism applying. To study deeper how this molecular refinement is generated we analyzed the behavior of cells with different rhombomeric identities during early embryonic development. We took advantage of two transgenic fish lines that express stable fluorescent protein reporters (mCherry or GFP) in r3 and r5 under the control of different *krx20* regulatory elements (Mü4127 and Tg[elA:GFP]; Fig 1A).

First, we characterized the two transgenic fish lines and revealed that in the Mü4127 line expression of *kalTA4* and *mCherry* mRNA spatially recapitulated endogenous *krx20* expression: fuzzy boundaries of expression at 11hpf (Fig 1G-I, see arrows in I) and sharp borders by 14hpf (Fig 1J-K,Q), with a slight temporal delay in respect to wt embryos (Distel et al, 2009). Analysis of *gfp* transcript expression and GFP protein in Tg[elA:GFP] line showed first jagged activation in r3, and then in r3 and r5, equivalent to *krx20* expression (Fig 1L-N,R), with complete straight gene expression

boundaries by 14hpf (Fig 1O-P,S). The *krx20* expression domain corresponded with the expression of the reporter genes (Fig 1K,P).

Because the two lines recapitulate the dynamics of *krx20* expression next we used them to trace rhombomeric cells using two approaches: i) *in vivo* imaging to follow single cells from different rhombomeres (Fig 2, Movies S1-S3), using Tg[elA:GFP] embryos injected with H2B-mCherry; and ii) fake cell-tracing analysis in fixed embryos (Fig 3). We first focused on detailed cell trajectories in the vicinity of rhombomeric borders and followed *in vivo* single r5 or r6 cells by tracking cell nuclei. We observed that cells located on either side of the r5/r6 boundary did not change their molecular identity (Fig 2A-L, see blue dots for single cells, Movies S1-S2). r5 GFP-positive cells were kept into r5 and maintained the GFP during the length of the movie (Fig 2A-F, see blue dot and white arrow for a given example; Movie S1). r6 GFP-negative cells behaved in a similar manner, namely, r6 cells that incurred into the r5 territory were sorted out and never changed their molecular identity even after cell division (Fig 2G-L, see blue dots and white arrows; Movie S2). These results show that when cells of a given identity are found within an environment of different identity are sorted out.

To explore the behavior of groups of cells in adjacent territories we followed several individual cells by time-lapse analysis during 5h (from 11 to 16hpf). Single red nuclei of GFP-positive and GFP-negative cells mainly located in the r3-r6 region, and at different positions along the rhombomeres (close/far to the boundary) were manually back-tracked (Fig 2M-R'; n=43). This means that cells that by the end of the movie were located in given positions of the hindbrain were followed back to their original positions at the beginning of the movie. As shown in Fig 2M-R' and Movie S3, analysis of several individual cell trajectories indicated that cells that at the beginning of the analysis (11hpf) were in the nearby of their future position but somehow intermingled (Fig 2M'-O'; see mixed blue, yellow and green dots), were

sorted out from the neighboring territory with distinct molecular identity by the end of the analysis (Fig 2P'-R'; see segregated blue, yellow and green dots). In Movie S3 it can be observed that cells do not migrate long distances, but they mainly intermingle. Thus, cells that are early located in the fuzzy boundary region, end up segregated along the sharp boundary of gene expression.

These results support cell sorting as the mechanism operating in the refinement of molecular rhombomeric boundaries in zebrafish, independently of the identity of the cell. However, to fully support this hypothesis we did a fake cell-tracing analysis in the transgenic zebrafish lines Tg[elA:GFP] and Mü4127 (Fig 3). The rationale of the experiment was that cells expressing *krx20* will switch on the reporter gene *mCherry/gfp* and then mCherry/GFP proteins will be synthesized. Since fluorescent proteins are more stable than *krx20* mRNA, we will be able to trace cells that once activated *krx20* by the expression of the fluorescent reporter even at a stage when normally *krx20* gene has already been switched off. If cell plasticity was the cellular mechanism used by the cells to generate the pattern we would find ectopic fluorescent cells in r2, r4 or r6 that no longer expressed *krx20* mRNA at late developmental stages (18hpf). On the other hand, if cell sorting was the main mechanism accounting for the sharpening of gene expression we should not expect any ectopic fluorescent cells, since *krx20* cells located in the "wrong" side (r2, r4 and r6) would segregate to the "right" side (r3 and r5). Following this hypothesis, we performed fluorescent *in situ* hybridization for *krx20* combined with antibody staining to detect the reporter fluorescent protein followed by confocal analysis (Fig 3A-F). When expression of *krx20* was analyzed in embryos at 18hpf (once molecular boundaries have been clearly refined; Fig 1), no ectopic *krx20*-cells were found in r2, r4 or r6 in any of the transgenic lines (Fig 3A,D). Moreover, in these same embryos no ectopic GFP-positive cells were observed (Fig 3B,E). Accordingly, the big majority of cells expressing GFP also expressed *krx20*

mRNA (Fig 3C,F). To quantify this, we counted the number of cells close to boundary regions that expressed both *krx20* and GFP, and found that over 95% of the cells in any of the rhombomeric boundaries shared both markers (Fig 3J-K). Since we observed jagged expression of *mCherry* and *gfp*/GFP at early developmental stages (see arrows in Fig 1D,I,N,R), these results strongly suggest that cell sorting plays a major role in the sharpening of *krx20* expression. However, to unveil any possible cell plasticity events that could take place but could be masked by the strength of the sorting mechanism, we knocked-down EphA4a function, which plays a known role in cell sorting (Xu et al, 1999). When EphA4a was downregulated, boundaries were jagged but all GFP-positive cells still expressed *krx20* (Fig 3G-I, see white arrow head pointing to an isolated cell expressing both markers). Cells not expressing *krx20*, did not have any GFP either (Fig 3G-I, see white arrows). No changes were detected when different rhombomeric boundaries were analyzed (Fig 3J-K), pointing to cell sorting as the sharpening mechanism in all hindbrain boundaries -independent of the cell position along the antero-posterior (AP) axis-.

Presence of an actomyosin cable in the interhombomeric boundaries

The border of expression of transcription factors prefigures the position of the morphological rhombomeric boundaries. As shown above, once gene expression domains achieve sharp boundaries due to cell sorting, morphological boundaries are visible as shallow indentations on the outside of the neural tube and cell mixing is restricted between rhombomeres. In zebrafish, hindbrain morphological boundaries are visible around 15hpf (Fig S4; Maves et al 2002). From this stage onwards, cells with different rhombomeric identities do not mix. We performed live imaging in the proliferating tissue and looked at cell behaviors upon cell division close to the boundaries. We found that interhombomeric boundaries could be transiently challenged by cell division, since cells incurred into the

neighboring compartment when they divided (Fig 4A-E, B'-E', see red cell indicated with white arrow heads, n=7; see as well Movie S5). Interestingly, when a dividing cell at the boundary rounded up and transiently invaded the adjacent compartment, it was pushed back to the original rhombomere (Fig 4B-E), suggesting there was an elastic barrier at boundary interfaces. Thus, we wanted to address how cell segregation is physically restricted during growth and morphogenesis.

Several mechanisms have been proposed for keeping cells segregated, mainly differential cell adhesion but also extracellular matrix fences (for review see Batlle ad Wilkinson, 2010). We investigated the role of mechanical barriers in maintaining distinct rhombomeric borders or keeping rhombomeric cells segregated, exploring two possible mechanisms: a barrier made of extracellular matrix deposition such as in the embryonic intersomitic boundaries in zebrafish (Jülich et al, 2009); or a barrier based in actomyosin fibers as previously described in Drosophila (Major and Irvine, 2005, 2006; Monier et al, 2010; Aliee et al, 2012; Becam et al, 2012). First, we investigated if there was any contribution of Fibronectin (FN) matrix deposition in the interhombomeric boundaries analyzing the presence of FN matrix assembly between rhombomeres (Fig S6). When embryos at 18hpf were immunostained with anti-FN, no FN matrix deposition was observed in the hindbrain boundaries although a clear staining was visible at the somites interface (Fig S6A-B). Similar results were obtained when we injected embryos with mRNA of the □ 5 integrin subunit, a FN receptor that clusters upon activation (Jülich et al, 2009), in order to visualize integrin clustering in rhombomeric boundaries (Fig S6C-F). These results suggest that fibronectin does not play a major role in keeping rhombomeric cells apart.

Next, we explored the presence of actin-filament structures in the hindbrain at the time morphological bulges appeared. For this purpose, we used the transgenic lines Tg[lifeactin:GFP] and Tg[utrophin:GFP] that allow the visualization of F-actin, and Tg[myoII:mCherry/GFP], which let us visualize

Myosin II when bound to actin filaments (Behrndt et al, 2012; Maitre et al, 2012). Since actomyosin cables are always located at the apical side of the cells, we did analyze the presence of Actin filaments in the hindbrain observing the apical side of the rhombomeric cells, which is located close to the midline (Fig 4F-G, G displays a view of the stacks contained within the orange frame in F). For this, we took confocal images of embryos in dorsal views and did Maximal Intensity Projections of only the most apical stacks in a sagittal-like view (see Materials and Methods, and Fig S7). Indeed, an enrichment of Actin cable-like structures was visible from 15hpf, coinciding with the stage where morphological boundaries were already visible (Fig 4H-M). These cables could not be observed earlier (Fig 4H-I) and were visible at least up to 24hpf (Fig 4J-M; data not shown). To demonstrate that these cables were formed by F-actin and Myosin II, we sought the presence of actomyosin fibers by crossing Tg[lifeactin:GFP] with Tg[myosinII:mCherry] and showed that indeed the rhombomeric cables contained both elements of the actomyosin structures (Fig 4N-N'). Finally, we demonstrated that these cables were specifically located in the interhombomeric boundaries, coinciding with the border of mCherry expression as a readout of *krx20* in Mü4127/Tg[myoII:GFP] embryos (Fig 3O). Next, we investigated in which rhombomere the cable was located, by immunostaining Tg[utrophin:GFP] embryos with anti-EphA4a. The actomyosin cable seems to localize in the EphA4-negative rhombomere (Fig 4P-P"), although the optical resolution of confocal and two-photon microscopy is at the limit to detect structures within that range.

These data demonstrate the local enrichment of contractile elements such as F-actin and Myosin II in hindbrain boundaries, as reported previously in Drosophila at the parasegment boundaries of the embryonic epidermis (Monier et al, 2010), and the boundaries of the different larval imaginal discs (Major and Irvine, 2005, 2006; Landsberg et al, 2009; Becam et al, 2012; Curt

et al, 2013). These results point to actomyosin cables as major players in restricting the intermingling of different rhombomeric cells.

Actomyosin barriers sort cells at rhombomeric boundaries

To know whether actomyosin cables were effectors of boundary formation it was important to determine their ability in restricting cell mixing. Therefore, to test whether the actomyosin cable does create a barrier, we disrupted the cables by inhibiting Myosin II function using two different drugs: i) Blebbistatin, which inhibits Myosin II by blocking the Myosin heads in a complex with low Actin affinity (Kovacs et al, 2004), and ii) Rockout, an ATP-competitive inhibitor that specifically blocks Rho kinase activity and therefore inhibits MRLC (non-muscle Myosin II regulatory light chain) by preventing its phosphorylation (Ernst et al, 2012). When double transgenic Mü4127/Tg[utrophin:GFP] embryos were treated with Blebbistatin or Rockout, the actomyosin cables in the apical side of the cells were dismantled (compare Fig 5C and D; 76% for Blebbistatin, 90% for Rockout not shown) and r3 or/and r5 ectopic cells were found in adjacent rhombomeres (Fig 5H, 60%, see white arrows pointing at ectopic cells) when compared with control embryos (Fig 5F, 0%). These results support the idea that actomyosin cables serve as mechanical barriers that restrict cell movement between rhombomeres during hindbrain segmentation. Interestingly, when Myosin II contractility was artificially enhanced exposing embryos to Calyculin A (a compound that overactivates Myosin II inhibiting Myosin phosphatase; Filas et al, 2012), the morphological bulges were more visible (see the indentations in the neural tube in Fig 5E, 100%). As expected no cell mixing was observed (Fig 5I, 100%) indicating that these actomyosin cables are indeed functional. We have found a clear correlation between the lack/disorganization of the actomyosin cables and the extent of cell intermingling. These results support the hypothesis that vertebrates have a mechanism based in actomyosin-dependent mechanical barriers to maintain

straight interfaces between different cell populations, and therefore to keep them segregated.

Rhombomeric cells on both sides of the boundary are perfectly aligned and form a straight interface (Fig 5G,J). We quantified the degree of misalignment when compartmentalization was compromised (Fig 5K) using as a readout *krx20*-expression. We measured the Index of Straightness (IS, Fig S7; Monier et al, 2010) considering that the straighter the boundary, the closer will be IS to 1, which corresponds to a perfect straight line. Quantification of the IS confirmed that interhombomeric interfaces were straighter in control embryos (Fig 5J,M, IS=1.1, n=10) than in Blebbistatin-treated embryos (Fig 5K,M, IS=1.2, n=13), and even straighter boundaries were observed in embryos where Myosin II activity was enhanced by addition of Calyculin A (Fig 5L-M, IS=1.05 n=8). These results support our previous conclusions in that mechanical barriers maintain the straightness of the boundaries.

To make sure that our time-controlled drug treatments were not disrupting too much the embryo development, we made sure that the disassembly of the actomyosin cable observed after pharmacological treatments was reversible. For this, we incubated Tg[myosinII:GFP] embryos with Blebbistatin and Rockout as depicted in Fig 5A, and then the pharmacological agent was washed out and embryos were let to develop few more hours. As shown in Fig 6A-D, in both cases the actomyosin cable is restored after the wash-out of the drug. Since actomyosin is required for interkinetic nuclear migration (Spear and Ericksson, 2012), a process that occurs within a time frame of very few hours (Leung et al, 2011), we wanted to make sure that the observed phenotype –lack of interhombomeric cables- was not due to a secondary effect resulting from the overall changes in morphogenesis and, in particular, to specific basal-to-apical nuclear migration defects in the rhombomeric cells. To investigate this issue we

closely analyzed the effects of Myosin II inhibitors and activators in the Interkinetic Nuclear Migration (INM) process upon our experimental conditions (Fig 6E-J). For this purpose, we sought the position and number of mitotic cells in the hindbrain (Fig 6E-I), and calculated the Interkinetic Nuclear Migration Ratio (apical nuclei/basal nuclei, Fig 6J, Fig S8). No differences in the apical position of the mitotic cell nuclei of embryos treated with DMSO, Blebbistatin, Rockout or Calyculin (Fig 6E-H), or in the total number of pH3-positive cells were observed (Fig 6I). Thus, our experimental conditions did not compromise the overall proliferation of the neural progenitors. On the other hand, when the INM Ratio was assessed, both for Blebbistatin or Calyculin A treated embryos, we consistently observed more cell nuclei in an apical location (Fig 6J). Nevertheless, given that both antagonistic treatments interfere with the basal-to-apical INM the dismantling of the cable cannot be explained by a disruption in basal-to-apical INM of rhombomeric cell progenitors. Thus, the phenotypes we observed are specific to the rhombomeric actomyosin cables.

Our next question was to address how these mechanical barriers were established. Interestingly, when cell sorting was compromised by EphA4a-MO injections, not only ectopic r3 and/or r5 cells were found outside their territory as expected (Fig 7D, 100%, see white arrows; Cooke et al, 2005), but actomyosin cables were highly disrupted (Fig 7I, 100%) when compared with control embryos (Fig 7C,D, respectively). In line with this observation, the IS in the boundaries of the morphants was increased when compared to control embryos (Fig 8D; IS=1.1 CTRL-MO n=31; IS=1.25 EphA4a-MO n=23); and accordingly, the interfaces between rhombomeres were jagged (compare Fig 8A to Fig 5J as control, n=10). To further support this, when EphA4a-morphants were treated with a Myosin II inhibitor the phenotype was enhanced and the hindbrain boundaries were further jagged, hence displaying a higher IS (Fig 8B,D) and as expected cell intermingling was

observed (Fig 7E). Interestingly, when actomyosin filament stability was enhanced treating EphA4-morphants with Calyculin A, no r3/r5 cells were found ectopically (Fig 7F, 100%) and actomyosin cables were partially rescued (Fig 7K, 60%), which strongly suggests that assembly of actomyosin cables is an event downstream of EphA/Ephrin signaling. Accordingly, boundaries were straighter and consequently the IS was closer to 1 (Fig 8C,D). Furthermore, when EphA4 was conditionally activated in r4 or in r6, enrichment of actomyosin fibers components was generated around the ectopic EphA4-positive cell (Fig 8H-I, see yellow arrows). When ectopic EphA4-cells were located in r3 or r5 territories (where there is no EphA4 ligand), no ectopic enrichment of cable structures could be observed (Fig 8H-I, see white arrow head). Overall, these results strongly suggest that indeed EphA/Ephrin pathway is the activator of the assembly of the cable and that mechanical barriers act downstream of EphA/Ephrin signaling to segregate cells from different rhombomeres.

DISCUSSION

We demonstrate by different approaches that cell sorting is the major mechanism operating in the sharpening of gene expression in rhombomeric boundaries, independently of the cell identity and the position along the AP axis. A recent report suggested that an attenuation mechanism relying on intracellular noise induces cells to switch their identity during r4/r5 boundary sharpening (Zhang et al, 2012). Their model proposes that noise in the Retinoic Acid (RA) morphogen gradient can lead to rough gene expression boundaries initially, and that sharpening is driven by noise in the expression of *hoxb1a* and *krx20*, due to induced switching between expression of one gene and the other (Zhang et al, 2012). However, we observe only cell sorting events at the rhombomeric boundaries, either by: i) analyzing single cell trajectories and behaviors (such as cell division), ii) cell tracing using

stability of fluorescent proteins versus less stability of mRNA, or iii) trying to unveil any possible cell plasticity events downregulating the cell sorting, and we could not find evidences for cell switching. Nevertheless, this difference between our results and theirs might be explained by the fact that the cells undergoing plasticity display very low *krx20*-expression, as they pointed out in their work, which might not be detectable with our transgenic lines. Interestingly, another difference in our study is that all rhombomeric boundaries behave similarly, regardless of their AP position, meanwhile Zhang et al describe cell switching depending on RA fluctuations mainly in r4/r5. Since r4/r5 is the first rhombomeric boundary to appear (Maves et al, 2002; Lecaudey et al, 2004) and it is evolutionary conserved (Jimenez-Guri and Pujades, 2011) it is possible that r4/r5 is under such evolutionary pressure of being properly regulated that it might undergo dual refining mechanism based in both cell sorting and cell plasticity events, acting with different temporal specificities, since we do not see cells losing *krx20*-expression and changing identity in our temporal frame study. Interestingly, a recent report discovered that the sharply delineated pattern of neural progenitor domains along the DV axis forms through sorting of specified cells. They found that specified progenitors of different fates are spatially mixed and cell sorting rearranges them into sharply bordered domains (Xiong et al, 2013). May be the *krx20* activation is the result of both, interpretation of morphogen concentration and a gene regulatory network, which are spatially inaccurate and a cell-autonomous mechanism (cell sorting) is needed for refinement. Since the formation of spatially distinct domains faces noise at multiple scales, most probably multiple strategies are used to achieve robust patterning.

The key challenge to rhombomeric boundaries we have detected is the division of the cells at the boundary. Mitotic cells incurring into the adjacent rhombomeres are pushed back to their rhombomere of origin, suggesting a

mechanical barrier is involved in keeping different cell populations segregated. Here, we provide evidences of the presence of actomyosin cables at the interhombomeric boundaries, and show that Myosin II function is required for restriction of cell intermingling. Experiments with pharmacological drugs that enhance or decrease the stability of the actomyosin complex in a very precise time window demonstrate that actomyosin cables are functional, and this can be modulated upon specific experimental conditions. Interestingly, it has been reported that Myosin II is active in the hindbrain at 18hpf peaking at 21hpf (Gutzman and Sive, 2010), the period when morphological rhombomeric bulges are visible. In addition, mutants for *mypt1*, a Myosin II phosphatase mutant that display an overactive Myosin II, display similar defects to our experiments with Calyculin A: the neural tube is narrower and indentations in the neural tube are deeper at the morphological boundaries than in control embryos. We have detected actomyosin cables in the apical side of the neuroepithelial cells, although a readout of Myosin II activity, pMRLC (phosphorylated Myosin Regulatory Light Chain), was reported to localize in the basal as well as in the apical side of the neural tube during lumen formation (Gutzman and Sive, 2010). This is probably due to the fact that Myosin II and Actin have pleiotropic functions: they are important for neuroepithelial cell shape, rhombomere morphogenesis and ventricle expansion from 24hpf onwards (Gutzman and Sive, 2010), and for actomyosin fiber assembly from 15hpf as we show in our report. We demonstrate that actomyosin-based barriers are involved in segregating cells at rhombomeric boundaries and keep them apart, since embryos in which the actomyosin fiber has been dismantled display a certain degree of rhombomeric cell mixing (see Fig 9 for model).

Previous models for cell sorting predicted that boundaries formed as a consequence of different rhombomeric cell types having distinct adhesive properties. They also brought up EphA/Ephrin signaling as an important factor in maintaining the boundaries between adjacent odd- and even-

numbered rhombomeres (for reviews see Dahmann et al, 2011; Batlle and Wilkinson, 2012). Our data helps to understand how the juxtaposition of different rhombomeric cells triggers actomyosin assembly interfaces along rhombomeric boundaries through EphA/Ephrin signaling. We showed the actomyosin cable is located apically; however, because insufficient optical resolution we have been unable to discriminate whether the cable is at the even-, odd-numbered rhombomeres, or both. Nevertheless, upon abrogation of EphA/Ephrin signaling actomyosin cables are perturbed and cells mix with the adjacent rhombomere neighbors. In addition, this phenotype is partially rescued by enhancing Myosin II function, suggesting that these cables, not completely dismantled in the downregulation of the EphA4a, upon favorable conditions can be functionally restored to a wt phenotype. These evidences suggest that assembly of actomyosin fibers is downstream of EphA/Ephrin signaling, and this is crucial to maintain rhombomere sharpening. Whether this mechanism acts in parallel or downstream to other known roles in cell adhesion/repulsion of EphA/Ephrin signaling remains to be shown. To this end, one possible molecular mechanism would be that ephrin-reverse signaling is responsible for recruiting PDZ-domain proteins involved in actomyosin assembly, and therefore the key factor for assembling the mechanical barrier (Klein, 2012). The other option is that Eph receptor upon ligand binding enhances Rock activation, which inhibits F-actin depolymerization and MLCP activity, favoring accumulation of actomyosin cables as shown in a recent work where actomyosin-based contraction is responsible for specific sorting of neuronal auditory projections (Defourny et al, 2013).

The picture that emerges from our results is the existence of a conserved strategy between vertebrates and Drosophila based in actomyosin-driven mechanical forces to sort cells at compartment boundaries. Another relevant aspect of our study, also related to EphA/Ephrin being upstream of

actomyosin cable formation, is that this sharpening mechanism can be a common strategy to be used for other boundaries where this signaling pathway is involved, such as gut or somites.

MATERIALS AND METHODS

Zebrafish strains and maintenance

Zebrafish embryos were obtained by mating of adult fish by standard methods. All fish strains were maintained individually as inbred lines. All procedures used have been approved by the institutional animal care and use ethic committee (PRBB–IACUC), and implemented according to national rules and European regulations. Mü4127 is an enhancer trap line in which the trap cassette containing a modified version of Gal4 (KalT4) and mCherry (KalTA4-UAS-mCherry cassette) was inserted in the 1.5Kb downstream of *krx20* gene (Distel et al, 2009). 4xKaloop is a stable transgenic effector strain that carries a bicistronic 4xUAS effector construct driving KalTA4-GFP fusion protein expression as a reporter that once activated, continuously maintains its own expression by constantly providing the Gal4 activator (KalT4) in a feedback loop (Distel et al, 2009). We used the crosses from Mü4127 with 4xKaloop to visualize the activity of the KalT4 in green due to expression of GFP under its control. Tg[elA:GFP] line, is a stable reporter line where chicken element A was cloned upstream of the *gfp* reporter in a modified pTol2 vector (Chomette et al, 2007; Stedman et al., 2009; Labalette et al, 2011). Tg[lifeactin:GFP] and Tg[utrophin:GFP] lines are reporters that allow the visualization of F-actin, and Tg[myosinII:mCherry/GFP] visualizes Myosin II (non-cardiac Myosin associated to Actin filaments) (Behrndt et al, 2012; Maitre et al, 2012). Tg[□ actin:HRAS-EGFP] homogenously labels cell membranes (Cooper et al, 2005).

Whole mount in situ hybridization and immunostaining

Whole-mount *in situ* hybridization was adapted from (Thisse et al, 1993). Riboprobes were as follows: *krx20* (Oxtoby and Jowett, 1993), *kalTA4* (Distel et al, 2009) and *gfp*. The chromogenic and fluorescent in situ hybridizations were developed with NBT/BCIP and FastRed substrates

respectively. For double fluorescent in situ hybridization of Fig S1, DIG-labeled riboprobes for *kalTA4* and *gfp* were developed with FastRed and FLUO-labeled krx20 with fluorescein-tyramide substrate (TSA system).

For immunostaining, embryos were blocked in 5%GS/PBT 1h at RT and incubated O/N at 4ºC with primary antibody. Primary pAbs were the following: anti-EphA4 (1:450) (Irving et al, 1996), anti-FN (1:200, Sigma), anti-GFP (1:200, Torrey Pines), anti-pH3 (1:200, Upstate). After extensive washings with PBST, embryos were incubated with secondary Ab conjugated with Alexa Fluor®488 or Alexa Fluor®555 (1:500, Invitrogen). Embryos were flat-mounted and imaged under a Leica DM6000B fluorescence microscope or SP5 confocal microscope with 20x or 40x objective.

Antisense morpholinos and mRNA injections

For morpholino knockdowns, embryos were injected at 1cell/stage with translation-blocking morpholino oligomers (MOs) obtained from GeneTools, Inc. MOs were as follows: MO-EphA4a, 5'-AAC ACA AGC GCA GCC ATT GGT GTC-3' (Cooke et al, 2005), p53-MO, 5'-GCG CCA TTG CTT TGC AAG AAT TG-3' (Langheinrich et al., 2002).

For mRNA expression, capped H2B-mcherry (Olivier et al, 2010), itga5:GFP (Jülich et al, 2009), and lyn:GFP/mem:mCherry mRNAs were synthetized with mMessage mMachine (Ambion). Embryos were injected at 1cell/stage and developed until the desired stages.

Time-lapse movies

Cell tracking experiments

Anesthetized live embryos were embedded in 1% low-melting point (LMP) agarose with the hindbrain positioned towards the glass-bottom of the Petri dish in order to have a dorsal view with an inverted objective. For cell tracking experiments, and in order to have a mosaic expression, Tg[elA:GFP] embryos were injected with H2B-mcherry mRNA at 4-8cell stage. Briefly,

back-tracking of red nuclei of GFP+ and GFP-cells was performed in 3 independent experiments and cells were tracked manually at different DV level using ImageJ software. Experimental parameters for Movies S2 and S3 were: voxel dimension (nm): x 378.8 y 378.8 z 1510.6, time frame: 90s; total time: 2h21 min; pinhole: 60.6 μm; zoom: 2; objective: 20x dry; NA: 0.70. Experimental parameters for Movie S4 were the following: voxel dimension (nm): x 378.8 y 378.8 z 1510.6, time frame: 155s; total time: 4h36 min; pinhole: 66.7 μm; zoom: 2; objective: 20x immersion; NA: 0.70. Videos were performed using SP5 Leica confocal system.

In vivo analysis of cell divisions in the rhombomeric boundaries

Anesthetized live double transgenic Mu4127 Tg[actin:HRAS-EGFP] embryos for Fig 3 and Fig S5 were embedded and mounted as previously described. Experimental parameters for the video were: voxel dimension (nm): x 303.0 y 303.0 z 1216.9, time frame: 423,1s; total time: 3h58 min; pinhole: 60.8 μm; zoom: 2.5; objective: 20x immersion; NA: 0.70.

Assessment of cable-like structures in live embryos and pharmacological treatments

Cable-like structures

Live embryos from Tg[lifeactin:GFP], Tg[utrophin:GFP] and Tg[myosinII:GFP/mCherry] lines were anesthetized with Tricaine and mounted as described before. For cable-structure analysis, 0.6μm z stacks were acquired in dorsal view and re-sliced to generate YZ confocal cross-sections. Images were re-sliced in XZ, and finally, a maximal projection of the XZ sections corresponding to the apical side of cells in the neural tube was generated (Fig S8A).

Pharmacological treatments

We found very important to apply the treatments once the neural tube was already formed to avoid interfering with early morphogenesis of the neural tube, but at a stage that we could still tackle the process of interest, the formation of rhombomeric bulges. Thus, in all experiments embryos at 14hpf were dechorionated and treated during 6h at 28ºC with: i) Myosin II inhibitors such as Blebbistatin (25 M), or Rockout (50nM); and ii) Calyculin A (100nM), an inhibitor of Myosin-phosphatase to enhance contractility of actomyosin cables, and iii) DMSO for control experiments. Afterwards, embryos were either taken to the confocal microscope for *in vivo* analysis or fixed in 4%PFA for immunostaining or in situ hybridization.

Quantification of the Index of Straightness (IS)

The quantification of the Index of Straightness was based in the sharpness of the border of *krx20* expression. Whole-mount *in situ* hybridization for *krx20* was performed on 18hpf fixed embryos from the same batch, after different experimental conditions: control embryos, CTRL-MO or EphA4a-MO injected embryos treated with either DMSO, Blebbistatin or Calyculin A. Confocal images were acquired in dorsal view of flat-mounted hindbrains covering the r3-r5 region with 1µm z distance. Images were then re-sliced to generate YZ confocal cross-sections to properly orient the embryos along the DV axis, and finally the same 5µm DV portion in every embryo was selected and re-sliced back to XY to obtain dorsal views. These stacks were then projected into a single dorsal view image (Fig S8B). Once images were obtained, we addressed the index of straightness (IS) of the *krx20* expression border doing the following: longitudes of the *krx20* expression border for r2/r3, r3/r4, r4/5 and r5/r6 boundaries were calculated with FIJI (yellow dotted line, α; Fig S8B), and also the theoretical straight distance of the *krx20*-expression border (white dotted line, β; Fig S8B). The IS is the ratio

between α and β. Since IS=1 would represent a completely straight boundary we plotted the values as a deviation from 1, representing a better indication of the deviation from straightness (Fig 5D, Fig 6M). In the plots SEM was used and the significance of results was assessed using the two-tailed Student's *t*-test.

Quantification of the Interkinetic Nuclear Migration (INM) Ratio

Tg[βactin:HRAS-EGFP] embryos at 18hpf after different pharmacological treatments were immunostained with: i) anti-pH3 to analyse the cells undergoing mitosis, ii) anti-GFP to visualize the plasma membranes and therefore singularize the cells, and iii) DAPI to position cell nuclei. Confocal image stacks with 1μm z and identical zoom were taken in the hindbrain region extending from r2 to r6. Then, an identical XY frame covering half of the neural tube from apical to basal side of the neuroepithelial cells was selected for each embryo (Fig S9A). Channels were split and green channel was subtracted from both blue channel and red channel to help to segment the cell nuclei (Fig S9B-D). Finally, we divided our chosen frame in two halves, one apical and one basal, and counted the number of nuclei located in both sides (Fig S9B'). To assess the Interkinetic Nuclear Migration Ratio we divided the number of apical and basal nuclei. The total number of pH3-positive cells was used as a readout of mitotic cells (Fig S9D'). Results were plotted in Fig 5I-J, SEM was used and the significance of the results was assessed using the two-tailed Student's *t*-test.

ACKNOWLEDGEMENTS

We are grateful to S Dyballa for her enormous help in imaging and developing ImageJ/FIJI analysis tools, and to M Milan and R Bradley for critical reading of the manuscript. We thank to the people who kindly provided us transgenic fish lines and reagents, especially P Charnay, CP

Heisenberg, G Koster, SA Holley and N Peyrieras. JT was a recipient of a postdoctoral Beatriu de Pinos fellowship (AGAUR, Generalitat de Catalunya). The work was funded by BFU2009-07010 and BFU2012-31994 (Spanish Ministry of Economy and Competitiveness, MINECO) to CP. The authors declare no competing financial interests.

AUTHOR CONTRIBUTIONS

SC and JT contributed to the design, execution and analysis of the experiments. CP contributed to the concept, design and analysis of the experiments, provided funding, and wrote the manuscript.

REFERENCES

Aliee M, Röper JC, Landsberg KP, Pentzold C, Widmann TJ, Jülicher F, Dahmann C (2012) Physical mechanisms shaping the Drosophila dorsoventral compartment boundary. Curr Biol 22(11):967-76

Batlle E, Wilkinson DG (2012) Molecular mechanisms of cell segregation and boundary formation in development and tumorigenesis. Cold Spring Harb Perspect Biol 4(1):a008227

Becam I, Rafel N, Hong X, Cohen SM, Milán M (2011) Notch-mediated repression of bantam miRNA contributes to boundary formation in the Drosophila wing. Development 138(17):3781-9

Behrndt M, Salbreux G, Campinho P, Hauschild R, Oswald F, Roensch J, Grill SW, Heisenberg CP (2012) Forces driving epithelial spreading in zebrafish gastrulation. Science 338(6104):257-60

Chomette D, Frain M, Cereghini S, Charnay P, Ghislain J (2006) Krox20 Hindbrain Cis-Regulatory Landscape: Interplay between Multiple Long-Range Initiation and Autoregulatory Elements. Development 133, 1253-1262

Cooke JB, Moens CB (2002) Boundary formation in the hindbrain: Eph only it were simple... Trends Neurosci 25(5):260-7

Cooke JE, Kemp HA, Moens CB (2005) EphA4 is required for cell adhesion and rhombomere-boundary formation in the zebrafish. Curr Biol 15(6):536-42

Cooper MS, Szeto DP, Sommers-Herivel G, Topczewski J, Solnica-Krezel L, Kang HC, Johnson I, Kimelman D (2005) Visualizing morphogenesis in transgenic zebrafish embryos using BODIPY TR methyl ester dye as a vital counterstain for GFP. Dev Dyn 232(2):359-68

Curt JR, de Navas LF, Sánchez-Herrero E (2013) Differential activity of Drosophila hox genes induces Myosin expression and can maintain compartment boundaries. PLoS One 8(2):e57159

Dahmann C, Oates AC, Brand M (2011) Boundary formation and maintenance in tissue development. Nat Rev Genet 12(1):43-55

Defourny J, Poirrier AL, Lallemend F, Mateo Sánchez S, Neef J, Vanderhaeghen P, Soriano E, Peuckert C, Kullander K, Fritzsch B, Nguyen L, Moonen G, Moser T, Malgrange B (2013) Ephrin-A5/EphA4 signalling controls specific afferent targeting to cochlear hair cells. Nat Commun 4:1438

Distel M, Wullimann MF, Köster RW (2009) Optimized Gal4 genetics for permanent gene expression mapping in zebrafish. Proc Natl Acad Sci 106(32):13365-70

Ernst S, Liu K, Agarwala S, Moratscheck N, Avci ME, Dalle Nogare D, Chitnis AB, Ronneberger O, Lecaudey V (2012) Shroom3 is required downstream of FGF signalling to mediate proneuromast assembly in zebrafish. Development 139(24):4571-81

Filas BA, Oltean A, Majidi S, Bayly PV, Beebe DC, Taber LA (2012) Regional differences in actomyosin contraction shape the primary vesicles in the embryonic chicken brain. Phys Biol 9(6):066007

Fraser S, Keynes R, Lumsden A (1990) Segmentation in the chick embryo hindbrain is defined by cell lineage restrictions. Nature 344:431-435

Gutzman, JH, Sive, H (2010) Epithelial relaxation mediated by the myosinphosphatase regulator Mypt1 is required for brain ventricle lumen expansion and hindbrain morphogenesis. Development 137: 795-804

Irving C, Nieto A, DasGupta R, Charnay P, Wilkinson DG (1996) Progressive spatial restriction of *Sek-1* and *Krox-20* gene expression during hindbrain segmentation. Dev Biol 173: 26-38

Jimenez-Guri E, Udina F, Colas JF, Sharpe J, Padron-Barthe L, Torres M, Pujades C (2010) Clonal analysis in mice underlines the importance of rhombomeric boundaries in cell movement restriction during hindbrain segmentation. PLoS One 5:e10112

Jimenez-Guri E, Pujades C (2011) An ancient mechanism of hindbrain patterning has been conserved in vertebrate evolution. Evol Dev 13(1):38-46

Jülich D, Mould AP, Koper E, Holley SA (2009) Control of extracellular matrix assembly along tissue boundaries via Integrin and EphA/Ephrin signaling. Development 136(17):2913-21

Kemp HA, Cooke JE, Moens CB (2009) EphA4 and EfnB2a maintain rhombomere coherence by independently regulating intercalation of progenitor cells in the zebrafish neural keel. Dev Biol 327(2):313-26

Klein, R (2012) EphA/Ephrin signaling during development. Development 139: 4105-4109

Kovács M, Tóth J, Nyitray L, Sellers JR (2004) Two-headed binding of the unphosphorylated nonmuscle heavy meromyosin ADP complex to actin. Biochemistry 43(14):4219-26

Laballete, C, Bouchoucha, YX, Wassef, MA, Gonagl, PA, Le men, J, Becjer, T, Gilardi-Hebenstreit, P, Charnay, P (2011) Hindbrain patterning requires fine-tuning of early *krox20* transcription by Sprouty 4. Development 138:317-326

Landsberg KP, Farhadifar R, Ranft J, Umetsu D, Widmann TJ, Bittig T, Said A, Jülicher F, Dahmann C (2009) Increased cell bond tension governs cell sorting at the Drosophila anteroposterior compartment boundary. Curr Biol 19(22):1950-5

Langheinrich, U, Hennen, E, Stott, G, Vacun, G (2002) Zebrafish as a model organism for the identification and characterization of drugs and genes affecting p53 signaling, Curr Biol 12(23): 2023-8

Lecaudey V, Anselme I, Rosa F, Schneider-Maunoury S (2004) The zebrafish iroquois gene iro7 positions the r4/r5 boundary and controls neurogenesis in the rostral hindbrain. Development 131:3121-3131

Leung L, Klopper AV, Grill SW, Harris WA, Norden C (2011) Apical migration of nuclei during G2 is a prerequisite for all nuclear motion in zebrafish neuroepithelia. Development 138(22):5003-13

Maître JL, Berthoumieux H, Krens SF, Salbreux G, Jülicher F, Paluch E, Heisenberg CP (2012) Adhesion functions in cell sorting by mechanically coupling the cortices of adhering cells. Science 338(6104):253-6

Major RJ, Irvine KD (2005) Influence of Notch on dorsoventral compartmentalization and actin organization in the Drosophila wing. Development. 132(17):3823-33

Major RJ, Irvine KD (2006) Localization and requirement for Myosin II at the DV compartment boundary of the Drosophila wing. Dev Dyn 235(11):3051-8

Maves L, Jackman W, Kimmel CB (2002) FGF3 and FGF8 mediate a rhombomere 4 signaling activity in the zebrafish hindbrain. Development 129(16):3825-3837.

Moens CB, Prince VE (2002) Constructing the hindbrain: Insights from the zebrafish. Dev Dyn 224:1-17

Monier B, Pélissier-Monier A, Brand AH, Sanson B (2010) An actomyosin-based barrier inhibits cell mixing at compartmental boundaries in Drosophila embryos. Nat Cell Biol 12(1):60-5

Olivier N, Luengo-Oroz MA, Duloquin L, Faure E, Savy T, Veilleux I, Solinas X, Debarre D, Bourgine P, Santos A et al. (2010) Cell lineage reconstruction of early zebrafish embryos using label-free nonlinear microscopy. Science 329(5994): 967-971

Oxtoby E, Jowett T (1993) Cloning of the zebrafish krox-20 gene (krx-20) and its expression during hindbrain development. Nucleic Acids Res 1993 Mar 11;21(5):1087-95

Schilling TF, Prince V, Ingham PW (2001) Plasticity in zebrafish hox expression in the hindbrain and cranial neural crest. Dev Biol 231(1):201-16

Spear PC, Erickson CA (2012) Interkinetic nuclear migration: a mysterious process in search of a function. Dev Growth Differ 54(3):306-16

Thisse C, Thisse B, Schilling TF, Postlethwait JH (1993) Structure of the zebrafish snail1 gene and its expression in wild-type, spadetail and no tail mutant embryos. Development 119(4):1203-15

Xiong, F, Tentner, AR, Huang, P, Gelas, A, Mosaliganti, KR, Souhait, L, Rannou, N, Swinburne, IA, Obholzer, ND, Cowgill, PD, Schier, AF, Megason, SM (2013) Specified neural progenitors sort to form sharp domains after noisy Shh signaling. Cell 153: 550-561

Xu Q, Alldus G, Holder N, Wilkinson DG (1995) Expression of truncated Sek-1 receptor tyrosine kinase disrupts the segmental restriction of gene expression in the Xenopus and zebrafish hindbrain. Development 121(12):4005-16.

Xu Q, Mellitzer G, Robinson V, Wilkinson DG (1999) In vivo cell sorting in complementary segmental domains mediated by Eph receptors and ephrins. Nature 399(6733):267-71

Zhang L, Radtke K, Zheng L, Cai AQ, Schilling TF, Nie Q (2012) Noise drives sharpening of gene expression boundaries in the zebrafish hindbrain. Mol Syst Biol 8:613

FIGURE LEGENDS

Figure 1: Characterization of the fish transgenic lines used in the study. (A) Scheme of the inserted transgenes in the fish lines. (B-P) Spatio-temporal characterization of the expression of the transgene (*kalta4*, *gfp*) in the different transgenic lines by in situ hybridization compared with endogenous expression of *krx20* in wt embryos. Note that at early stages of embryonic development in all zebrafish strains, *krx20*, *kalt4* or *gfp*-positive cells are found surrounded by cells of different identity (D,I,N, for magnifications, see arrows); later on, clear and sharp gene-expression domains are generated (E,J,O). (Q,S) Spatial characterization of the reporter fluorescence protein expression in the two different transgenic lines injected with mRNA driving expression to the plasma membrane such as lyn:GFP and or mem:mCherry. (R) anti-GFP immunostaining of Tg[elA:GFP] embryos at 3ss. Note that GFP-positive cells within the jagged boundary are found surrounded by GFP-negative cells (see white arrows). Dorsal views with anterior to the left.

Figure 2: Tracking of single cells shows that rhombomeric cells are sorted out from territories with different rhombomeric identity

In vivo imaging of Tg[elA:GFP] embryos injected with H2B-mcherry mRNA at 4-8cell stage. (A-L) Time-lapse of an embryo from 12hpf where we tracked: (A-F) a single GFP-positive cell from r5 (see blue dot pointed with white arrow); (G-L) a single GFP-negative cell from r6 that divides in two GFP-negative cells (see blue dots pointed with white arrows). See Movies S1 and S2 for original movies. (M-R) Time-lapse of an embryo at 12hpf where several single cell trajectories within r3-r6 were back-tracked. Merge of green and red channels, displaying in green the emergence of r3 first and later r5 and in red all labeled cell nuclei; (M'-R') Green channel displayed in white, to observe the appearance of r3 first and then r5, and the

position of tracked-cells with colored dots. Blue dots correspond to r4-cells, yellow dots to r5-cells and green dots to r6-cells. See Movie S3 for original data. Note that cells at the boundaries that at the last time point are segregated were intermingled at the beginning of the movie. Dorsal views with anterior to the left.

Figure 3: Cell sorting is the main cellular mechanism involved in molecular boundary refinement

(A-I) Fluorescent *krx20* in situ hybridization (red) followed by anti-GFP immunostaining (green) to detect the expression of the reporter gene under the control of *krx20* in the different transgenic zebrafish lines: (A-C) Tg[elA:GFP] and (D-F) double transgenic Mü4127 4xKaloop embryos, which express GFP in r3 and r5; (G-I) Tg[elA:GFP] embryos injected with MO-EphA4a. Note that in all cases cells co-express *krx20* (red) and GFP (green). Even when cell sorting is disrupted after morpholino-injection and a given cell is found isolated, it expresses either both markers (see white arrow heads), or it expresses none (see white arrows). All images are dorsal views with anterior to the left. (J-K) Quantification of cells expressing *krx20* and GFP in the vicinity of all rhombomeric boundaries. Green bars: Tg[elA:GFP] embryos; dashed bars: Tg[elA:GFP] embryos injected with MO-EphA4a; grey bars: Tg[elA:GFP] embryos injected with MO-CTRL.

Figure 4: Actomyosin cables are present in the interhombomeric boundaries.

(A-E') Dorsal views of time-lapse stacks of rhombomeres 3 (red) and 4 of Tg[actin:HRAS-GFP] Mü4127 embryos from 21hpf onwards. (B-E') Inserts of the region framed in (A). Note that cell division challenges the boundary (see white arrow head). Anterior is to the top. See Movie S5 for the original data. (H,J,L) Dorsal views of Tg[utrophin:GFP] embryos from 14 to 18hpf. (I,K,M) Sagittal-optical sections of same embryos obtained as

Maximal Intensity Projections of the XZ apical planes depicted in (H,J,L) within the orange frame. See scheme in (F-G) for further clarity and Fig S7A for more exhaustive explanations. Arrows point to the enrichment of F-actin. Note that the enrichment of F-actin structures can be observed from 15hpf, once the morphological rhombomeric bulges are visible (Fig S4). Anterior is always to the left. (N-N') Sagittal-optical views obtained as in (I,K,M) of double transgenic Tg[lifeactin:GFP]/Tg[myoII:mCherry] embryos showing that interhombomeric cables are formed by F-actin and Myosin II (see arrows). Myosin II can be seen in red (N), and the merge of F-actin and Myosin II in yellow (N'). (O) Sagittal-optical view from double transgenic Tg[utrophin:GFP]/Mü4127 embryos where Myosin II cables are located in the interhombomeric boundaries (see arrows). (P-P") Tg[utrophin:GFP] embryos immunostained for anti-EphA4. (P'-P") is an insert of the region framed in (P) where the actomyosin cable is observed in the EphA4-negative territory. Anterior is always to the left.

Figure 5: Actomyosin barriers prevent cell intermingling between rhombomeres.

(A) Scheme depicting the experiment: double transgenic Tg[utrophin:GFP]/Mü4127 embryos at 14hpf were treated with different pharmacological agents that modulate the function of the actomyosin cable, such as: (C,G) DMSO as control, (D,H) Blebbistatin and (E-I) Calyculin. (B-E) show the presence/absence of the actomyosin cable in apical sagittal-like views, and (F-I) display dorsal views of r2-r6 region to observe the extent of cell mixing. Note that once the actomyosin cable is disrupted (D), ectopic r3/r5 cells are found in r4 (see white arrows in (H). Anterior is always to the left. (B,F) are schemes to help in the comprehension the 3D-tissue organization. (J-M) Analysis of the Index of Straightness (IS) within the *krx20*-expression border: (J-L) wt embryos were treated with same pharmacological agents as in previous experiments and assayed for *krx20*

situ hybridization. Note that upon Blebbistatin treatment the border of *krx20*-expression is very fuzzy compared with the sharp border displayed by DMSO or Calyculin treated embryos. Anterior is to the left. (M) Quantification of the Index of Straightness (IS) upon different conditions. IS was measured according to Fig S8B. *** $p<0.001$, ** $p<0.005$.

Figure 6. Effects of the pharmacological treatments on the Interkinetic Nuclear Migration (INM).

(A-D) Wash-out experiments.

(E-H) Tg[actin:HRAS-GFP] embryos upon different treatments were stained for anti-pH3 to visualize mitotic cells and counterstained with DAPI to singularize cell nuclei. Dorsal views of half-side hindbrains with anterior to the left and apical to the bottom. Images were analyzed according to Fig S8 and the data obtained was plotted as: (I) number of cells undergoing mitosis in the hindbrain (pH3-positive cells), and (R) Interkinetic Nuclear Migration Ratio, which is calculated as the number of nuclei located in the apical side of the cells divided by the number of nuclei located in the basal side of the cells (DAPI-positive cells). *** $p<0.001$ ** $p<0.005$

Figure 7: EphA/Ephrin signaling is upstream of the generation of the actomyosin cables.

(A) Scheme of the functional experiment: double transgenic embryos Mü4127/Tg[utrophin:GFP] injected with CTRL-MO (C,H) or EphA4a-MO (D-K) at 1-4 cells stage, incubated from 14hpf for 6h with DMSO (C-D,H-I), Blebbistain (E,J) or Calyculin A (F,K). After the treatment, the degree of cell mixing (C-F) and the presence of actomyosin cables (H-K, see arrows) were assessed. Embryos injected with CTRL-MO behave as control embryos in previous experiments. Note the cell mixing in embryos where the cable was disrupted (D,E, see white arrows), and the partial rescue of the cable in EphA4a-MO embryos treated with Calyculin A (K) resulting in no cell

mixing (F). Dorsal views (B-F) and sagittal-optical views of apical stacks (H-K) with anterior to the left.

Figure 8. Ectopic EphA/Ephrin signaling can induce ectopic enrichment of cable structures.

(A-C) Analysis of the Index of Straightness (IS) in wt embryos injected with EphA4-MO at 1-4 cells stage, incubated from 14hpf for 6h with different pharmacological agents and assayed for *krx20* in situ hybridization. Note that the jagged *krx20*-expression domains upon Blebbistatin treatment, and how this enhances the effect of EphA4a-MO. IS is partially rescued in morphants upon Calyculin treatment. Dorsal views with anterior to the left. (D) Quantification of the IS for embryos in experiment (A-C) (dashed bars), and comparison with control embryos (solid bar). (E-J) Gain-of-function experiments. Conditional ectopic expression of EphA4 in even- and odd-numbered rhombomeres in Tg[myoII:mCherry] embryos using the Ubi:Gal4-ERT2xUAS:GFP system. Ectopic EphA4 expression (H-J) or GFP as control (E-G) can be followed in green, and Myosin II structures in red. (E,H) are dorsal views of embryos, (F,I) are sagittal-like views, and (G-J) are transverse views.

Figure 9: Model for the requirement of actomyosin cables in the interhombomeric boundaries to keep different rhombomeric cell populations segregated.

Schematic 3D-representation of a hindbrain territory depicting two adjacent rhombomeres. Three different orthogonal views are taken from this scheme: transverse (Blue), sagittal (Yellow) and dorsal (Purple). Actomyosin cables are represented as green lines in transverse and sagittal views and as green dots in the dorsal view. To help clarity, in the dorsal view cells are represented only for the posterior rhombomere (red cells). A) DMSO, Calyculin or CRTL-MO embryos. Note the sharp boundary in the dorsal

view. B) Blebbistatin, Rockout and EphA4a-MO embryos. Actomyosin cables are dismantled and cells from the posterior compartment cross the boundary to the anterior compartment. AP axis is indicated in the diagram.

SUPPLEMENTARY MATERIAL

Movie S1: In vivo imaging of Tg[elA:GFP] embryos injected with H2B-mcherry mRNA, from 12hpf-13hpf, focusing on a single GFP-positive cell from r5. Dorsal views with anterior to the left.

Movie S2: In vivo imaging of Tg[elA:GFP] embryos injected with H2B-mcherry mRNA, from 11hpf-13hpf, focusing on a single GFP-negative cell from r6. Note that GFP-negative cell at the boundary that undergoes cell division is sorted out from r5 along the movie (see blue dot). Dorsal views with anterior to the left (see blue dots).

Movie S3: In vivo imaging of an Tg[elA:GFP] embryo injected with H2B-mcherry mRNA at 4-8cell stage, from 11hpf to 16hpf. Several single cells were back-tracked within r3 to r6. Dorsal views with anterior to the left.

Figure S4: In vivo imaging of wt embryos injected with lyn-GFP mRNA at 1cell/stage. Time-lapse frames at 14hpf, 15.5hpf and 18hpf. Note that the morphological rhombomeric boundaries are clearly visible from 15.5hpf onwards (see white arrows). Dorsal views with anterior to the left.

Movie S5: In vivo imaging of double transgenic Mu4127 Tg[actin:HRAS-GFP] embryos from 21hpf to 30hpf. Partial sequence (21hpf-25hpf) of the acquired time-lapse. Dorsal views with anterior to the top.

Figure S6: Extracellular matrix deposition does not contribute to interhombomeric fences. (A-B) Dorsal views of Tg[elA:GFP] embryos immunostained with anti-FN. Note that there is not enrichment of FN in the hindbrain although there is a clear FN-deposition in the intersomitic boundaries (ISB). (C-E) Mü4127 embryos were injected with itga5:GFP

mRNA in order to visualize the clustering –and therefore the activation- of 5 integrins in the hindbrain boundaries. Note that as FN, no enrichment of itga5 was found in the hindbrain although it can be clearly observed in the ISB (D).

Figure S7: Scheme depicting the processing of the samples to obtain: (A) sagittal-like optical sections to observe actomyosin-cables in the apical side of the cells; and (B) dorsal view images to calculate the IS. (A) Embryos were mounted and dorsal images in XY are acquired in the confocal microscope. Using ImageJ/FIJI, all dorsal images are re-sliced in YZ and rotated if need to have a perfect DV orientation. Afterwards, re-slice all images in XZ to obtain sagittal views and select the apical XZ stacks to MIP. (B) Embryos were mounted and dorsal images in XY are acquired in the confocal microscope. Using ImageJ/FIJI, all dorsal images are re-sliced in YZ and rotated if need to have a perfect DV orientation. Then, re-slice images back to XY and select the stacks from the medial part of the neural tube to MIP.

Figure S8: Scheme depicting the processing of the samples for the quantification of the Interkinetic Nuclear Migration Ratio and the number and position of mitotic cells. Tg[βactin:HRAS-GFP] embryos were stained for anti-pH3 (red) and DAPI (blue) at 18hpf. To clearly singularize the cell nuclei, the intensity of GFP labelling the plasma membrane (C) was subtracted from the blue channel and the red channel (D). Then, either nuclei (DAPI-staining) or pH3-positive cells were counted in the desired regions.

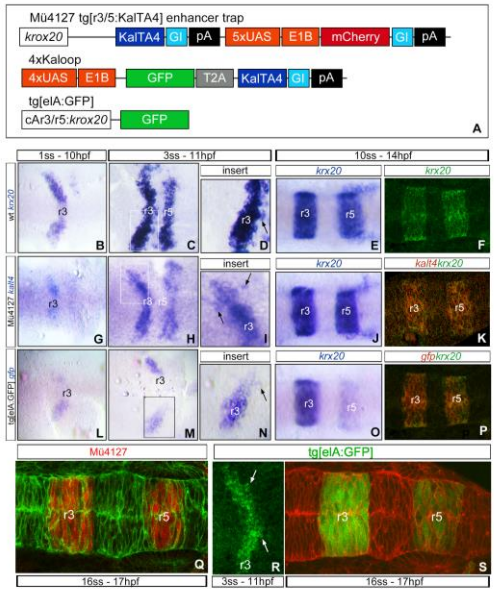

Figure 1

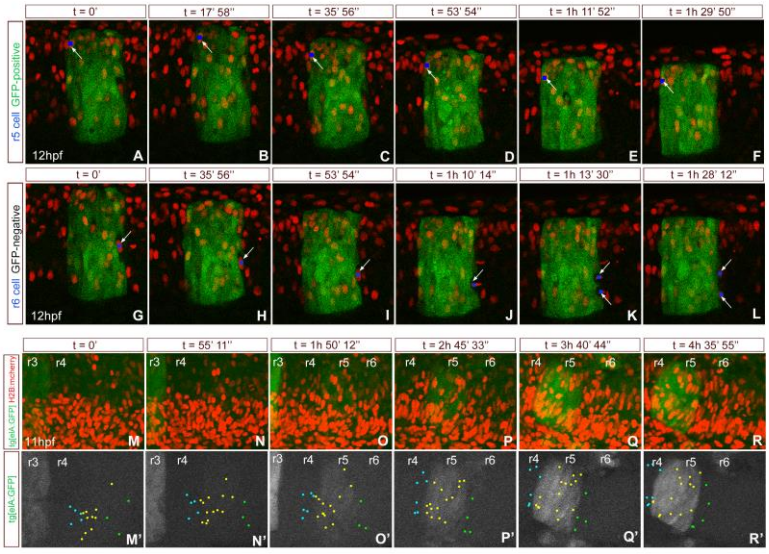

Figure 2

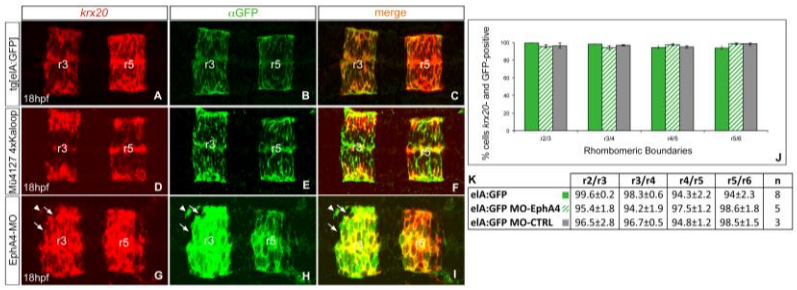

Figure 3

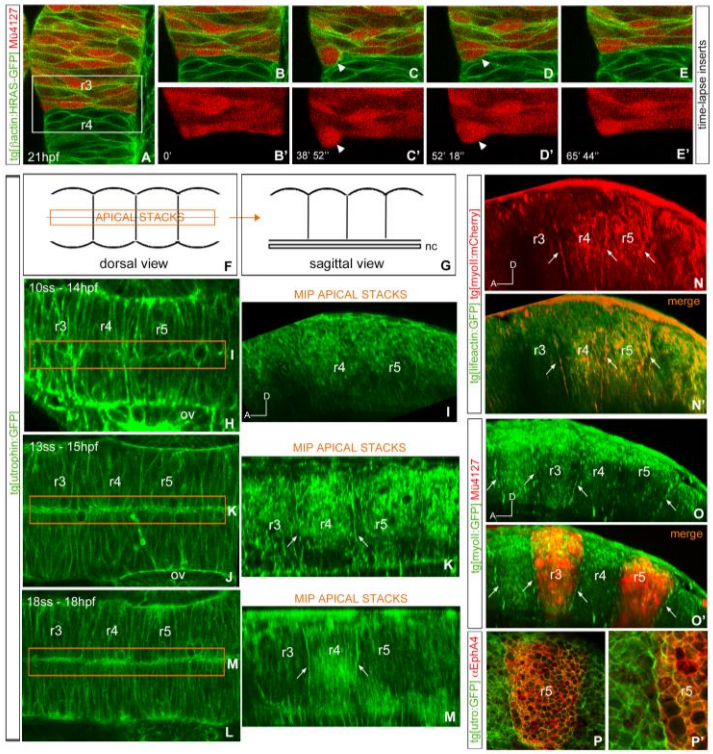

Figure 4

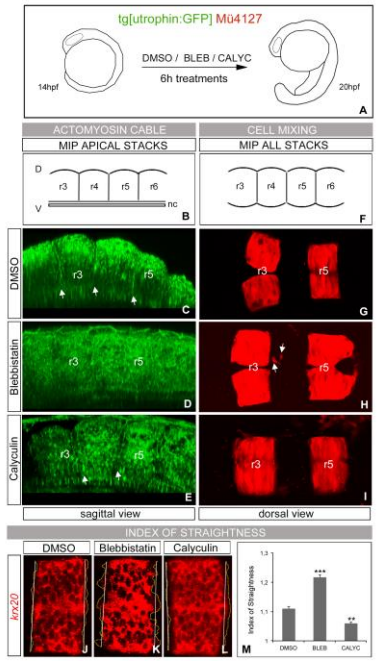

Figure5

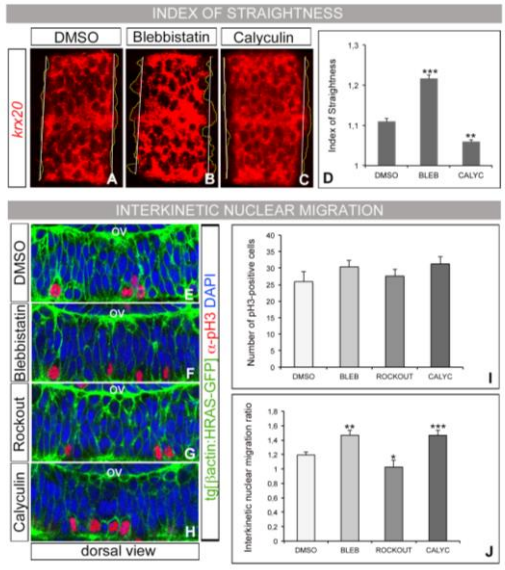

Figure6

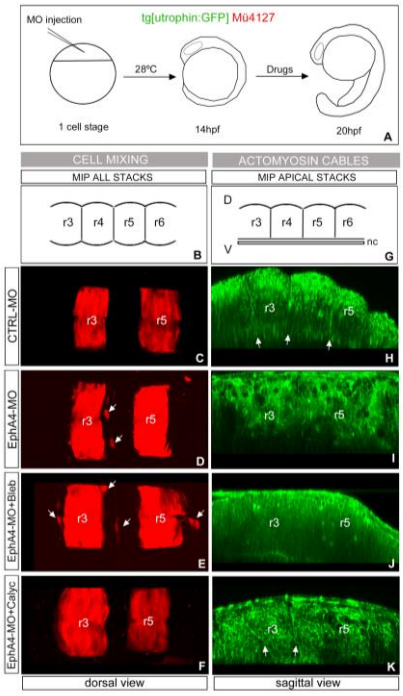

Figure7

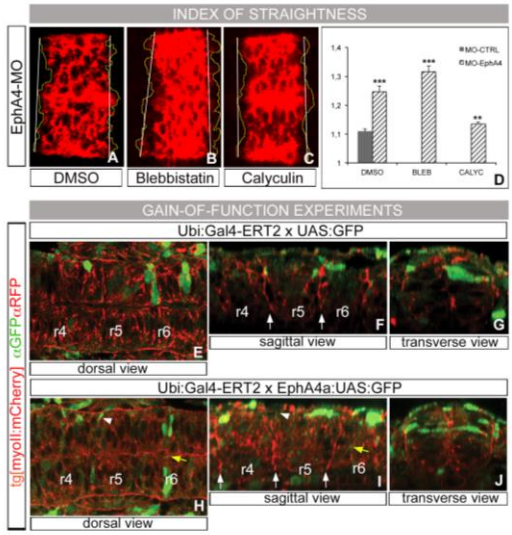

Figure 8

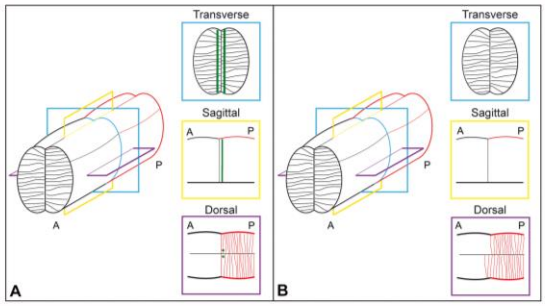

Figure 9

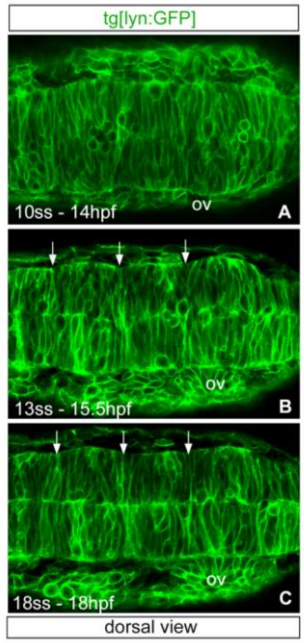

Figure S4

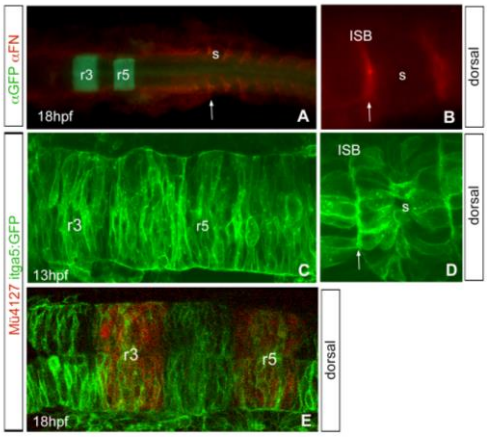

Figure S6

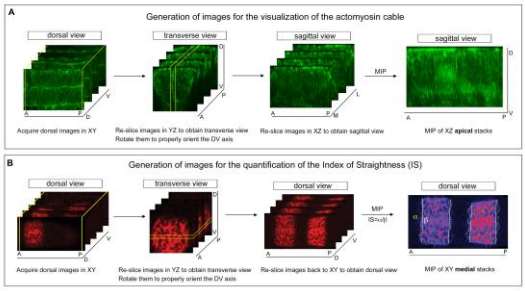

Figure S7

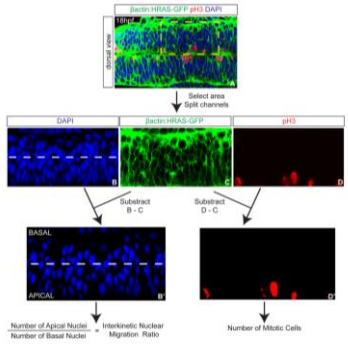

Figure S8